Habib Fathallah

NARROWBAND INTERFERENCE SUPPRESSION IN SPREAD SPECTRUM CDMA COMMUNICATIONS VIA BLIND EQUALIZATION

Mémoire présenté
à la Faculté des études supérieures
de l'Université Laval
pour l'obtention
du grade de maître ès arts (M.A.)

Département de Génie Électrique et Génie Informatique
FACULTÉ DES SCIENCES ET DE GÉNIE
UNIVERSITÉ LAVAL

Avril 1997

Habib Fathallah

NARROWBAND INTERFERENCE SUPPRESSION IN SPREAD SPECTRUM CDMA COMMUNICATIONS VIA BLIND EQUALIZATION

Mémoire présenté
à la Faculté des études supérieures
de l'Université Laval
pour l'obtention
du grade de maître ès arts (M.A.)

Département de Génie Électrique et Génie Informatique
FACULTÉ DES SCIENCES ET DE GÉNIE
UNIVERSITÉ LAVAL

Avril 1997

Table of contents

Figures

Résumé

Dans ce mémoire, nous nous sommes intéressés à la possibilité de faire coexister un système de communication à spectre étalé CDMA avec le système classique à bande étroite. Nous avons étudié la réjection de l'interférence à bande étroite modélisé comme un système virtuel d'interférents CDMA. D'abord, nous avons étudié le détecteur MMSE (Minimum Mean Square Error), et nous avons évalué ses performances. Ensuite, nous avons focalisé notre étude sur sa version adaptative aveugle qui a l'avantage de ne nécessiter aucune connaissance préalable sur l'interférence. Une analyse spatiale du signal reçu nous a permis de décrire avec précision la trajectoire d'évolution du détecteur aveugle et d'en identifier plusieurs inconvénients et anomalies. On a défini deux nouvelles contraintes sur le pas de convergence, qui en ont nettement amélioré la vitesse et la qualité. Enfin, nous avons proposé un nouveau détecteur adaptatif et aveugle qui évite les anomalies du détecteur précédent et qui tire profit des nouvelles contraintes de convergence.

Prof. Leslie Ann Rusch
Directrice de recherche

Habib Fathallah
Étudiant à la Maîtrise

Abstract

In this dissertation, we study the coexistence of two different communications techniques in a given frequency band: narrowband and direct sequence spread spectrum (DSSS). We interpret the digital narrowband interferer as a set of virtual, orthogonal code division multiple access (CDMA) system users. We first applied the fixed minimum mean square error (MMSE) receiver to our system, and analyzed its performance in terms of probability of error, and signal to noise ratio. We next focused on a blind adaptive suppression technique, which has the major advantage of only requiring knowledge of the desired user's spreading code to recover the data bits. We used subspace analysis to describe the mean tap weight vector trajectory. We identified some convergence anomalies in the blind algorithm and derived two improved constraints on the adaptation step size, both fixed and variable. Finally, we proposed a new blind adaptive detector that avoids the convergence anomalies, while capitalizing on the new constraints on the step size for faster and better quality of convergence.

Prof. Leslie Ann Rusch
Research Advisor

Habib Fathallah
Master's Candidate

I dedicate this work to my love

Jihen *...*

Remerciements

Je tiens à exprimer ma reconnaissance et ma gratitude au Dr Leslie Ann Rusch, ma directrice de recherche, qui m'a aidé, soutenu, encouragé, et n'a cessé de me prodiguer ses précieux conseils. Ces judicieuses directives m'ont été d'une grande utilité. Je ne peux passer sous silence l'impact des qualités humaines du Dr Rusch sur l'avancement de ce travail. Qu'elle trouve dans ce travail le témoignage de ma gratitude et de mon profond respect. Enfin, je dirai que j'étais entre bonnes mains.

Je remercie spécialement le Dr Vincent Poor, professeur à Princeton University d'avoir accepté d'être l'un des correcteurs de ce mémoire. Je me sens fier d'être le premier étudiant de son ex-étudiante. C'est grâce au Dr Vincent Poor, un des pionniers des techniques CDMA, que j'ai eu la chance de travailler dans cet axe de recherche.

Je remercie également le Dr Huu Tuê Huynh, professeur au département de génie électrique et génie informatique à l'Université Laval, d'avoir accepté d'être aussi l'un des correcteurs de ce mémoire.

De plus, mes remerciements s'adressent à toutes et tous mes collègues étudiantes et étudiants du Centre d'Optique Photonique et Laser du département de génie électrique et génie informatique (COPGEL), particulièrement à Dominique Brichard qui, avec ses qualités humaines, m'a énormément aidé à m'intégrer dans l'équipe COPGEL. Mes remerciements s'adressent également aux professeures et aux professeurs du laboratoire pour l'effort qu'ils déploient pour diriger, former, et motiver les étudiants. Un merci spécial pour les collègues Jean-François Cliche, André Fekecs, Bernard Ruchet pour le temps et l'effort qu'ils ont investis au profit de tout le laboratoire. Un remerciement s'adresse également aux collègues James Babineau, Louis-Patrick Boulianne, Jean-François Lemieux, Jean-Philippe Laflamme, Martin Rochette, Antoine Bellemare, Jean

Martin, Vincent Delisle, Christine Latrasse, Normand Cyr, Fakher Ayadi et tous ceux qui contribuent à générer un climat aussi propice dans le laboratoire.

Ma mère, mes frères, mes sœurs, mes belles-sœurs, mes beaux-frères, mes nièces, mes neveux, ma grande famille et mes ami(e)s ne peuvent être récompensés pour leur amour. J'aimerai aussi témoigner ma gratitude à la famille de Mer Zoubeir Ben Hassine. Je les remercie toutes et tous et je pense à eux à 10000 km.

Introduction

Code division multiple access (CDMA) implemented with direct sequence spread spectrum (DSSS) signaling is among the most promising multiplexing technologies for cellular telecommunications services such as personal communications, mobile telephony, and indoor wireless networks. The advantages of direct-sequence spread spectrum for these services include superior operation in multipath environments, flexibility in the allocation of channels, the ability to operate asynchronously, enhanced privacy, and increased capacity in bursty or fading channels [1].

The spread-spectrum communication is inherently resistant to the narrowband interference (NBI) caused by coexistence with conventional communications signals. This follows from spread spectrum's jamming resistance that made it originally attractive for military applications. To combat an adversary who deliberately attempts to jam the frequency of military communications, the military signal is spread out in the frequency domain. The jammer power density is by its nature concentrated at a relatively very narrow bandwidth of frequency. At reception, the despreading operation spreads the narrowband signal across a large bandwidth, while the military signal is despread and collapses back to its original data bandwidth. It's interesting to note that after despreading the situation is reversed between the original narrowband interferer (now wideband), and the original data signal (now narrowband). This process is illustrated in the Figure 2.1.

Due to these original characteristics, it has been proposed that spread spectrum be overlaid on existing frequency band occupants. These existing users would have very narrow bandwidth compared to the spread spectrum signal. The ability of spread spectrum systems to coexist with narrowband communication systems on the same bandwidth without degrading either the narrowband or the CDMA system's performance is a very attractive feature of this technique. The inherent processing gain of a spread spectrum system provides a great degree of interference rejection capability, reducing interference by as much as one

over the spreading code length. At times the interfering signal is powerful enough so that even with this advantage communication becomes effectively impossible. Over the past two decades, a significant body of research has been concerned with the development of techniques for active narrowband interference (NBI) suppression in spread spectrum systems. Milstein [22] offers an excellent review of those methods developed prior to 1988. Research has shown that performance can be increased by processing to suppress narrowband interference especially for commercial applications that presuppose a powerful licensed interferer and a spread spectrum system constrained in power so as not to disrupt existing communications systems.

The narrowband users in spread spectrum communication can be viewed as an additive noise with a non-gaussian distribution. The presence of the narrowband signal makes the environment non-gaussian. Several schemes have been proposed to filter out such narrowband signals before going to matched filter the received waveform [26-30]. The narrowband signal is predictable, while the wideband spread spectrum signal is not. One of the most common approaches uses filtering to predict narrowband signals and to subtract these predictions from the received signals. Such a scheme is termed a predictor/subtractor detector. Analysis of this filtering technique has modeled the narrowband signal as either a deterministic sinusoidal signal or an autoregressive signal (AR). These models greatly simplify analysis, yet still capture the narrowband property of the interferer. They do not apply, however, to a digital interference signal.

Poor and Rusch [29] provide an overview of more recent NBI suppression techniques, especially those employing non-standard signal processing methods to enhance the interference rejection capabilities in CDMA systems. They consider nonlinear filtering techniques [27-30] in which the spread spectrum CDMA signal (digital) is modeled as a non-Gaussian noise in the interference suppression process. We are more interested in [30] where Rusch and Poor first apply the techniques of multiuser detection to remove a digital narrowband interference signal. They interpret each interfering bit as a virtual SS user (Figure 2.10). Suppose we have m+1 narrowband bits occurring in the time of a single SS

bit. This can be interpreted as a code division multiple access (CDMA) system with m+2 users.

Multiuser detection theory gives us the optimal and various sub-optimal receivers for such a system. These receivers require information on some, or perhaps all, of the following parameters: signature sequences, received energies, timing delays, etc. of all users. In particular, the NBI suppression method of [30] is based on the use of the decorrelating detector for removing digital interferers from the channel. The major significant practical disadvantage of the decorrelating detector is that it requires the knowledge of waveforms of all users in the channel, including the narrowband interferers. The MMSE receiver proposed by Rusch and Fathallah [31] and reproduced in section 2.5, provides a slight increase in performance in terms of probability of error in the range of high signal to interference ratio, but it also requires the knowledge of all users waveforms, as well as the spread spectrum and interference powers.

The need for blind adaptation

The minimum mean square error (MMSE) detector is of interest as an adaptive version can be implemented which does not require knowledge of the interfering signals characteristics. Minimizing the mean square error (MSE) directly requires a training sequence for every active user during initial adaptation. Each transmitter sends a training sequence at start-up which the receiver uses for initial adaptation. After the training sequence, the receiver can switch to a decision-directed mode. However, the decision directed adaptation becomes unreliable during drastic changes in the interference environment, and consequently, data transmission of the desired user must be suspended and the training sequence must be retransmitted. The above observations motivate the need for a blind adaptation technique in volatile multi-access channels, particularly in the presence of narrowband interference. In our NBI suppression it is also unrealistic to expect interferers to submit to the transmission of training sequences.

Overview

We begin in chapter 1 with a brief review of spread spectrum communications and various multiple access techniques. We consider in particular direct-sequence spread spectrum with code division multiple access (DSSS/CDMA), and introduce both the mathematical and the geometric model of this system. We present useful performance measures for CDMA systems, and briefly review the most important multiuser detectors.

In chapter 2, we consider the narrowband interference problem. In sections 2.1 to 2.4, we present previous work in narrowband interference mitigation in (DSSS/CDMA). In section 2.2 we briefly treat the principal linear methods that have been proposed, devoting most of our attention to the most recently proposed methods. We describe nonlinear filtering methods that offer improved suppression capability over linear methods in the estimator/subtractor configuration. NBI has typically been modeled as a sinusoidal signal or as a narrowband autoregressive signal. We exploit the structure of the digital NBI to further improve the performance of active NBI suppression.

We present the first of our contributions in the section 2.5. We take the general expression for the minimum mean square error (MMSE) receiver and apply it to the narrowband suppression problem when the NBI is a binary signal, arriving at a closed-form solution for the MMSE detector and its probability of error. We describe the theoretical and simulation results of the MMSE receiver compared of other receivers previously applied to the interference suppression problem [30].

In chapter 3, we focus on the blind multiuser detection algorithm proposed by Honig, Madhow and Verdú [14]. This detection approaches the MMSE detector, yet unlike this detector, it only requires knowledge of the spreading code of the desired user (in our case, the true SS user). The discrete time received signal can also be interpreted as a vector which has components due to the different users and noise. The geometric description of the channel is of great interest. In fact, it allows us to describe the evolution of the blind adaptive algorithm. In section 3.2, we define several bases for the space spanned by all possible signature sequences, as well as important subspaces. We examine the eigenspaces

of the received signal's covariance matrix to partition the signal space in three subspaces, Γ_{NO}, $\Gamma_{I\&N}$ and Γ_E. We demonstrate the significance of these subspaces in terms of how energy from the desired user, the AWGN and the narrowband interference is distributed among them. In particular, the subspace Γ_E is a two dimensional subspace which contains all the energy of the desired signal and a subset of the interference and noise energies. Γ_{NO} contains only noise, and $\Gamma_{N\&I}$ contains only a subset of interference and noise energies.

In section 3.3, we show that for this virtual CDMA system, the three fixed receivers of interest [the matched filter (or conventional detector), the decorrelating detector, and the MMSE receiver] all project the received signal onto this two-dimensional subspace Γ_E. Previous subspace analysis of systems with wideband interference has not identified this two dimensional space, but always involved much higher dimensional spaces. By identifying this space we are able to parameterize the receivers of interest by a single variable in contrast of m+1 variables in a system with m+1 wideband interferers. Because the space is of low dimension, we describe in sections 3.4 and 3.5 the mean trajectory of the stochastic blind adaptive detector. We find that the mean trajectory also falls in the two dimensional subspace Γ_E. Because the above observations, we are able to improve the criteria on the step size for stability in the adaptive algorithm which searches for the MMSE solution. In section 3.6, we propose two new limits on the step size that allows for much faster convergence. The first new limit is independent of time, whereas the second is a variable step size that decreases with the iteration number.

In chapter 4, the low dimension of the effective energy space allows us to define a general linear receiver as a function of one parameter. Each linear receiver of interest is characterized by a particular value of this parameter. We use this derivation to formulate a paramaterized version of the probability of error, the asymptotic efficiency, the near far resistance, the mean output energy (MOE), and the signal to interference ratio (SIR). This parameterization allows an alternate derivation of the MMSE receiver and also allows us to see the effect of weak interference on the mean output energy (MOE). Using our single parameter model of the MOE we identify an anomaly in the convergence for weak interferers. We show that while the MOE is always convex, it is extremely shallow for weak

interference signals. The adaptive version of the MMSE receiver minimizes the mean output energy via a gradient descent. Using our single parameter model we easily describe the mean evolution of the adaptive detector in a simple two-dimensional subspace, especially in the most important eigenvectors directions. Because the minimization function is convex, the algorithm will not be trapped by local minima, however when this function extremely shallow it is easily lead astray by spurious noise samples. In section 4.3 we examine how system parameters affect the efficiency of the convergence of the adaptive algorithm. We find the algorithm cannot effectively converge to the MMSE receiver when the narrowband interference power is weaker than the spread spectrum signal's power.

In section 4.4, we present simulation results for the fixed and adaptive receivers. Monte Carlo simulations confirm theoretical calculations of the probability of error for all receivers. We show faster convergence of the stochastic gradient algorithm when the new, looser constraint is applied to the step size, focusing on convergence along the eigenvectors of interest. We also match Monte Carlo results to theoretical results for the parameterized mean output energy illustrating sensitivity to interference power. Finally, we propose a new adaptive receiver that avoids the convergence anomalies while capitalizing on the new step size for faster convergence.

CDMA Communications

Code division multiple access implemented with direct sequence spread spectrum signaling is among the most promising multiplexing technologies for cellular telecommunications services such as personal communications, mobile telephony, and indoor wireless networks. The advantages of the direct-sequence spread spectrum for these services include superior operation in multipath environments, flexibility in the allocation of channels, the ability to operate asynchronously, enhanced privacy, and increased capacity in bursty or fading channels. The ability of spread spectrum systems to coexist with narrowband communication systems on the same bandwidth without significantly degrading either the narrowband or the CDMA system's performance is another attractive feature of this technique.

We begin in sections 1.1 and 1.2 with a brief review of various multiple access techniques and spread spectrum communications. In section 1.3, we consider in particular a direct-sequence spread spectrum with code division multiple access (DSSS/CDMA) system. We introduce both the mathematical and the geometric model of this system. In section 1.4 we present useful performance measures for CDMA system. In section 1.5 we present a brief review of the most important multiuser detectors.

1.1. Multiaccess techniques

1.1.1. Random multiaccess techniques

Different approaches can be applied to dynamic channel sharing. For example, random *multiaccess communication techniques,* in which a user initiates communications as if it were the sole user of the channel. If there are no simultaneous transmissions, the message is received successfully. Two popular implementations of random multiaccess communication are the ALOHA and carrier sense multiple access with collision detection protocols (CSMA/CD). The main difference between these two protocols is in the algorithm used to determine the retransmission delay when simultaneous transmissions lead to data loss. ALOHA is the first random multi-access communication system proposed for a radio channel in 1969 [2,5]. CSMA/CD is used in the Ethernet coaxial-cable local area networks. In the CSMA protocol, each terminal on the network monitors the status of the channel before transmitting information. If the channel is idle (*i.e.,* no carrier is detected), the user transmits a packet of data. As transmissions are uncoordinated, simultaneous transmissions can occur. In such cases a collision is detected, and the transmission is immediately aborted in midstream. Thus all users must be capable of "listen-while-talk" operation [4]. These approaches to sharing a channel are based on the philosophy of having no more than one transmitter active of given time. When more than one users are active, (*i.e*. when they overlap in both frequency + time), the receiver is not able to recover any of the colliding transmissions.

1.1.2. TDMA, FDMA, and CDMA

Three major multiple access techniques are used to share the available bandwidth in a wireless communications. The three techniques are time division multiple access (TDMA), frequency division multiple access (FDMA), and code division multiple access (CDMA). TDMA allows users to share the same frequency band, but allocates a unique time slot to each user in a cyclical fashion, as seen in (Figure 1.1 a). In FDMA a user is assigned a particular frequency band which is not shared by other users in the geographic vicinity as

illustrated (Figure 1.1 b). In a CDMA system (Figure 1.1 c), the receiver need not concern itself with the fact that signals overlap both in frequency and in time. Instead unique "signatures" waveforms (or codes) are used by each user. The actual, or near orthogonality of these codes allows successful communications in the presence of simultaneous transmissions.

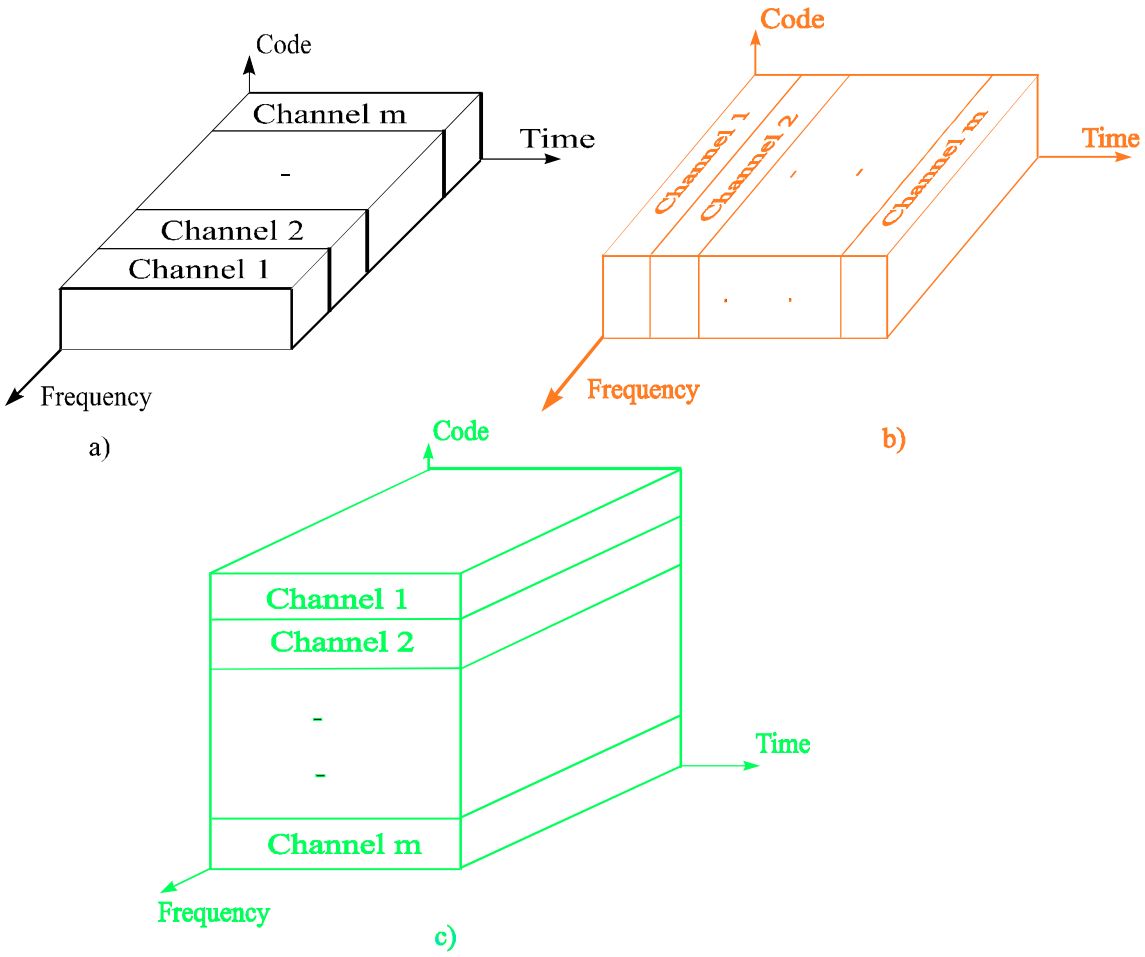

Figure 1.1 a) FDMA, b) TDMA, and c) CDMA.

An interesting comparison for the three multiple access techniques is given by Verdù [2]:

> *"From the view point of utilization of channel resources, orthogonal CDMA has no advantage over FDMA or TDMA ... The only advantage of CDMA over TDMA and FDMA is the extra flexibility it affords in order to shape the time and frequency domain*

waveforms....the orthogonality of the signature waveforms is not necessary for CDMA to work, in the sense that the various signals can still be demodulated. Indeed, this a major reason why CDMA is an attractive multi-access technique for many multiuser communication systems. Dropping the restriction of orthogonal signature waveforms has two major consequences: (a) The users need not be synchronized; (b) A greater number of signatures can be assigned."

The two digital communication techniques TDMA and FDMA can be seen as a special cases of CDMA where the signatures waveforms are non-overlapping in the time domain and the frequency domain, respectively.

1.2. Spread spectrum system

We only consider direct sequence spread spectrum which employs a pseudonoise (PN) sequence to modulate the phase of the data. The alternatives, "frequency hopping", whereby the carrier frequency is shifted in a pseudorandom way is not discussed here. Direct-sequence spread spectrum was originally designed for single-user military communication systems to provide privacy (to demodulate the signal you need special information of the chip modulation sequence); low probability of intercept (the power spectral density of the transmitted signal is comparable to that of the ambient noise); and immunity to jamming interference.

One method of spreading the spectrum of a data-modulated signal is to modulate the signal a second time using a very wideband spreading signal (or PN code) (Figure 1.2). The second modulation usually takes the form of digital phase modulation. The spreading signal is chosen to have properties which facilitate demodulation of the transmitted signal by the intended receiver, and while making demodulation by unintended receiver as difficult as possible [4]. Typically, the different signature waveforms used in implementations of CDMA systems are constructed from pseudonoise (PN) sequences which can be easily generated by linear feedback shift-registers.

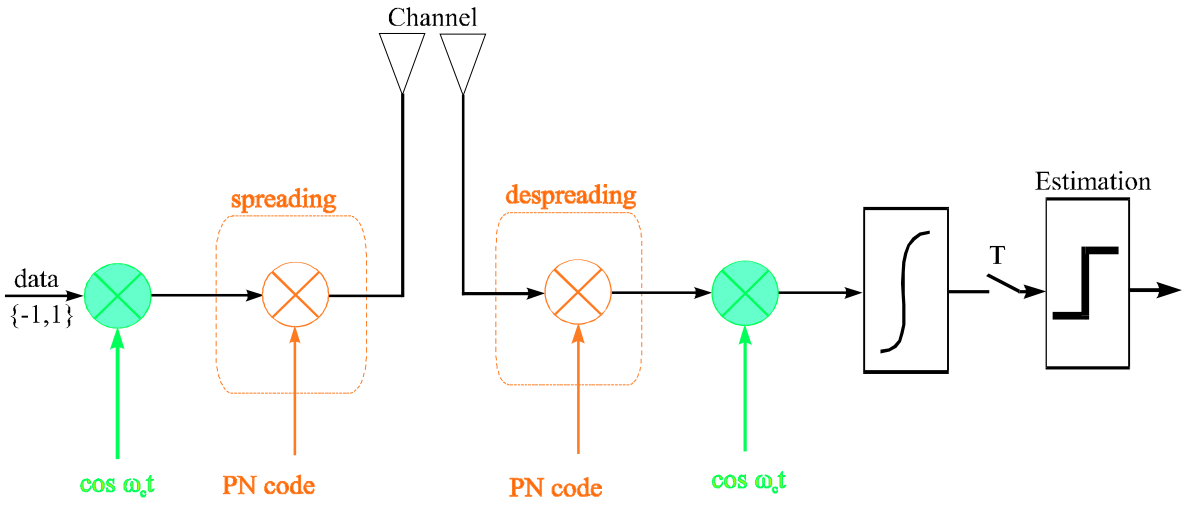

Figure 1.2 Direct sequence spread spectrum system

To demodulate a DSSS signal, it is shifted to baseband and correlates with a replica of the PN sequence used for transmission. Note that this requires that the transmitters maintain synchronization, so that their data bit epochs coincide.

In a spread spectrum system there are two modulations, (1/T) corresponding to the data modulation rate and ($1/T_c$) corresponding to the chip modulation rate, or the code rate. As illustrated in Figure 1.3, the transmission bandwidth ($1/T_c$) employed is much greater than the minimum bandwidth required to transmit the digital information (1/T). A definition of spread spectrum that reflects the characteristics of this technique is given by Pickholtz et *al.* in[1]:

> *"Spread spectrum is a means of transmission in which the signal occupies a bandwidth in excess of the minimum necessary to send the information, the band spread is accomplished by means of a code which is independent of the data, and a synchronized reception with the code at the receiver is used for despreading and subsequent data recovery."*

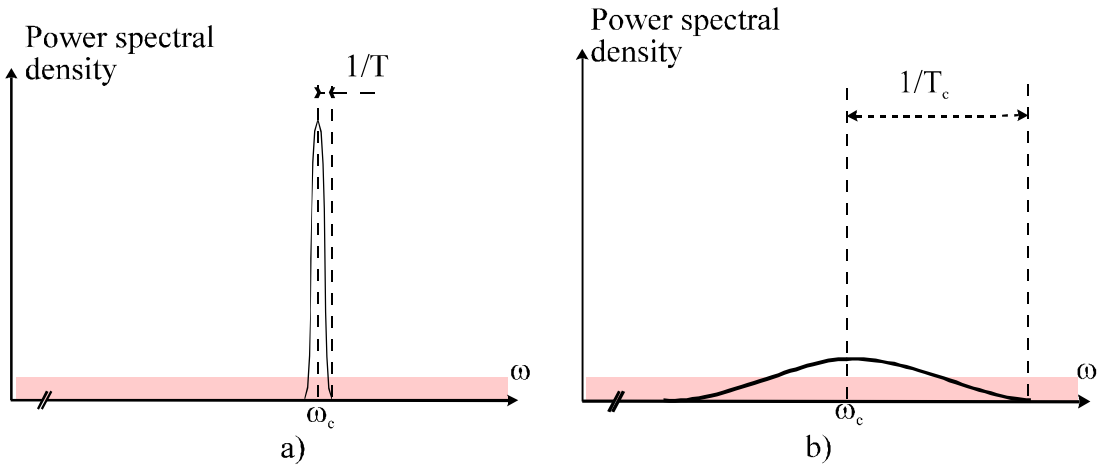

Figure 1.3 The signal power spectral density: a) before spreading, b) after spreading.

Figure 1.3 shows the power spectral density of the signal before and after spreading, where $N=T/T_c$ is the spreading gain, T is a bit period, T_c is a chip period, and ω_c is the carrier frequency. The shaded area represents additive white Gaussian noise (AWGN).

1.3. DS-CDMA

In the CDMA channel sharing strategy, each user is assigned a different signature waveform. We have seen in the last section that the orthogonality of signature waveforms is not necessary for reliable DS-CDMA communications. We replaced the requirement that the signature waveforms be orthogonal by the requirement that their mutual interference be tolerable. The signature waveforms or codes can be viewed as a vectors in the N-dimensional space. The cross-correlation between the vector codes measures the mutual interference between the signature waveforms. The cross-correlation between the codes is a very important parameter in the design and selection of codes. The PN codes sequences are usually generated by shift registers. Good autocorrelation properties means that PN sequences facilitate synchronization and are good choices for channels subject to multipath propagation, where it is important to be able to distinguish between delayed replicas of the signal [3]. We note also that the number of simultaneous users should not exceed a predetermined design parameter in order that the interference remains tolerable.

1.3.1. System mathematical model

We consider a K+1 users DS-CDMA system in an otherwise additive white Gaussian noise channel. The received signal r(t) is expressed as a function of the multiple access data SS signal $S_t(\mathbf{b})$, and the channel noise N_t

$$r(t) = S_t(\mathbf{b}) + N_t \tag{1}$$

where $N_t = \sigma\, n(t)$ is a zero mean additive white Gaussian noise (AWGN) process with power spectral density σ^2, and the baseband synchronous multiple access data DS/CDMA signal coming from the K+1 CDMA users is

$$S_t(\mathbf{b}) = w_0 \sum_{i=-M}^{M} \left\{ \mathbf{b}(0,i)s_0(t-iT) + \sum_{k=1}^{K} w_k \left(\sum_{i=-M}^{M} \mathbf{b}(k,i)s_k(t-iT) \right) \right\} \tag{2}$$

where a user $k \in \{0,1,..K+1\}$ is assigned a unit energy signature waveform $s_k(t)$, which is zero outside the interval [0,T], where T is the information bit interval, assumed to be equal for all users, the matrix $\mathbf{b}[(K+1)x(2M+1)]$ is the information bit sequences of the several users, 2M+1 is the bit sequence length, w_k is the energy, and $\mathbf{b}(k,i) \in \{-1, 1\}$ is the i^{th} bit of the k^{th} user. The carrier frequency is denoted by ω_c.

The signature waveform $s_k(t)$ of the k^{th} user, $k \in \{0, 1,..K\}$ is given by

$$s_k(t) = \sum_{j=0}^{N-1} a_k(j)\Pi(t - jT_c)$$

where $a_k(j) \in \{-1,1\}$ is the j^{th} element of the spreading sequence user k, N is the processing gain, $T_c=T/N$ is the chip duration, and $\Pi(t)$ is the rectangular chip waveform with duration T_c.. The transmitted bits are assumed mutually independent, and they are also independent of the Gaussian channel noise. In such a scenario, the received signal includes contributions from CDMA users, narrowband users, and Gaussian noise. The narrowband interference can be, analog or digital. In chapters 2, 3, and 4 we will study different cancellation methods for digital narrowband interference.

1.3.2. System geometric model

In order to describe the channel geometrically, we switch from a continuous time model to a discrete time model. We assume the received signal is passed through a filter matched to the chip waveform and is then chip-synchronously sampled once during each chip interval (Figure 1.4). The result of this manipulation is the discrete time received signal r_i.

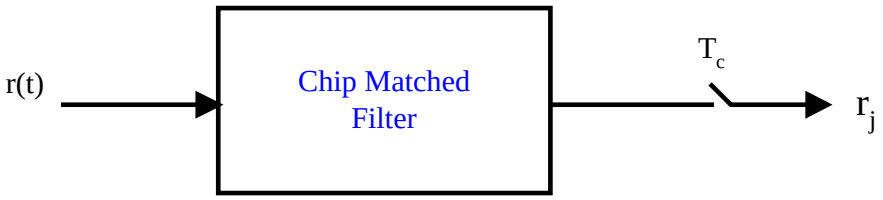

4

The sample r_j is the sum of the contributions of all the active CDMA users sharing the channel plus the AWGN contribution. We examine the synchronous channel, where the observation vector =$[r_0,r_1,..,r_{N-1}]$ relative to one bit interval is

$$\mathbf{r} = \pm\sqrt{w_0}\mathbf{s}_0 + \sum_{k=1}^{K+1} b_k\sqrt{w_k}\mathbf{s}_k + \sigma\mathbf{n} \qquad (3)$$

The discrete time received signal will have a component due to the desired user plus components due to each k^{th} spread spectrum signal $\sqrt{w_k}\mathbf{s}_k$ times the bit value b_k, and the ambient white noise σ . Note that for the asynchronous channel, additional cross-correlations occur which are time-variant, and the geometric interpretation is much more difficult to visualize.

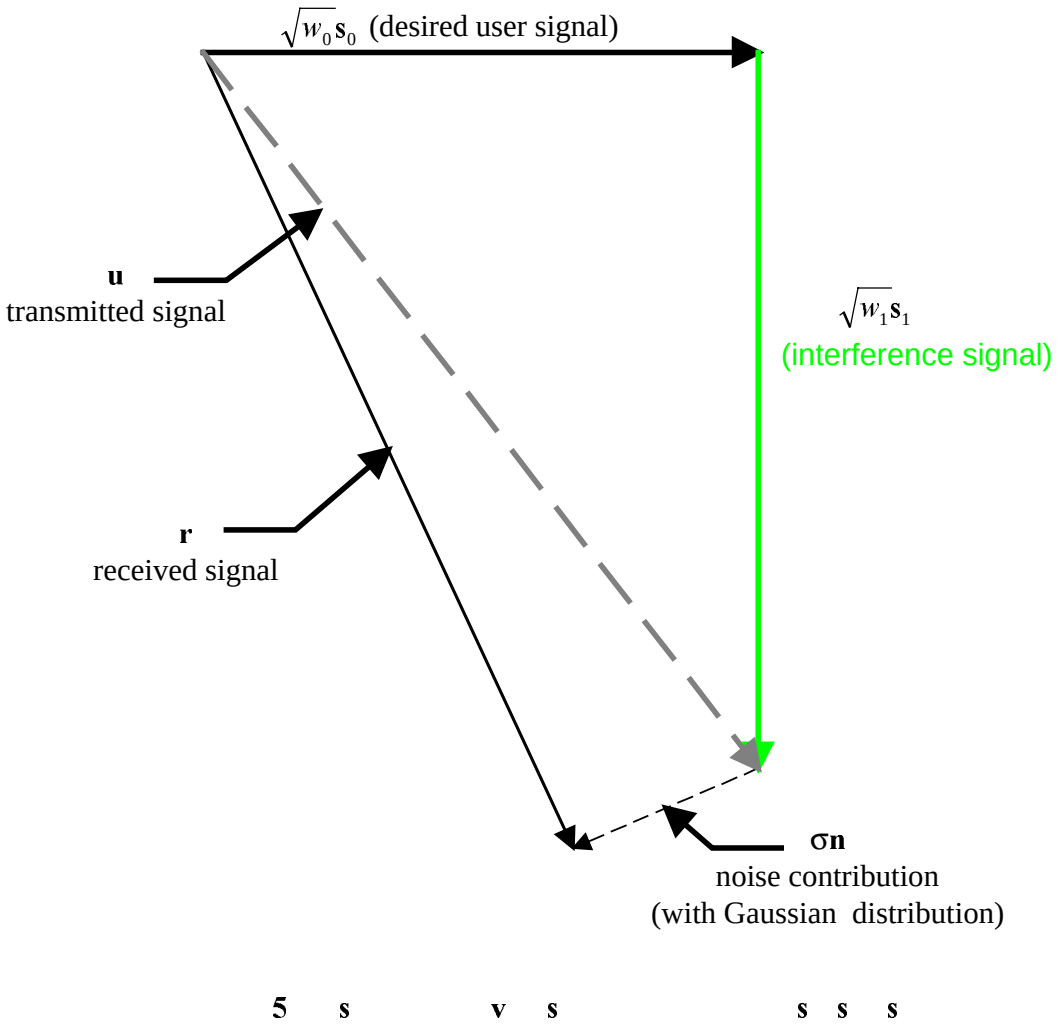

5 s v s s s s

Figure 1.5 describes the geometric interpretation of the discrete time system with two users in AWGN. The transmitted signal is represented by the vector ; this is the sum of two vectors $b_0\sqrt{w_0}\mathbf{s}_0$ and $b_1\sqrt{w_1}\mathbf{s}_1$ representing user zero and user one for the particular bit values b_0=1 and b_1=-1. The vector σ represents the AWGN contribution. To be precise, σ is the component of the AWGN realization which falls in the plane described by $\mathbf{s}_0$ and $\mathbf{s}_1$. The direction of the noise realization is uniformly distributed, while the amplitude has a Gaussian distribution. The vector represents the entire received signal including the noise contribution and the transmitted signal. We interpret each linear detector in the following sections as a vector in the space of N dimensions, (N is the length of the signature sequences) and the despreading operation as an inner product between the received signal vector and the detector vector.

1.4. Performance measures:

There are several common performance measures in multiuser detection [2]. The main performance measure is the bit error rate. Other measures are motivated in the analysis and design of various detectors. Clearly, the presence of more than one user in an AWGN channel will increase the bit error rate to each user. We define the of user j, $_j(\sigma)$, as the energy that user j requires to achieve a bit error rate equal to that of a single-user Gaussian channel with the same background noise level σ.

We define the as the ratio between the effective and actual energies; it quantifies the performance loss (in dB) due to the existence of other users in the channel. The measures the slope with which the logarithm of the probability of error decreases to zero as the signal to noise ratio increases.

In some multiuser channels the received users' powers can be different. This happens for example when the users are placed at different distances from the receiver. Naturally, the stronger users are easier to detect than the others. In this situation a strong interference can seriously disturb a desired user with weaker power. This is known as the near-far problem. The of a detector quantifies the degree of robustness against the near far problem. The near far resistance is defined as the minimum asymptotic efficiency over all possible relative energies of the other users. We will measure the performance of the conventional detector with these parameters in the following section.

1.5. Multiuser detectors

For the synchronous channel, observation of the received waveform in isolated symbol intervals is a sufficient statistic for that symbol decision. For asynchronous signals, observation of sequences of symbols is required as overlapping symbols of the other users gives additional information about the received signal. Any reduction in the observation interval leads to suboptimal bit decision. We examine only the synchronous case, in order to

introduce several interesting receivers. In most cases these receivers can be generalized to the asynchronous case [2].

1.5.1. Conventional detector:

The matched filter is the simplest strategy to demodulate CDMA signals. This demodulator was the first adopted in the implementation of CDMA systems. Thus, it is referred to also as the conventional receiver. The conventional receiver correlates the received signal with a replica of the spreading code to despread the signal and recover the data.

1.5.1.1. Single-user conventional detector

We consider first a single-user white Gaussian noise channel with binary phase shift keying (BPSK) modulation

$$r(t) = \sqrt{w_0}\, b_0 s_0(t) + \sigma\, n(t) \qquad (4)$$

where $s_0(t)$ is a signature waveform assigned to user zero, with amplitude $\sqrt{w_0}$, bit value $b_0 \in \{-1,+1\}$, n(t) is a unit spectral density, white zero-mean Gaussian noise, and σ^2 is the channel noise spectral density.

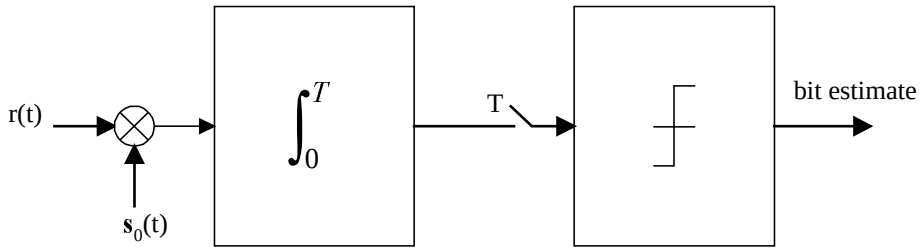

6 S - s v

The optimal receiver for a binary signal in AWGN is the matched filter, as seen in figure 1.6. The error probability of the matched filter is as follows:

$$\text{Prob}\left[b_0 \neq \hat{b}_0\right] = \text{Prob}\left[b_0 = +1\right]\text{Prob}\left[y_0 < 0 / b_0 = 1\right] + \text{Prob}\left[b_0 = -1\right]\text{Prob}\left[y_0 > 0 / b_0 = -1\right]$$

$$= \frac{1}{2}\text{Prob}\left[y_0 < 0 / b_0 = 1\right] + \frac{1}{2}\text{Prob}\left[y_0 > 0 / b_0 = -1\right]$$

by symmetry

$$\text{Prob}\left[\text{b}_0 \neq \hat{\text{b}}_0\right] = \text{Prob}\left[\text{y}_0 < 0 / \text{b}_0 = +1\right]$$

We let Q be the complementary cumulative distribution function of the unit normal random variable

$$\text{Q}(\text{x}) = \int_{\text{x}}^{\infty} \frac{1}{\sqrt{2\pi}} \text{e}^{-\frac{\text{t}^2}{2}} \text{dt}$$

We then find the probability of error for CDMA single-user channel is

$$\text{p}_0(\sigma) = \text{Prob}\left[\text{b}_0 \neq \hat{\text{b}}_0\right] = \text{Q}\left(\frac{\sqrt{\text{w}_0}}{\sigma}\right) \tag{5}$$

1.5.1.2. The multiuser conventional detector

In the multiple access systems, the conventional receiver which demodulates each and every user is simply a bank of independent conventional receivers (Figure 1.7). When all the signatures are orthogonal, the conventional receiver is optimal, in fact, all the users are transparent one another. In practice, however, orthogonality is lost with random delays between users. Therefore, the question of interest is how to demodulate the transmitted messages when the assigned signatures are not orthogonal.

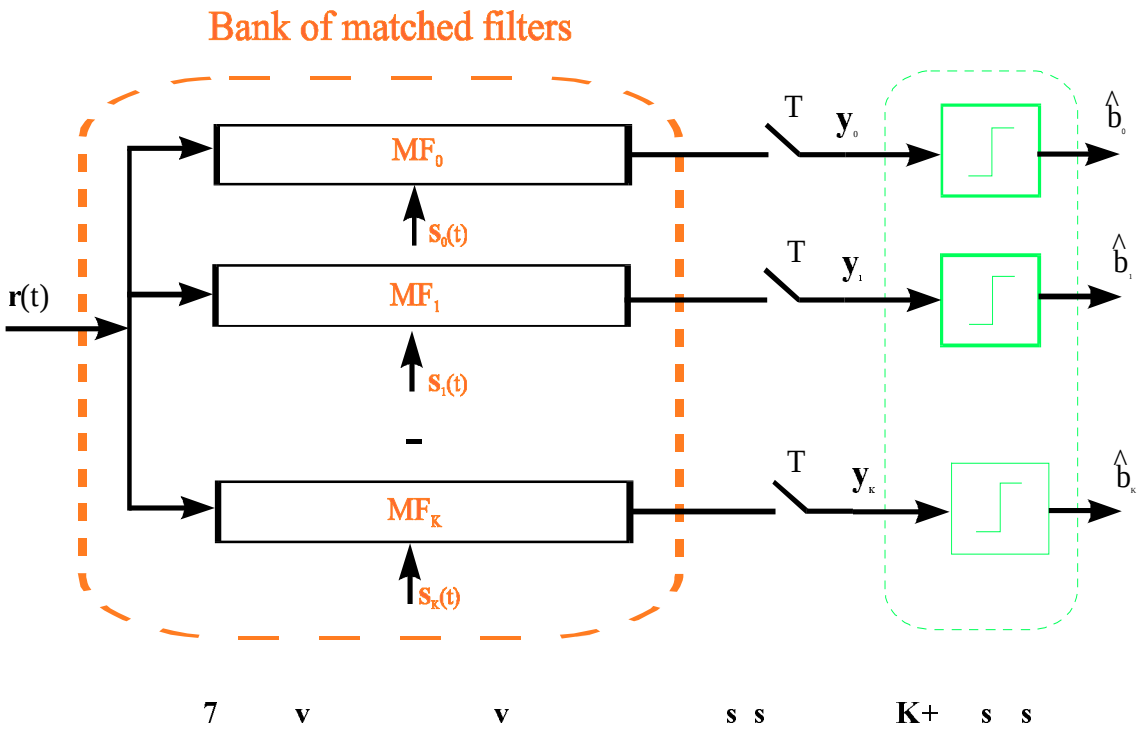

7 v v s s K+ s s

The matched filter output for user zero in Figure 1.7 is equal to

$$y_0 = \int_0^T r(t)s_0(t)dt = \sqrt{w_0}b_0 + \sum_{k=1}^{K}\sqrt{w_k}b_k\rho_{0k} + \sigma n_0 \qquad (6)$$

where $\rho_{0k} = \int_0^T s_k(t)s_0(t)dt$ (k≠0) is the cross-correlation coefficient, and n_0 is a Gaussian random variable with zero mean and power spectral density equal to σ^2. Thus, in general each matched filter output has a component due to the cross correlation with the signals of the other users, which is called multiple access interference (MAI).

Acceptable performance of the system will require that the MAI and AWGN be small relative compared to the desired user's signal. To study the effect of multiple access interference on the performance of the single-user conventional receiver, we focus especially on the two-user case.

The probability of error

The probability of error for user zero [2] is

$$P_e = \Pr ob\left[b_0 \neq \hat{b}_0\right] = \frac{1}{2}Q\left(\frac{\sqrt{w_1} - \sqrt{w_0}\rho_{10}}{\sigma}\right) + \frac{1}{2}Q\left(\frac{\sqrt{w_1} + \sqrt{w_0}\rho_{10}}{\sigma}\right) \qquad (7)$$

It has been shown that if the relation $\sqrt{w_1 / w_0} > 1/|\rho_{10}|$ holds, the conventional receiver exhibits extremely poor performance. To achieve acceptable performance, the cross-correlation's between the signals must be kept to a low level. One way to achieve low cross-correlation is to choose a very long spreading sequence. When the power of any of the interfering users is dominant, performance degradation will occur nonetheless. This is known as the near-far effect. It is interesting to note that most commercial systems using multiuser CDMA techniques employ the conventional detector. To avoid the near far problem they use power control. Power control strives to provide similar power among all channel users at the base station receiver. Basically, they amplify the weak users' signals and/or attenuate the strong users' signals.

To summarize, when the channel output is corrupted by additive white Gaussian noise, the conventional single-user receiver is only optimal in the absence of interfering users. This is the reason for the emergence of multiuser detection theory. In the following section we will explain the basic elements of the optimum multiuser detector proposed by Verdù [7].

1.5.2. Optimum multiuser detector:

Verdù [7] found that the optimum multiuser detector is a maximum-likelihood sequence detector consisting of a bank of single-user matched filters followed by a Viterbi algorithm (Figure 1.8)

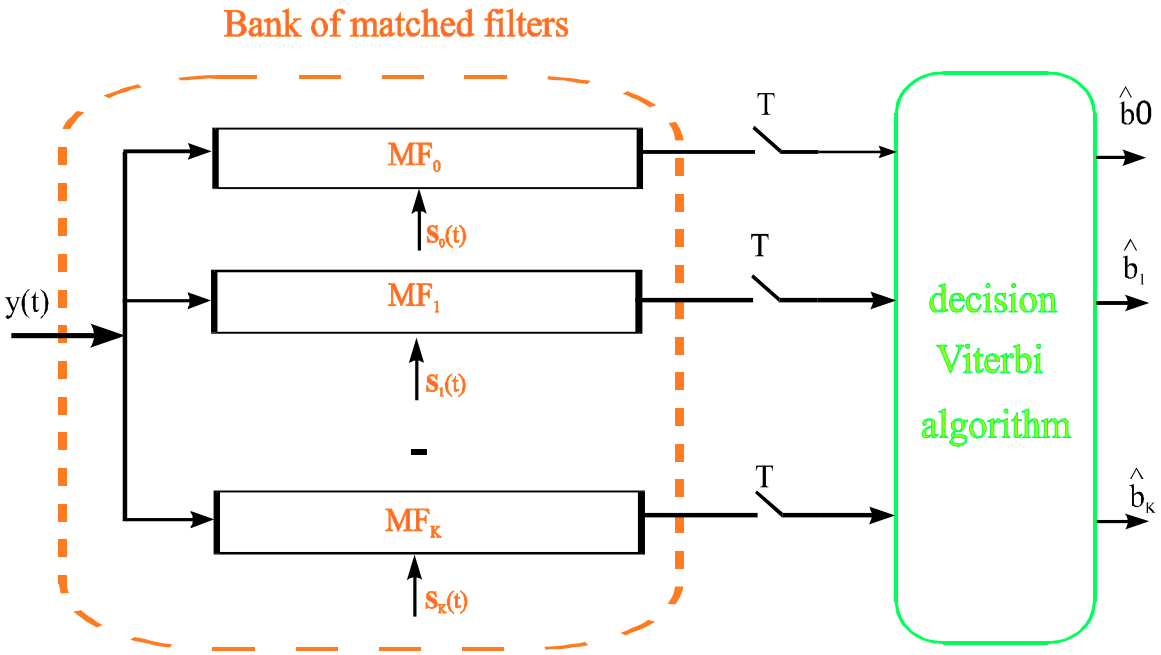

8 O v

The optimum detector affords important performance gains over the conventional single-user detector, including resolution of the near far problem. However, the detector is exponentially complex in the number of users, making implementation problematic. The optimum receiver also requires knowledge of the received energies. In the following section we investigate low-complexity multiuser detection strategies with performance that approaches that of the optimum detector [8-12].

1.5.3. Decorrelating detector

It is of interest to explore whether there are multiuser demodulators that are more economical to implement than the optimum detector while retaining similar performance. Consider the synchronous case where the outputs of a bank of matched filters are given by

$$y_k = \int_0^T r(t)s_k(t)dt \text{, for } k = 0,\ldots K \qquad (8)$$

The vector $\mathbf{y} = (y_0, y_1, \ldots y_K)$ forms a sufficient statistic for demodulating $\mathbf{b} = (b_0, b_1, \ldots b_K)$. The matched filter bank outputs can be presented compactly as

$$\mathbf{y} = \mathbf{R}\mathbf{w}^{\frac{1}{2}}\mathbf{b} + \mathbf{n} \tag{9}$$

where $\mathbf{R}$ is the nonnegative definite correlation matrix between the assigned signature waveforms defined by $(\mathbf{R})_{ij} = \int_0^T s_i(t)s_j(t)dt$. W is the diagonal matrix of the received energy, $\mathbf{w}^{\frac{1}{2}} = \text{diag}\left[\sqrt{w_0}, \sqrt{w_1}, .., \sqrt{w_m}\right]$, and is a zero-mean Gaussian m-vector with covariance matrix equal to σ^2 . As an intuitive motivation for the decorrelating detector consider that in the absence of noise, the matched filter output vector is

$$\mathbf{y} = \mathbf{R}\mathbf{w}^{\frac{1}{2}}\mathbf{b} \tag{10}$$

Thus if the signals are linearly independent (invertible), the natural strategy to follow in this hypothetical situation is

$$\hat{\mathbf{b}} = \text{sgn}\left(\mathbf{w}^{-\frac{1}{2}}\mathbf{R}^{-1}\mathbf{y} \right) \tag{11}$$

Note that the noise components in $\mathbf{R}^{-1}\mathbf{y}$ are correlated, and therefore $\mathbf{R}^{-1}\mathbf{y}$ does not result in optimum decisions when noise is present. With a simple mathematical manipulation below we point out that this detector does not require knowledge of the energies of any of the active users

$$\text{sgn}\,\mathbf{R}^{-1}\mathbf{y} = \text{sgn}\,\mathbf{w}^{\frac{1}{2}}\,\hat{\mathbf{b}}$$

which means that (since the entries of $\mathbf{w}^{\frac{1}{2}}$ are nonnegative) in the absence of noise

$$\hat{\mathbf{b}} = \text{sgn}\,\mathbf{R}^{-1}\mathbf{y} \tag{12}$$

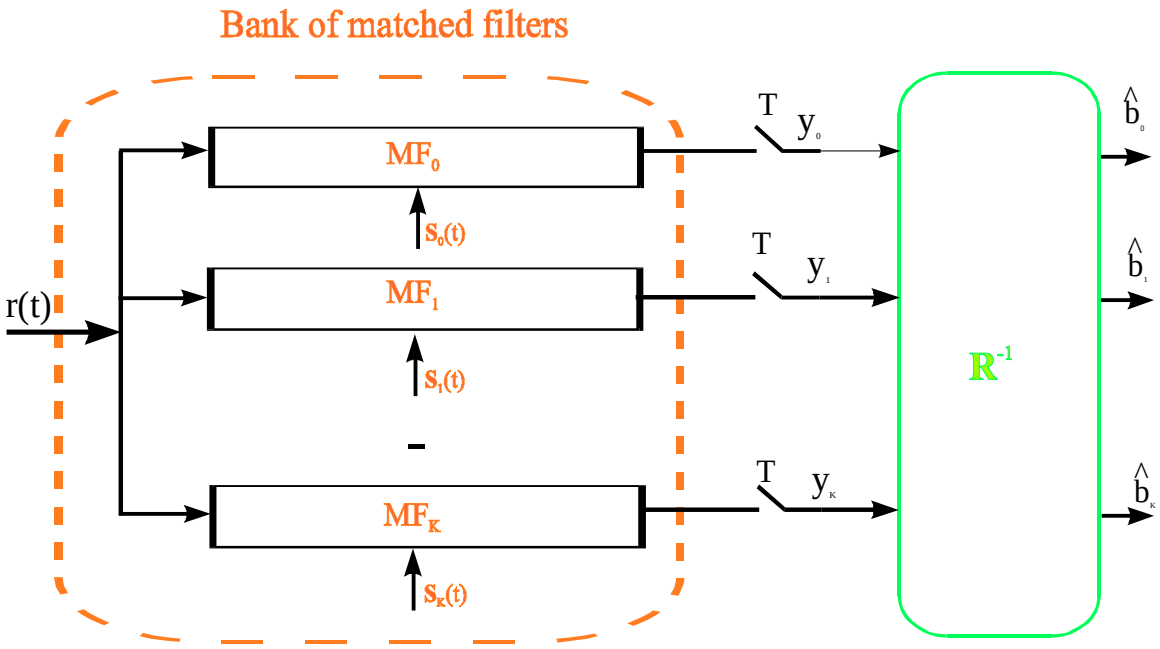

9

The decorrelating detector estimates the data bits by multiplying the vector of matched filter outputs by the inverse of the cross-correlation matrix **R**. The detector is a solution to the generalized likelihood ratio test or maximum likelihood detector when the energies are not known by the receiver [10]. This detector selects the decisions that maximize the maximum likelihood function over the unknown parameters,

$$\begin{aligned}\hat{\mathbf{b}} &= \arg \min_{\mathbf{b}\in\{-1,1\}^{K+1}} \min_{\substack{w_k\in[0,+\infty)\\ k=0,\ldots,K}} \int_0^T \left(r(t) - \sum_{i=1}^{K} \sqrt{w_i}\, b_i s_i(t) \right)^2 dt \\ &= \arg \min_{\mathbf{b}\in\{-1,1\}^{K+1}} \min_{\substack{w_k\in[0,+\infty)\\ k=0,\ldots,K}} \left\{ \mathbf{y}^T \mathbf{w}^{-\frac{1}{2}} \mathbf{R}^{-1} \mathbf{w}^{-\frac{1}{2}} \mathbf{y} + \mathbf{b}^T \mathbf{w}^{-\frac{1}{2}} \mathbf{R}^{-1} \mathbf{w}^{-\frac{1}{2}} \mathbf{b} - 2\mathbf{b}^T \mathbf{y} \right\}\end{aligned} \tag{13}$$

The first term is a non-negative and independent for the data bits values, thus we can eliminate it from the minimization. Let $\mathbf{x} = \mathbf{w}^{\frac{1}{2}}\mathbf{b}$, transforming the two minimizations to one minimization over an N-fold real vector. The minimization of this above equation is equivalent to selecting the bits that minimize the following expression

$$\min_{\mathbf{x}\in\{-\infty,+\infty\}^N} \mathbf{x}^T\mathbf{R}\,\mathbf{x} - 2\mathbf{x}\mathbf{w}^{-\frac{1}{2}}\mathbf{y}$$

If the cross-correlation matrix **R** is invertible, the solution to the above equation is

$$\mathbf{x} = \mathbf{R}^{-1}\mathbf{w}^{-\frac{1}{2}}\mathbf{y}$$

and the most likely bits are given by

$$\hat{\mathbf{b}} = \operatorname{sgn}\mathbf{x} = \operatorname{sgn}\mathbf{R}^{-1}\mathbf{y}$$

Note that this form is very practical if only one user need be demodulated. Instead of matched filtering the incoming signal with the signature waveform of the k^{th} user $s_k(t)$, we use a matched filter for the k^{th} line of the inverse cross correlation matrix $\mathbf{R}^{-1}$

$$\mathbf{c}_k = \left[\left(\mathbf{R}^{-1}\right)_{0k}, \left(\mathbf{R}^{-1}\right)_{1k}, \ldots \left(\mathbf{R}^{-1}\right)_{Kk}\right]$$

and the bit estimate is

$$\hat{b}_k = \operatorname{sgn}\left(\left\langle \mathbf{c}_k, \mathbf{y}_k \right\rangle\right)$$

where < , > denotes the inner product between a given two vectors and Consider the two user case, that is, one interferer in the system. The decorrelating detector can be expressed as

$$\mathbf{c}_k = \mathbf{s}_0 - \rho_{10}\mathbf{s}_1 \tag{14}$$

Figure 1.10 shows that the decorrelating detector can be expressed as the component of $_0$ which is orthogonal to the interference subspace. This is because the decorrelating detector is the projection of the signature of the desired user onto the space orthogonal to the space spanned by the interfering users. Figure 1.10. a) shows the simple two users case, while the b) presents the most general scenario.

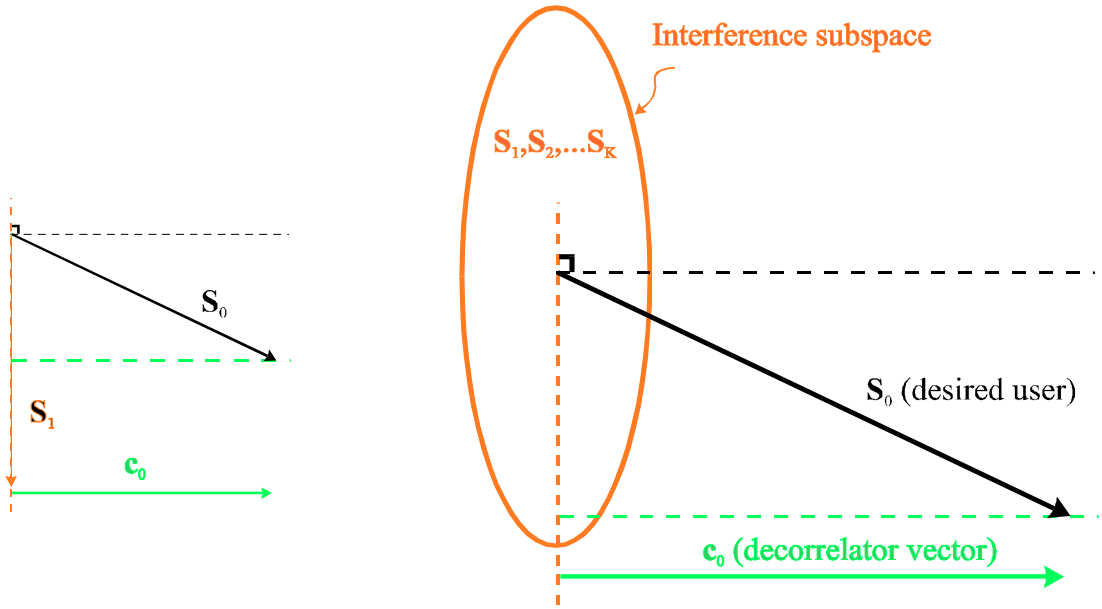

a) b)

0

The dimension of the interference subspace is equal to the number of interferers in the channel. Thus, the decorrelation operation is equivalent to a single user channel with a higher noise power level. The decorrelating detector eliminates multiaccess interference at the expense of a degradation in the signal to noise ratio. The decorrelating detector requires knowledge of signatures for all active users, but does not require the received energies.

1.5.4. Minimum mean square error detector (MMSE)

As described earlier, the decorrelating detector tunes out the interference at the expense of a smaller projection of the signal of interest, or equivalently, the noise variance at the output of the filter is enhanced. This situation can be improved if the received energies are known. For this reason, another multiuser detector was developed which provides a trade-off between suppression of the multiuser interference and noise enhancement. This detector estimates the bit value via the following linear transformation determined by Madhow and Honig [12]

$$\hat{b} = \mathrm{sgn}\left(\left(\mathbf{R} + \sigma^2 I_{K+1}\right)^{-1}\mathbf{y}\right) \tag{15}$$

The estimate minimizes the mean square error $E\left\{(\mathbf{b}-\mathbf{M}\mathbf{y})^T(\mathbf{b}-\mathbf{M}\mathbf{y})\right\}$ over all nonnegative definite matrices with dimension N. When $\sigma \to 0$ this detector reduces to the decorrelating detector.

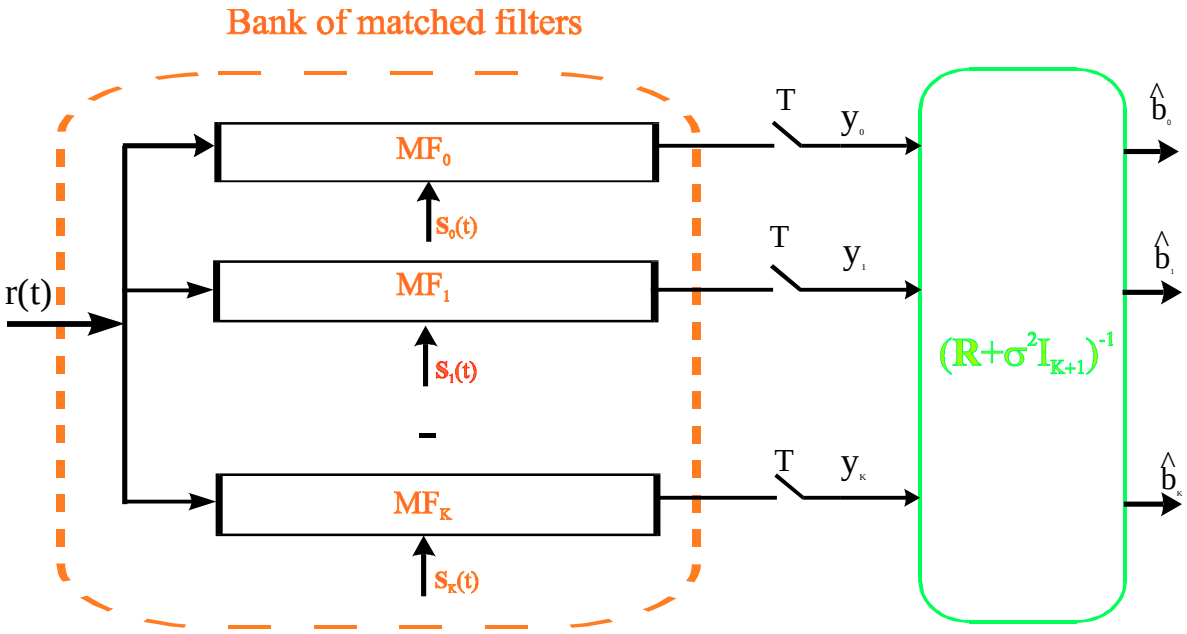

(E

We find an alternative derivation of the MMSE receiver in [13]. The authors rewrite the matched filters output as

$$\begin{aligned}\mathbf{y} &= \mathbf{R}\mathbf{w}^{\frac{1}{2}}\mathbf{b} + \mathbf{n} \\ &= \mathbf{R}\mathbf{x} + \mathbf{n}\end{aligned}$$

The random vector **x** and noise vector **n** are statistically independent. A new random vector can be defined by combination of **x** and **n**; we define

$$\mathbf{v} = \begin{bmatrix}\mathbf{x}\\ \mathbf{y}\end{bmatrix} = \begin{bmatrix}\mathbf{w}^{\frac{1}{2}}\mathbf{b}\\ \mathbf{y}\end{bmatrix} = \begin{bmatrix}\mathbf{w}^{\frac{1}{2}} & \mathbf{0}\\ \mathbf{R}\mathbf{w}^{\frac{1}{2}} & \mathbf{I}\end{bmatrix}\begin{bmatrix}\mathbf{b}\\ \mathbf{n}\end{bmatrix} = \mathbf{H}\begin{bmatrix}\mathbf{b}\\ \mathbf{n}\end{bmatrix}$$

The expectation and the covariance matrix of the new vector , can be easily derived

$$\mathrm{E}(\mathbf{v}) = \mathbf{0}$$

and eventually the covariance matrix is

$$\begin{aligned}\mathrm{cov}(\mathbf{v}) &= \mathbf{H}\,\mathrm{cov}\left(\begin{bmatrix}\mathbf{b}\\ \mathbf{n}\end{bmatrix}\right)\mathbf{H}^{\mathrm{T}} \\ &= \begin{bmatrix}\mathbf{w} & \mathbf{wR}\\ \mathbf{Rw} & \mathbf{RwR}+\sigma^2\mathbf{R}\end{bmatrix} = \begin{bmatrix}\sum_{\mathbf{xx}} & \sum_{\mathbf{xy}}\\ \sum_{\mathbf{yx}} & \sum_{\mathbf{yy}}\end{bmatrix}\end{aligned}$$

$\hat{\mathbf{x}}_{\mathrm{mmse}}$ can be directly calculated

$$\begin{aligned}\hat{\mathbf{x}}_{\mathrm{MMSE}} &= \mathrm{E}(\mathrm{x}) + \sum_{\mathbf{xy}} \sum_{\mathbf{yy}}^{-1} \left(\mathbf{y} - \mathrm{E}(\mathbf{y})\right) \\ &= \sum_{\mathbf{xy}} \sum_{\mathbf{yy}}^{-1} \left(\mathbf{y} - \mathrm{E}(\mathbf{y})\right)\end{aligned}$$

we arrive at

$$\hat{\mathbf{x}}_{\mathrm{MMSE}} = \left(\mathbf{R} + \sigma^2\mathbf{w}^{-\frac{1}{2}}\right)^{-1}\mathbf{y}$$

An implantation of the MMSE detector requires the knowledge of the signatures waveforms, as well as the received powers for all the active users sharing the channel. When only one user need be detected a simple implementation of the MMSE is possible. As is done for the decorrelating detector, we match filter the incoming signal with the kth line of the inverse matrix

$$\left(\mathbf{R} + \sigma^2\mathbf{w}^{-\frac{1}{2}}\right)^{-1}$$

to decode user k.

1.5.5. Adaptive MMSE multiuser detector

The modified matched filter structures of linear multiuser detectors (such as the decorrelating detector and the MMSE detector) are attractive in the simplicity of their

implementation. However, these detectors require the knowledge of the signature waveforms (and the received energies in the case of the MMSE detector).

In a practical channel, the cross-correlation and the received energies are time-varying, thus, it is important to find a detector that does not require this information. This goal can be accomplished with an adaptive implementation of the MMSE linear detector [12]. In practice, the adaptive MMSE detector requires the transmission of a training sequence, ., a bit sequence known by the receiver, prior to the transmission of the real information bit sequence. If the channel is such that the cross-correlation and amplitudes vary over time, training sequences must be sent periodically to readjust the receiver. The adaptation rule for the MMSE linear detector is based on the gradient descent stochastic algorithm. This stochastic algorithm (also known as the Newton algorithm) minimizes any convex function.

As we saw in section 5.4, the MMSE linear detector for user zero correlates $_0$ with the sampled received waveform . Let $_0$ minimizes the following expression over all possible linear detectors .

$$\mathrm{E}\left[\left(\sqrt{w_0}b_0 - < \mathbf{c}, \mathbf{r} >\right)^2\right] \tag{16}$$

This is a convex function, where < , > denotes the inner product between a given two vectors and . To specify the gradient descent algorithm used to find the minimum, we first obtain the gradient of $\left(\sqrt{w_0}b_0 - < \mathbf{c}, \mathbf{r} >\right)^2$ with respect to **c**, which is equal to $2\left(\sqrt{w_0}b_0 - < \mathbf{c}, \mathbf{r} >\right)\mathbf{r}$. The adaptive algorithm for bit interval i is

$$\mathbf{c}[i] = \mathbf{c}[i-1] - \mu\left(< \mathbf{c}[i-1], \mathbf{r}[i] > - b_0[i]\right)\mathbf{r}(i) \tag{17}$$

where μ is the convergence step size of the algorithm. Therefore, the update of the impulse response is equal to the received waveform times the error between the known data and the filter output.

Note that the algorithm requires no knowledge of the signature waveforms (not even that of the desired user) or of the received amplitudes. To conclude, the MMSE linear detector is the minimum of a convex function which can be obtained adaptively when a training sequence is available.

1.5.6. Blind Adaptive multiuser detector

The typical operation of the adaptive MMSE detector (section 1.5.5) requires each transmitter to send a training sequence at start-up, which the receiver then uses for initial adaptation. After transmission of the known training sequence, the unknown information bit sequence is transmitted. Any time there is a drastic change in the interference environment, the detector becomes unreliable, and data transmission of the desired user must be temporarily suspended and yield to a fresh training sequence. Honig, Madhow, and Verdù [14] succeed in deriving an algorithm that requires only the spreading code of the desired user (as does the conventional single user detector). We introduce the following canonical representation for a linear detector of user zero:

$$\mathbf{c}_0 = {}_0 + {}_0 \tag{18}$$

where $< {}_0, {}_0>=0$, and $< \mathbf{c}_0, \mathbf{s}_0 >= \|\mathbf{s}_0\|^2 = 1$. $\|\mathbf{u}\|$ is the module of the vector $\mathbf{u}$.

The mean output energy, or MOE, is defined as the mean square output value of this linear detector

$$\mathrm{MOE}(\mathbf{x}_0) = \mathrm{E}\left[< \mathbf{s}_0 + \mathbf{x}_0, \mathbf{r} >^2\right] \tag{19}$$

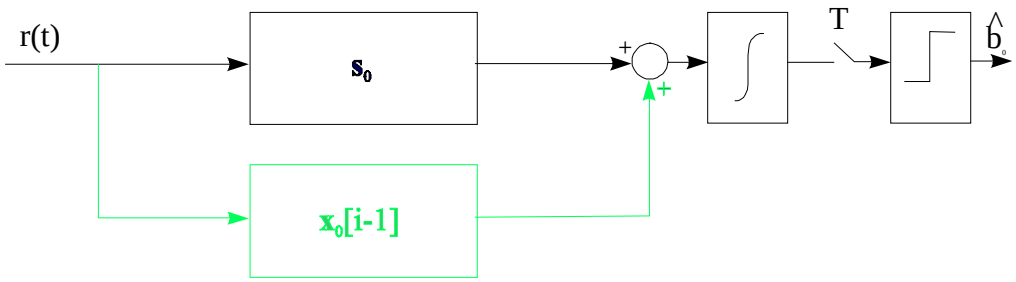

u **B**

The mean square error at the output is

$$\mathrm{MSE}(\mathbf{x}_0) = \mathrm{E}\left[\left(\sqrt{w_0}b_0 - < \mathbf{s}_0 + \mathbf{x}_0, \mathbf{y} >\right)^2\right] = \mathrm{MOE} - w_0 \tag{20}$$

The MSE and the MOE differ by a constant, so that the detector which minimizes the MSE necessarily minimizes the MOE as well. MOE($\mathbf{x}_0$) is a strictly convex function over the set of signals orthogonal to $\mathbf{s}_0$, thus, the MOE lends itself to a simple stochastic gradient descent adaptation rule. The minimization problem of the MOE ($\mathbf{x}_0$) is solved analogously to the minimization of section 1.5.5. The blind adaptation algorithm is formed by the following equations

$$\mathbf{x}_0[0] = 0\,;$$

$$\mathbf{x}_0[n] = \mathbf{x}_0[n-1] - \mu\, z[n](\mathbf{y}[n] - z_{MF}[n]\mathbf{s}_0)\,;$$

and $\mathbf{c}[n] = \mathbf{s}_0 + \mathbf{x}_0[n]$;

where $z_{MF}[n] = < \mathbf{s}_0, \mathbf{y}[n] >$, is the matched filter output; and $z[n] = < \mathbf{s}_0 + \mathbf{x}_0[n-1], \mathbf{y}[n] >$ the blind detector output. The blind detector decision output is

$$\hat{b}_0 = \mathrm{sgn}(z[n]) \tag{21}$$

In chapter 3, we apply this blind adaptive detector to suppression of a digital narrowband interferer.

Narrowband interference suppression in DSSS/CDMA communications

In chapter one we introduced spread spectrum systems and several receiver types for both single user and multiple user systems. In this chapter we describe how such systems are affected by the presence of a narrowband interferer. In section 2.1 we describe how this situation arises. In sections 2.2 - 2.4 we discuss previous methods to mitigate the narrowband interference problem, with section 2.2 concerning linear predictive measures, 2.3 nonlinear predictive measures and multiuser detection techniques. Finally, in section 2.5 we introduce a new multiuser receiver to combat narrowband interference, the MMSE detector. In Chapters three and four we present an adaptive version of this receiver.

2.1. Narrowband interference problem

Because of the growing demand for mobile radio and personal communications services, it has been suggested that personal communications networks (PCN) be established in the 1850-1990 MHz range [17]. However, that band of frequencies is currently occupied by various microwave signals transmitted by users ranging from utility companies to state and local agencies. In order to allow both sets of users to occupy these frequencies, as well as improve the spectral efficiency of this band, a spread-spectrum overlay is proposed, whereby a code-division multiple access personal communication networks (PCN) would share the spectral band with the existing narrowband microwave traffic.

We note that spread spectrum communication is inherently resistant to the narrowband interference (NBI) caused by coexistence with the pre-existing, licensed communications. At reception, the despreading operation of Figure 1.3 in effect spreads the narrowband signal across a large bandwidth, while the spread spectrum signal is despread and collapses back to its original data bandwidth. It is interesting to note that after despreading the situation is reversed between the original narrowband interferer (now wideband), and the original data signal (now narrowband). This process is illustrated in the Figure 2.1. A bandpass filter can be employed at the receiver so that only the interferer power that falls in the bandwidth of the despread signal causes any interference. Only a fraction, one over the spreading gain, of the original narrowband interference contributes to receiver noise. At times the interfering signal is powerful enough so that despite this attenuation by spreading the spectrum, communication is still impaired.

Milstein et al. [17] describe the results of several field tests which have been designed to demonstrate the feasibility of overlaying new mobile systems on existing band occupants, relieving the demand for new allocations. Traditional approaches to frequency allocation are based on standard processing techniques that work well only for moderate signal to noise ratio (SNR). In [21] the authors demonstrate that spread-spectrum users can share a frequency band with conventional microwave-radio users without one group

interfering with the other thereby increasing the efficiency with which the band is used. For example, mobile cellular telephone systems, already feeling a capacity squeeze in some areas, will be able to accept many more new customers. From [15]

> *"Initial field tests have already been performed in Houston Orlando, San Diego, and New York by Millicom, Inc., LOCATE, Inc,, and COX Inc., using broadband CDMA equipment developed by SCS Mobilecom, Inc.. These equipment had the following as fundamental goals.*
>
> *a) verify that the spread-spectrum overlay would not cause excessive interference to collocated fixed-service microwave signals.*
>
> *b) verify that PCN users can operate effectively in the presence of the interference produced by the fixed-service microwave signals.*
>
> *c) confirm the basic design philosophy of the PCN system, wherein handsets operating at an effective radiated power of 100 μ W are communicating with base stations in cells having a 183 m radios in congested areas″ .*

It is shown in [15] that the amount of interference that the CDMA network imposes upon the overlaid microwave signals must be such that they cause no more than 1dB degradation in the output signal-to-noise ratio of the microwave receiver. Equivalently, the total interference power must be about 6 dB below the thermal noise level. This criterion is used in simulations presented in chapter four.

Gilhousen et *al*. [23] study especially the capacity of a cellular CDMA system. They demonstrate that in contrast of the conventional techniques which must provide for different frequency allocation for contiguous cells, only CDMA can reuse the same (entire) spectrum for all cells, thereby increasing capacity by a large percentage of the normal frequency reuse factor.

2.2. Previous suppression techniques

It has been demonstrated that the interference immunity of a PN spread spectrum communication system corrupted by narrowband interference can be improved significantly by using signal processing techniques which complement the spread spectrum modulation. The objective is to reduce the level of the interference at the expense of introducing some distortion on the desired signal.

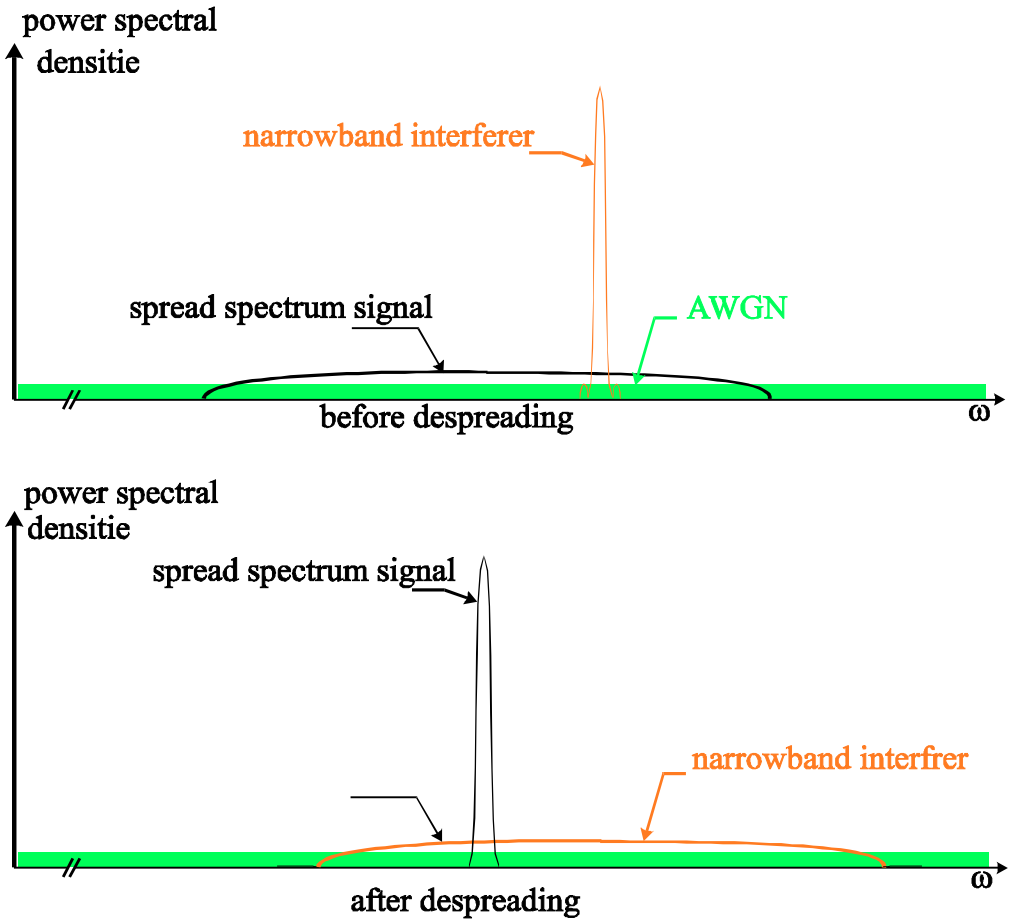

Figure 2.1 Spectral effects of Direct Sequence Spread Spectrum

Over the past two decades, a significant body of research has been concerned with the development of techniques for active NBI suppression in spread spectrum systems. An excellent review of those methods developed prior to 1988 can be found in a survey paper authored by Milstein [6] and in a more recent treatment by Poor and Rusch [29]. Research has shown that performance can be increased by processing to suppress narrowband

interference especially for commercial applications that presuppose a powerful licensed interferer and a spread spectrum system constrained in power so as not to disrupt existing communications systems. We briefly review the methods of linear and nonlinear prefiltring in sections 2.2.2 and 2.2.3. When the NBI is a digital signal, multiuser detection theory offer receivers with better performance than prefiltring. This approach, as described in section 2.2.4, involves modeling the NBI as a virtual CDMA system.

We will present the first of our contributions in the section 2.5. We take the general expression for the minimum mean square error (MMSE) receiver for a CDMA system and apply it to the narrowband suppression problem. We are able to determine a closed-form solution for the MMSE detector and its probability of error. We present theoretical and simulation results comparing the MMSE receiver with other receivers previously applied to the narrowband interference problem [30].

2.2.1. Linear techniques

If the interference is relatively narrowband compared with the bandwidth of the spread spectrum waveform, then the technique of interference cancellation by the use of notch filters often results in a large improvement in system performance, and the purpose of this section is to illustrate several such linear spectral filtering techniques. Theses notch filters are used to further enhance the performance of the spread spectrum system over and above what the inherent processing gain of the system provides, and so, they complement the spreading technique.

It should be noted that the NBI suppression methodology based on linear signal processing theories represents a large part of the work in NBI mitigation [22]. The signal processing methods have been mostly investigated extensively in theoretical analyses, as well as in implementation.

The development of this family of suppression methods has focused on two basic types of techniques (Figure 2.2 and 2.3): transform-domain and predictive methods. The

transform-domain methods suppress narrowband energy in the frequency domain, and estimator/subtractor methods perform time domain notch filtering.

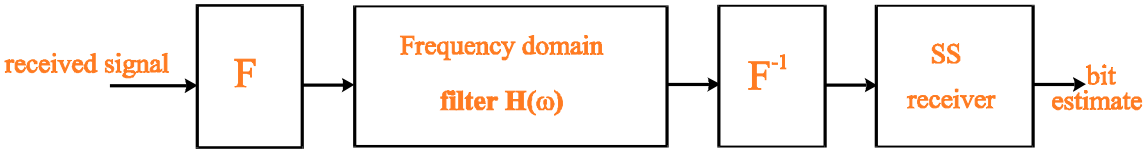

Figure 2.2 Transform-domain processing receiver

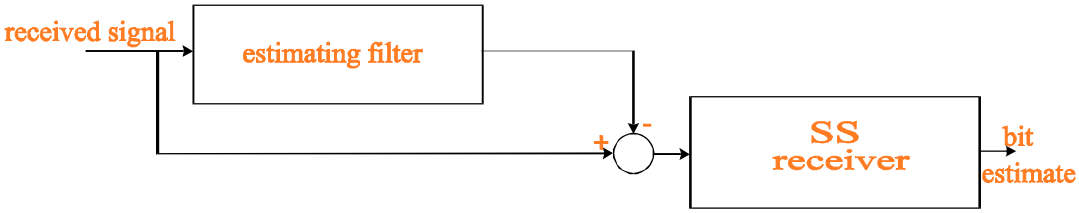

Figure 2.3 Estimator/subtractor receiver

Transform-domain processing:

In the NBI suppression based on the transform-domain techniques (Figure 2.2), the basic building block is a device which performs a real-time Fourier transform followed by a filter to notch out the NBI.

The Fourier transform of the input is taken, the transform is multiplied by the transfer function of some appropriate filter (mask) H(ω), the inverse transform of the product is taken, and the resulting waveform is put through a detection filter matched to the SS signal, as illustrated in Figure 2.2. Since the output of the Fourier transform is a waveform evolving in real-time which looks qualitatively like the one shown in Figure 2.4 a), multiplying that output by the waveform shown in Figure 2.4 b) should suppress a significant amount of interference power while only slightly reducing the power of the desired signal.

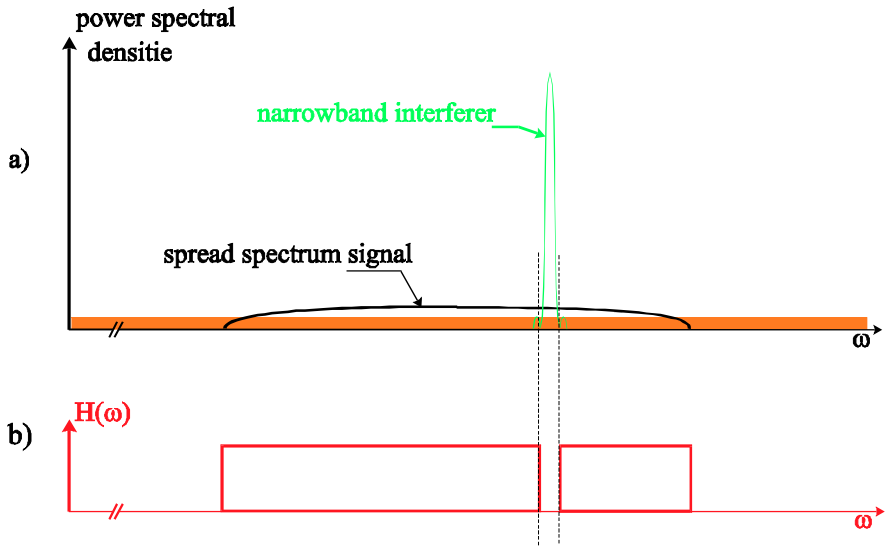

Figure 2.4 Notch filter

Depending on the overall system bandwidth and on the consequent processing speed requirements, the Fourier transforms required by this technique can be performed in hardware such as surface-acoustic-wave (SAW) technology or in software using the fast Fourier transform (FFT) as in [22]. It's interesting to note that it is possible to implement an adaptive version of this system as described in [22]. Figure 2.6 illustrates the process. The Fourier transformed receiver signal is fed into an envelope detector, and the output of the envelope detector is fed into a switch controlled by a threshold device. The upper branch passers the Fourier transformed input directly to the multiplier. The switch in the lower branch is set so that any time the output of the envelope detector exceeds a predetermined level, the output of the switch is forced to zero (and hence the lower input to the multiplier is also zero). The main idea of this adaptive transform-domain technique is to consider an adaptive mask that excises those Fourier components whose energy levels exceed a set threshold.

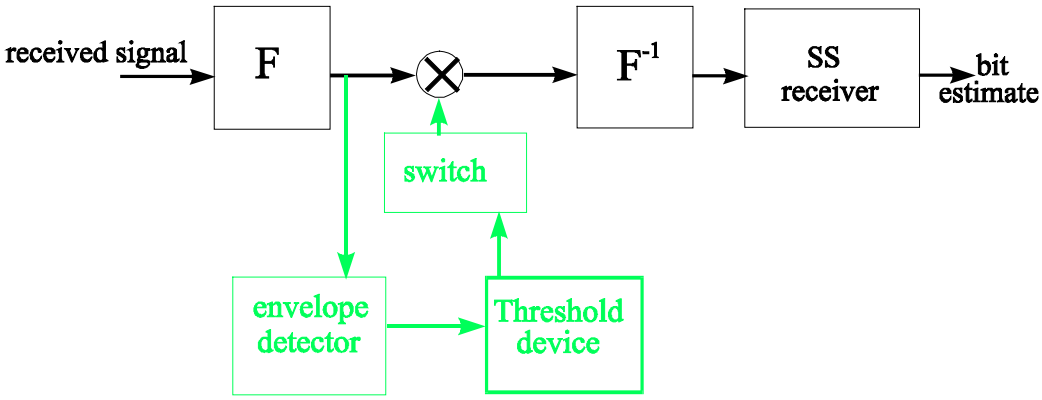

Figure 2.5 Block diagram of adaptive transform domain processing receiver

Linear predictive techniques

Predictive suppression techniques exploit the disparity in bandwidth between the SS signal and the NBI. The spread spectrum signal is essentially unpredictable, while the narrowband signal can be predicted with some accuracy, consequently, any prediction of the received signal will be a prediction primarily of the interfering narrowband signal [27,28]. Hence, a prediction of the received signal based on previously received values will, in effect, be an estimate of the interfering signal. By subtracting predicted values of the received signal obtained from the actual received signal and using the resulting prediction error as the input to the SS correlator, the effect of the interfering signal can be reduced significantly. This procedure is, in effect, performing a whitening operation on the received signal, and is illustrated in Figure 2.3. Fixed linear filters cannot be found for NBI suppression when the statistics for the interference are not known, and an adaptive algorithm must be used in such case. It forms a replica of the NBI by exploiting the discrepancy in bandwidth of the two signals. We will assume that the received signal is passed through a filter matched to the chip waveform and a chip synchronously sampled once during each chip interval, per Figure 2.6. The equivalent discrete time received signal will have components due to the spread spectrum signal s_k, the narrowband interference i_k, and the ambient white noise n_k. The observation of sample k is then given by

$$\mathbf{y}_k=\mathbf{s}_k+\mathbf{i}_k+\mathbf{n}_k \quad (1)$$

The SS signal $\mathbf{s}_k=\pm1$ with equal probabilities, $\mathbf{i}_k$ is the interference contribution, and the ambient noise n_k can be modeled as being AWGN. The three signals can be modeled as mutually independent.

Figure 2.6 Chip matched filtering.

The first important estimator/subtractor implementation is the linear predictive filter, or time-domain notch filter, as indicated in [22,26-28] and reproduced in Figure 2.7. Such a filter forms a linear prediction of the received signal based on a fixed number of previous samples. This estimate is subtracted from the received signal to obtain the residual signal. The residual signal is sent to the SS receiver, as well as being used to update the filter tap coefficients via a suitable adaptive algorithm, *e.g.* as the least mean squares (LMS) algorithm.

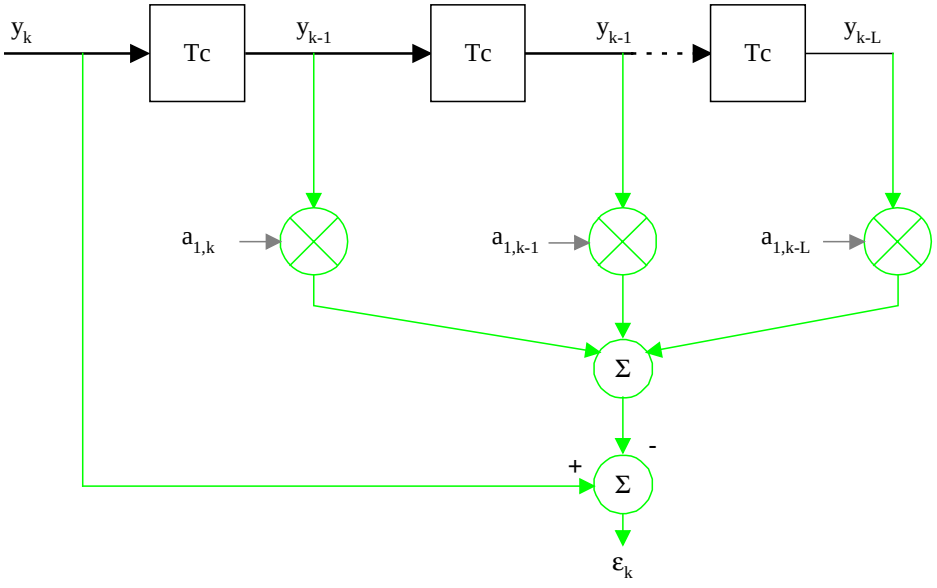

Figure 2.7 Linear LMS predictor filter

It should be noted that the LMS algorithm is one of the simplest adaptive algorithms to analyze and implement. The observation vector $\mathbf{X}_k$ and the tap vector θ_k are defined as follows

$$\mathbf{X}_k = \left[y_{k-1}\ y_{k-2} \cdots y_{k-L} \right]^T$$

$$\theta_k = \left[a_{1,k}\ a_{2,k} \ldots a_{L,k} \right]^T$$

The LMS estimate is determined by the following equations

$$\hat{y}_k = \mathbf{X}_k^T q_{k-1}$$

$$\theta_k = \theta_{k-1} + \mu_k (y_k - \hat{y}_{k-1}).\mathbf{X}_k \qquad (2)$$

where μ_k is a step size normalized to make the step size less dependent on the signal amplitude in $\mathbf{X}_k$ and also to speed convergence while guarding against instability.

A second useful implementation is an interpolating filter (Figure 2.8), where the estimate of a given value of the interference is based upon both past and future values. The linear interpolating filters have been found to have good phase characteristics as well as greater SNR improvement for NBI suppression, than do linear predicting filters [27, 28].

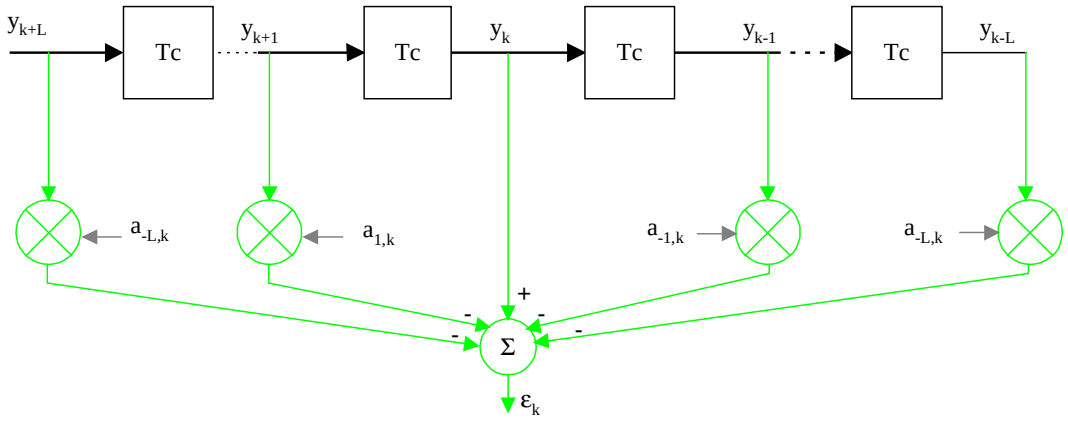

8

a *a* *a* *a*

2.2.2. Nonlinear predictive techniques

Linear prediction techniques are optimal for NBI in AWGN. The presence of the spread spectrum signal in addition to AWGN makes the optimal prediction filter nonlinear. In 1991, Vijayan and Poor [26] proposed nonlinear methods for predicting the narrowband signal that led to significant increases in the SNR improvement due to filtering. These nonlinear methods were derived from a system model that takes into account the non-Gaussian distribution of the observation noise (from the point of view of predicting the interferer, the observation noise consists of AWGN and the data signal). In 1994, Rusch and Poor [27-29], derive an enhancement to this nonlinear prediction and achieved further improvement by applying the technique to interpolating filter structures.

The non-Gaussian measurement noise in the prediction process requires a nonlinear filter for minimum mean square error (MMSE) prediction. As this optimal filter is too complex to implement, a suboptimal approximate conditional mean (ACM) nonlinear recursive filter was introduced in [24]. Adaptive filtering is examined in [27-29] for the more realistic case when the statistics of the narrowband process are unknown. The linear least mean squares predictor suggested by the ACM filter, as seen Figure 2.9 was modified to incorporate a non-linearity. In essence, a soft estimate of the SS value is made and subtracted from the received signal before the tap weights are calculated. The more reliable the soft estimates, the more Gaussian the adaptation noise.

Let $\overline{y}_k$ represent the observation less the soft decision on the spread spectrum signal, that is,

$$\overline{y}_k = y_k - \tanh\left(\frac{\varepsilon_k}{\sigma_k^2}\right) \tag{3}$$

where ε_k is the reduced signal at time k, and σ_k^2 the residual variance. Rusch [28] derives a new adaptation algorithm for tap weight update

$$\theta_k = \theta_{k-1} + \mu_k(\overline{y}_k - \hat{y}_k)[\overline{y}_{k-1}\ \overline{y}_{k-2} \ldots \overline{y}_{k-1}] \tag{4}$$

the nonlinear prediction is given by

a *a* *a* *a*

$$\hat{y}_k = \theta_{k-1}.\left[\bar{y}_{k-1}\ \bar{y}_{k-2} \ldots \bar{y}_{k-1}\right]^T \quad (5)$$

as illustrated in Figure 2.9.

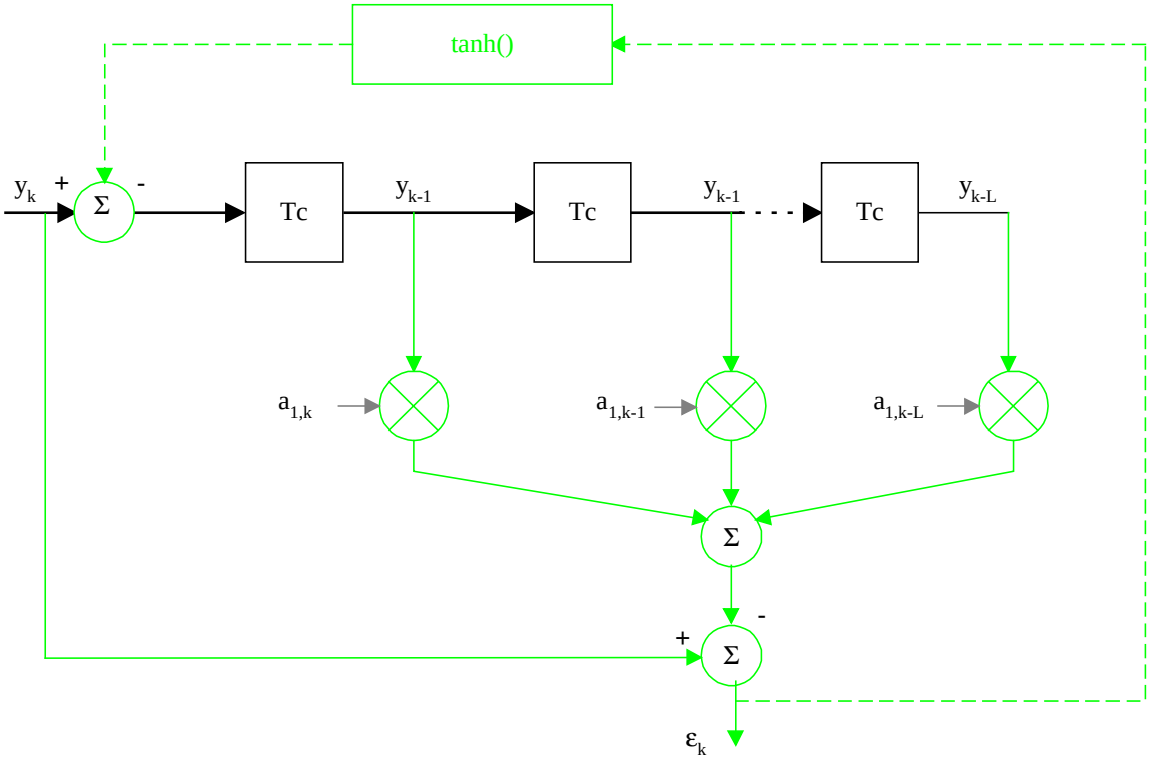

9

Note that with the approach explained in the previous sections we have separated the problem of narrowband interference rejection from that of signal detection and estimation. While we lose some optimality because of this separation, we reduce the complexity and gain flexibility in design. The spread spectrum receiver can be a simple matched filter, or a more sophisticated multiuser receiver that combats multiple access interference. When the interferer is actually a digital communications signal, we will see in the following section that it makes sense to combine these two functions for better performance.

a *a* *a* *a*

2.3. Multiuser detection techniques

Analysis of most of the methods of interference suppression discussed so far has involved modeling the narrowband signal as either a deterministic sinusoidal signal or an autoregressive signal (AR), the output of a linear filter driven by AWGN. These models greatly simplify analysis and have characteristics that capture the narrowband property of the receiver. However, the case of a digital narrowband interferer is poorly modeled as either a sinusoid or an AR process.

Suppose that the interferer is a digital communications signal with a data rate much lower than the spread spectrum chip rate. In such a situation, the structure of the digital interferer can be exploited to develop a SS receiver that optimally rejects the interference. In [30] Rusch and Poor apply the techniques of multiuser detection to this model to derive new methods for decoding the SS user while simultaneously suppressing the interferer. For simplicity they address the case of one true spread spectrum system user and one narrowband interferer. Analogously with the analysis of CDMA systems, they adopt use of the efficiency, asymptotic efficiency and the near-far resistance (presented in section 1.4) to gauge the effectiveness of these detectors.

System model

We consider a system with one SS signal and one digital narrowband signal in an otherwise AWGN channel with variance σ^2. Each data bit of the SS user has duration and is modulated by a unit energy pseudonoise signature sequence $s_0(t)$, which spreads the signal in the frequency domain. We assume a relationship between the data rates of the two users, m+1 bits of the narrowband user occur for each bit of the SS user (Figure 2.10) [30].

a *a* *a* *a*

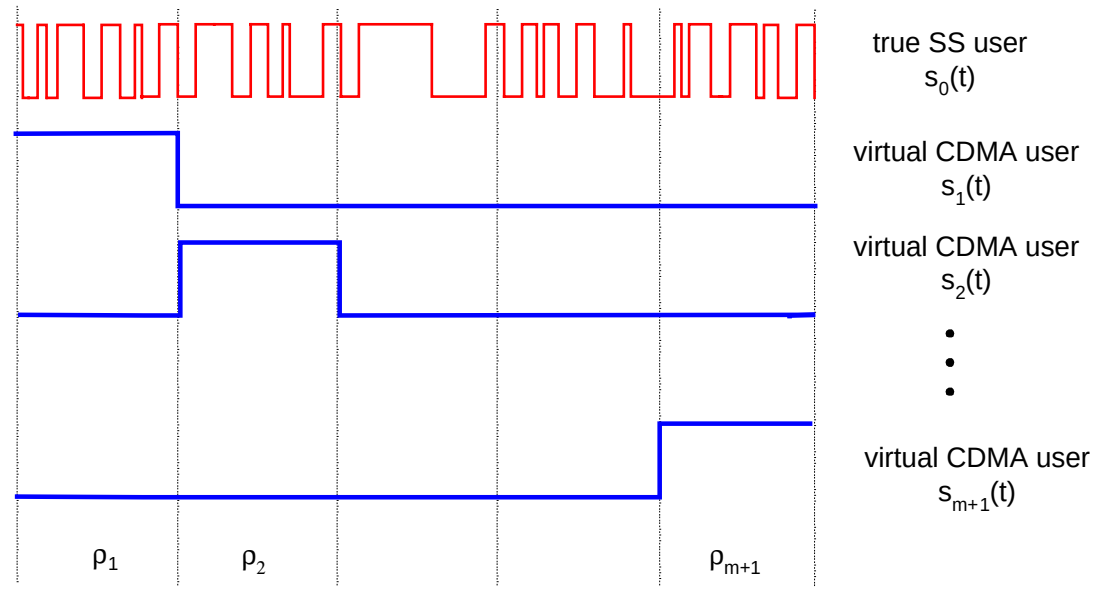

0 V **A** **,**

In Figure 2.10 we present the set of m+1 virtual signature sequences, and the SS spreading code. The first virtual user's signature sequence is constant during the first narrowband user's bit interval and zero everywhere else. Similarly each narrowband user's bit can be thought of as a signal arising from a virtual user with a signature sequence with only one non-zero interval. These form a set of orthogonal users, uncorrelated with one another. However, in general, the i^{th} virtual user's signature sequence $s_i(t)$, taken to have unit energy will have some cross correlation, ρ_i, with the spread spectrum user: $\rho_i = \int_0^T s_0(t)s_i(t)dt$ for i from 1 to m+1, forming the vector ρ. We see that the cross-correlation matrix **R** for this virtual multiuser system has a very simple structure,

$$\mathbf{R} = \begin{bmatrix} 1 & \rho^T \\ \rho & \mathbf{I}_m \end{bmatrix} \tag{6}$$

when $\mathbf{I}_{m+1}$ is the m+1 dimensional identity matrix.

We assume that the received signal strength for both signals remains constant for the SS bit interval. Let $_I$ be the received energy of the narrowband signal, and $_0$ the received energy of the SS user (including the processing gain). We will use the notation that

a *a* *a* *a*

the narrowband user data bits during the interval (are b_0, …, b_{m+1} or , and the SS bit is b_0. The received signal during one bit interval of the SS user is thus

$$y(t) = \sqrt{w_0}\, b_0 s_0(t) + \sqrt{w_I} \sum_{i=1}^{m} b_i s_i(t) + \sigma n(t), \quad t \in [0, T] \tag{7}$$

where n(t) is an AWGN process with zero mean and unit variance.

Conventional detector

As mentioned in section 1.3, the conventional detector sends the received signal directly to a single filter matched to the spreading code. The output of this matched filter is

$$y_0 = \sqrt{w_0}\, b_0 + \sqrt{w_I}\, \boldsymbol{\rho}^T \mathbf{b} + n_0, \quad t \in [0, T] \tag{8}$$

which is then compared to a threshold, to yield the estimate $\hat{b}_0$ of the spread spectrum bit. The probability of error is thus

$$\begin{aligned} P_r(\cdot) &= p_r\left(n_0 > \sqrt{w_0} - \sqrt{w_I}\, \boldsymbol{\rho}^T \mathbf{b}\right) \\ &= \frac{1}{2^{m+1}} \sum_{i=0}^{2^{m+1}-1} Q\left[\frac{\sqrt{w_0} - \sqrt{w_I}\, \boldsymbol{\rho}^T \mathbf{b}^i}{\sigma_0}\right] \end{aligned} \tag{9}$$

where $\mathbf{b}^i$ is an ordering of the 2^{m+1} possible values of the vector of narrowband bits, and n_0 is the noise contribution at the receiver output, a Gaussian random variable with zero mean and variance σ^2.

Optimum (maximum likelihood) detector

The optimum receiver feeds the received signal into a bank of matched filters, as indicated in section 1.5. The output of the matched filters, shown in Figure 1.7, form a sufficient statistic for determining the user's bits. The outputs of the matched filters form a vector **z** that can be written as

$$\mathbf{z} = \mathbf{R}\mathbf{W}^{\frac{1}{2}} \begin{bmatrix} b_0 \\ \mathbf{b} \end{bmatrix} + \mathbf{n} \tag{10}$$

p *pp*

where is Gaussian with zero mean and covariance matrix σ^2 , and

$$\mathbf{W}^{\frac{1}{2}} = \mathrm{diag}\left[\sqrt{w_0}, \sqrt{w_1}, .., \sqrt{w_I}\right] \tag{11}$$

The maximum likelihood estimate for the vector of narrowband and SS bits is given by

$$\hat{\mathbf{b}}_0 = \arg\max_{\mathbf{b}} \; 2\begin{bmatrix} b_0 \\ \mathbf{b} \end{bmatrix}\mathbf{W}^{\frac{1}{2}}\mathbf{z} - \begin{bmatrix} b_0 \\ \mathbf{b} \end{bmatrix}\mathbf{W}^{\frac{1}{2}}\mathbf{R}\mathbf{W}^{\frac{1}{2}}\begin{bmatrix} b_0 \\ \mathbf{b} \end{bmatrix} \tag{12}$$

The complexity of the is exponential in the number of narrowband bits m, which may be quite large. Attention has therefore focused on other sub-optimum linear detectors with much lower complexity.

Decorrelating detector

In the search for low complexity receiver, because of the complexity of the maximum likelihood and minimum probability of error, several performance criteria other than probability of error have been proposed to gauge receiver effectiveness. As defined earlier in section 1.4, the efficiency, the asymptotic efficiency and the near-far resistance are such performance measures. The decorrelating detector is a linear detector which achieves the near far resistance of the optimal (maximum-likelihood) detector. This receiver is given by the inverse of the cross-correlation matrix, which for our system is

$$\mathbf{R}^{-1} = \frac{1}{1-\rho^{\mathrm{T}}\rho}\begin{bmatrix} 1 & -\rho^{\mathrm{T}} \\ \rho^{\mathrm{T}} & \mathbf{I}_{\mathrm{m}} \end{bmatrix} \tag{13}$$

The decorrelating detector for the true SS user is the first row

$$\mathbf{c}_{\mathrm{dec}} = \begin{bmatrix} 1 & -\rho^{T} \end{bmatrix} \tag{14}$$

which estimates the SS bit as

$$\begin{aligned} \hat{\mathrm{b}}_0 &= \mathrm{sgn}\left(\mathbf{c}_{dec}^{T}\mathbf{y}\right) = \mathrm{sgn}\left(y_0 - \sum_{i=1}^{\mathrm{m+1}} \rho_i y_i\right) \\ &= \mathrm{sgn}\sqrt{w_0}\left(1-\rho^{\mathrm{T}}\rho\right) + \mathbf{n}^{*} \end{aligned} \tag{15}$$

with **n*** Gaussian with zero mean and covariance $\sigma^2\left(1-\rho^{\mathrm{T}}\rho\right)$. Therefore the probability of error is

$$Q\left(\frac{\sqrt{w_0\left(1-\rho^T\rho\right)}}{\sigma}\right) \tag{16}$$

By this expression, we see the decorrelation operation suppress the virtual multiple access interference (i.e. the NBI), at the expense of enhancing the AWGN. Per [11], the asymptotic multiuser efficiency is

$$\eta = \frac{1}{\left(\mathbf{R}^{-1}\right)_{1,1}} = 1-\rho^T\rho \tag{17}$$

which is independent of the received energies, the near-far resistance is consequently equal to the asymptotic efficiency. The decorrelating detector has the same near-far resistance as the optimal maximum likelihood detector (nonlinear) detector.

2.4. MMSE detector[1]

In [30] and as summarized in section 2.2.4, Rusch and Poor demonstrated how the multiuser detectors can outperform the conventional detector and predictor/subtractor detectors in the case of digital NBI. They examined fixed, linear detectors, above all the matched filter detectors and decorrelating detector. The matched filter detector is near-far limited, by which we mean that as the interferer power becomes arbitrarily large, the probability of error approaches one half. While the decorrelating detector offers good performance over a large spectrum of interference powers and bandwidths, it is not easily cast as an adaptive receiver when system parameters (such as the number and the spreading

[1] The section 2.5 was presented in the *Interference Rejection and Signal Separation in Wireless Communications Symposium*, New Jersey Institute of Technology, March 19, 1996 [31].

codes of active users) are not known. In this section we determine the minimum mean square error (MMSE) detector for the virtual CDMA system presented.

In [14] Honig, & develop a general expression for the receiver which minimizes the mean square error (MSE) between the outputs and the data in the CDMA channel case with no narrowband interference. This linear detector is of interest as an adaptive version can be implemented which does not require knowledge of the narrowband signal characteristics. We take the general expression for the MMSE receiver and apply it to the narrowband suppression problem, arriving at a closed-form solution for the MMSE detector and its probability of error.

As described in [30], and reproduced in section 2.4, we assume the interferer is a binary signal with m+1 narrowband bits in one SS bit. The cross-correlation matrix of this virtual CDMA is given by (6), with the received signal described by equation (8).

Per [12], the multiuser detector which minimizes the mean square error MSE defined in section 1.5 is determined by the inverse of the matrix $+\sigma^2\mathbf{W}^{-1}$. While this matrix inversion can not be simplified in a true CDMA system, our virtual CDMA system has a structure which can be exploited to find a closed-form solution. For our system this inverse is a function of the interference power and the cross correlation vector ρ.

$$\begin{aligned}\mathbf{R}+\sigma^2\mathbf{W}^{-1} &= \begin{bmatrix}1 & \rho^T\\ \rho & \mathbf{I}_{m+1}\end{bmatrix}+\frac{\sigma^2}{w_I}\begin{bmatrix}w_I/w_0 & 0\\ 0 & \mathbf{I}_{m+1}\end{bmatrix}\\ &= \begin{bmatrix}1+\sigma^2/w_0 & \rho^T\\ \rho & \mathbf{I}_{m+1}\left(1+\sigma^2/w_I\right)\end{bmatrix}\\ &= \left(1+\sigma^2/w_I\right)\begin{bmatrix}\dfrac{1+\sigma^2/w_0}{1+\sigma^2/w_I} & \dfrac{\rho^T}{1+\sigma^2/w_I}\\ \dfrac{\rho}{1+\sigma^2/w_I} & \mathbf{I}_{m+1}\end{bmatrix}\end{aligned} \tag{18}$$

the inverse can be expressed by

$$\frac{1}{1+\sigma^2/\mathrm{w_I}}\begin{bmatrix}\dfrac{1+\sigma^2/\mathrm{w_0}}{1+\sigma^2/\mathrm{w_I}} & \dfrac{\rho^T}{1+\sigma^2/\mathrm{w_I}}\\ \dfrac{\rho}{1+\sigma^2/\mathrm{w_I}} & \mathbf{I}_{m+1}\end{bmatrix}^{-1} \tag{19}$$

where σ^2 is the additive white Gaussian noise power. We have used the matrix identity

$$\begin{bmatrix}\mathrm{A} & \mathrm{B}\\ \mathrm{B^T} & \mathrm{D}\end{bmatrix}^{-1}=\begin{bmatrix}\mathrm{A^{-1}+FE^{-1}F^T} & -\mathrm{FE^{-1}}\\ -\mathrm{E^{-1}F^T} & \mathrm{E^{-1}}\end{bmatrix},$$

where $\mathrm{E=D-B^TA^{-1}B}$, and $\mathrm{F=A^{-1}B}$. In this case

$$\mathrm{A}=\frac{1+\sigma^2/\mathrm{w_0}}{1+\sigma^2/\mathrm{w_I}},\ \mathrm{B}=\frac{\rho^T}{1+\sigma^2/\mathrm{w_I}},\ \text{and D=}\mathbf{I}_{\mathrm{m}}$$

The inverse is given by

$$\left[\mathbf{R}+\sigma^2\mathbf{W}^{-1}\right]^{-1}=\frac{1}{1+\sigma^2/\mathrm{w_I}}\begin{bmatrix}\dfrac{\left(1+\sigma^2/\mathrm{w_I}\right)^2}{\left(1+\sigma^2/\mathrm{w_I}\right)\left(1+\sigma^2/\mathrm{w_0}\right)-\rho^T\rho} & \dfrac{-\rho^T\cdot\left(1+\sigma^2/\mathrm{w_I}\right)}{\left(1+\sigma^2/\mathrm{w_I}\right)\left(1+\sigma^2/\mathrm{w_0}\right)-\rho^T\rho}\\ \dfrac{-\rho\cdot\left(1+\sigma^2/w_I\right)}{\left(1+\sigma^2/\mathrm{w_I}\right)\left(1+\sigma^2/\mathrm{w_0}\right)-\rho^T\rho} & \dfrac{\rho\rho^T}{\left(1+\sigma^2/\mathrm{w_I}\right)\left(1+\sigma^2/\mathrm{w_0}\right)-\rho^T\rho}\end{bmatrix}$$

For our system, only the true SS bit is of interest; it is only this bit we wish to estimate. In our ordering, the SS bit is the first of the vector of "virtual" CDMA bits. Therefore we focus our efforts on the first row of the matrix, the vector

$$\frac{1}{\left(1+\sigma^2/\mathrm{w_I}\right)\left(1+\sigma^2/\mathrm{w_0}\right)-\rho^T\rho}\cdot\begin{bmatrix}1+\sigma^2/\mathrm{w_1} & -\rho^T\end{bmatrix}^T \tag{20}$$

It is this vector that we use to generate the MMSE estimate of the SS bit

$$\mathrm{c_0}(t)=\sum_{i=0}^{m+1}c_{0,i}s_i(t) \tag{21}$$

$$\hat{\mathrm{b}}_0=\mathrm{sgn}\left[\int_0^T\mathrm{c_0(t)y(t)dt}\right] \tag{22}$$

To find the canonical form (defined in [15] and reproduced in section 1.5) of this receiver, we normalize to arrive at a receiver whose inner product with the SS waveform has unit length.

$$\mathbf{c}_{\mathrm{MMSE}} = \frac{1}{1+\sigma^2/\mathrm{w}_{\mathrm{I}} - \rho^T\rho}\cdot\left[1+\sigma^2/\mathrm{w}_1 \quad -\rho^T\right]^T \tag{23}$$

The filter then takes the form

$$\mathrm{c}_{\mathrm{MMSE}}(t) = \frac{1}{1+\sigma^2/\mathrm{w}_{\mathrm{I}} - \rho^T\rho}\cdot\left[\left(1+\sigma^2/\mathrm{w}_{\mathrm{I}}\right)s_0(t) - \sum_{i=1}^{\mathrm{m}+1}\rho_i s_i(t)\right] \tag{24}$$

In order to determine the probability of error we examine the decision statistic for the SS bit. For convenience we reference all powers to the desired user power, $_0$ supposed equal to 1. The near-far ratio is therefore given by $_{\mathrm{I}}$, and σ^2 is the signal-to-Gaussian-noise ratio for the desired user. The received signal, r(*t*), is the sum of the SS signal and the narrowband user and the additive white Gaussian noise:

$$\mathrm{r}(t) = \mathrm{b}_0\mathrm{s}_0(\mathrm{t}) + \sqrt{w_1}\sum_{i=0}^{m-1}\mathrm{b}_{\mathrm{i}}\mathrm{s}_{\mathrm{i}}(\mathrm{t}) + \sigma\mathrm{n}(\mathrm{t}) \tag{25}$$

where n(t) is a zero mean, unit variance white Gaussian noise process.

Decision statistic (receiver output)

We now calculate the output of the MMSE detector. This decision statistic will be used to estimate the SS bit.

$$\begin{aligned} D.S. &= \int_0^T \mathbf{c}_{MMSE}(t)\mathrm{r}(t)dt \\ &= \frac{1}{1+\sigma^2/\mathrm{w}_{\mathrm{I}} - \rho^T\rho}\cdot\int_0^{\mathrm{T}}\left(\left(1+\sigma^2/\mathrm{w}_{\mathrm{I}}\right)\mathrm{s}_0(\mathrm{t}) - \sum_{i=1}^{\mathrm{m}+1}\rho_i\mathrm{s}_{\mathrm{i}}(\mathrm{t})\right)\left(\mathrm{b}_0\mathrm{s}_0(\mathrm{t}) + \sqrt{w_1}\sum_{i=1}^{\mathrm{m}+1}\mathrm{b}_{\mathrm{i}}\mathrm{s}_{\mathrm{i}}(\mathrm{t}) + \sigma\mathrm{n}(\mathrm{t})\right)\mathrm{dt} \end{aligned}$$

we calculate

t t s ss t s

$$\begin{aligned}\left(1+\sigma^2/\mathrm{w_I}-\rho^T\rho\right)D.S. &= \mathrm{b_0}\left(1+\sigma^2/\mathrm{w_I}\right)\int_0^{\mathrm{T}}\mathrm{s_0^2(t)dt}+\left(1+\sigma^2/\mathrm{w_I}\right)\sqrt{\mathrm{w_I}}\sum_{i=0}^{\mathrm{m+1}}\mathrm{b_i}\int_0^T \mathrm{s_i(t)s_0(t)dt}\\ &+\sigma\left(1+\sigma^2/\mathrm{w_I}\right)\int_0^{\mathrm{T}}\mathrm{s_0(t)n(t)dt}-b_0\sum_{i=0}^{\mathrm{m+1}}\rho_i\int_0^{\mathrm{T}}\mathrm{s_i(t)s_0(t)dt}\\ &-\sqrt{\mathrm{w_I}}\sum_{i=1}^{\mathrm{m+1}}b_i\rho_i\int_0^{\mathrm{T}}\mathrm{s_i^2(t)dt}-\sigma\sum_{i=1}^{\mathrm{m+1}}\rho_i\mathrm{s_i(t)n(t)}\\ &=\mathrm{b_0}\left(1+\sigma^2/\mathrm{w_I}-\rho^T\rho\right)+\sigma^2/\sqrt{\mathrm{w_I}}\sum_{i=1}^{\mathrm{m+1}}b_i\rho_i\\ &+\sigma\left(\left(1+\sigma^2/\mathrm{w_I}\right)\int_0^T\mathrm{s_0(t)n(t)dt}-\sum_{i=1}^{\mathrm{m+1}}\rho_i\mathrm{s_i(t)n(t)}\right)\\ &=\mathrm{b_0}\left(1+\sigma^2/\mathrm{w_I}-\rho^T\rho\right)+\sigma^2/\sqrt{\mathrm{w_I}}\sum_{i=1}^{\mathrm{m+1}}b_i\rho_i+\tilde{n}\end{aligned}$$

we arrive at

$$D.S.=b_0+\frac{\sigma^2/\sqrt{\mathrm{w_I}}\sum_{i=1}^{\mathrm{m+1}}b_i\rho_i+\tilde{n}}{\left(1+\sigma^2/\mathrm{w_I}-\rho^T\rho\right)} \tag{26}$$

with

$$\tilde{\mathrm{n}}=\sigma\left[\left(1+\sigma^2/\mathrm{w_I}\right)\int_0^{\mathrm{T}}\mathrm{s_0(t)n(t)dt}+\sum_{\mathrm{i=1}}^{\mathrm{m+1}}\rho_{\mathrm{i}}\int_0^{\mathrm{T}}\mathrm{s_i(t)n(t)dt}\right]$$

The receiver output can be expressed then as the sum of the contributions of the SS signal, the interference, and the noise

$$\mathrm{D.S.}=\mathrm{b_0}+\frac{\sigma^2}{\sqrt{\mathrm{w_I}}}\frac{\mathbf{b}^{\mathrm{T}}\rho}{1+\sigma^2/\mathrm{w_I}-\rho^{\mathrm{T}}\rho}+\frac{\tilde{\mathrm{n}}}{1+\sigma^2/\mathrm{w_I}-\rho^{\mathrm{T}}\rho} \tag{27}$$

where the effective additive white Gaussian noise, ñ, has zero mean and variance

$$\tilde{\sigma}^2=\sigma^2\left[\left(1+\frac{\sigma^2}{\alpha^2}\right)^2-\left(1+2\frac{\sigma^2}{\alpha^2}\right)\rho^{\mathrm{T}}\rho\right]$$

b n n n n n DSSS D n n

The Probability of error

The probability of error using this decision statistic against a zero threshold is

$$\begin{aligned} P_e &= \frac{1}{2}\Pr\left(\hat{b}_0 = 1 / b_0 = -1\right) + \frac{1}{2}\Pr\left(\hat{b}_0 = -1 / b_0 = 1\right) \\ &= \frac{1}{2}\Pr\left(D.S. > 0 / b_0 = -1\right) + \frac{1}{2}\Pr\left(D.S. < 0 / b_0 = 1\right) \\ &= \frac{1}{2}\Pr\left(\tilde{n} > 1 + \frac{\sigma^2}{\alpha^2} - \rho^T\rho - \frac{\sigma^2}{\alpha}\rho^T\underline{b}\right) + \frac{1}{2}\Pr\left(\tilde{n} < -1 - \frac{\sigma^2}{\alpha^2} + \rho^T\rho - \frac{\sigma^2}{\alpha}\rho^T\underline{b}\right) \end{aligned}$$

because of the symmetry, we have

$$P_e = \frac{1}{2^m}\sum_{i=0}^{2^m-1} Q\left(\frac{1 + \frac{\sigma^2}{\alpha^2} - \rho^T\rho - \frac{\sigma^2}{\alpha}\rho^T\mathbf{b}^i}{\tilde{\sigma}}\right) \tag{28}$$

where $\mathbf{b}^i$ is an ordering of the m+1 narrowband bits and Q the cumulative distribution function of Gaussian random variable.

From these equations we also arrive at some asymptotic results. As the near far ratio goes to zero, the probability of error for the MMSE detector approaches that of the single user case, $Q(\ \sigma\ )$. As the near far ratio goes to infinity, the probability of error is equal to that of the decorrelating detector,

$$\left(P_e\right)_{dec} = Q\left(\frac{\sqrt{1-\rho^T\rho}}{\sigma}\right) \tag{29}$$

For weak interferers the MMSE receiver has an advantage over the decorrelating detector, but this is not a scenario of interest. For very small cross-correlation, the performance of both the MMSE and the decorrelating detector approaches that of the single-user system.

b n n n n n DSSS D n n

Simulation results

Figure 2.11 shows the probability of error versus the near far ratio for three different receivers: the conventional (matched filter) detector, the decorrelating detector, and the MMSE detector. We use a noise power that is 6 dB above the spread signal, as suggested by field tests [4] of overlay spread spectrum systems. An -sequence of length 63 was used as the spreading code. Square waves at baseband were used for bit and chip waveforms. We see that simulation (continuous lines) and theory (dashed lines) match well.

For the case m=1, one narrowband bit coincides with exactly one spread spectrum bit. The cross correlation is very low, and we see that the MMSE and decorrelating detector each have performance equal to that of the single-user case. For larger values of m the cross correlations become larger and performance falls off slightly. For all the simulated systems, however, the MMSE and the decorrelating detectors show the same performance and their curves overlap.

For heuristic reasons we examined a synchronous system where one-shot detection (bit buy bit decisions sequence detection) is optimal. While in the asynchronous case one-shot detection is sub-optimal, it greatly reduces complexity and still offers good performance. Our analysis hinges on the narrowband users being cast as a set of an equal power orthogonal virtual CDMA users. This model can be applied to asynchronous systems as well as synchronous, therefore our results are valid in the realistic scenario of a time delay between the start of the SS bit and the narrowband bit. In the asynchronous case, each actual narrowband bit might need to be subdivided into further virtual users to ensure equal power (assume one bit was severely curtailed). While the complexity of the MMSE receiver increases with the number of virtual users m, it does not grow prohibitively. Furthermore, subdivision of narrowband bits leads to correlations between virtual signature sequences assures the validity of our analysis despite the correlations.

b n n n n n DSSS D n n

2.5. Conclusion

We have demonstrated that the MMSE detector can be very effective in removing a binary narrowband interference signal from a direct sequence spread spectrum signal overlaid on the narrowband system. We presented the MMSE receiver and its probability of error in closed-form, as a function of a) the bit waveform of narrowband signal, b) the cross correlation with the spread spectrum signal, and c) the relative powers of the signals and noise. We note that for both decorrelating and MMSE receivers, we suppose that the receiver can acquire the timing (bit epoch and carrier phase) of the desired user. Both receivers require the knowledge of the signatures waveforms of each active user. The MMSE also requires the interfering powers. Theses requirements are the major disadvantages of the both receivers. In Chapter 3, we study a blind adaptive technique which is previously proposed by Honig et [14] in the domain of multiple access interference rejection, and apply this method to our narrowband problem.

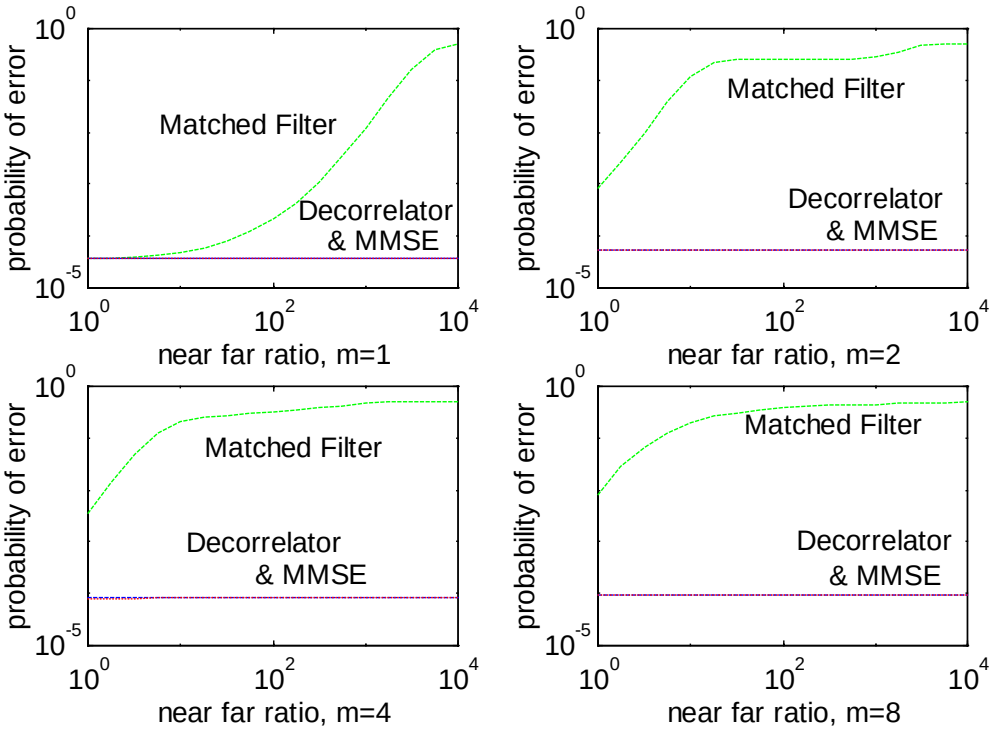

Figure 2.11 Results for Matched Filter, Decorrelating and MMSE detector

Subspace approach to blind adaptive narrowband interference suppression in DSSS[2]

3.1. Introduction

In chapter 2, it is shown that multiuser theory gives us an optimal and various sub-optimal receivers for a scheme of one digital narrowband signal and one CDMA signal. These receivers require information on some, or perhaps all, of the following parameters: signature sequences or codes, received energies, timing delays, etc. of all users. For instance, the NBI suppression method of [30] is based on the use of the decorrelating detector for removing digital interferers from the channel. The major significant practical disadvantage of the decorrelating detector that it requires the knowledge of all waveforms of all users in the channel, including the narrowband interferers. The MMSE receiver proposed in section 2.5 and appearing in reference [34], provides a slight improvement in probability of error in the range of high signal to interference ratio, but it also requires knowledge of all users' waveforms or codes, in addition to all users powers, including the narrowband interfering powers. These detectors also require knowledge of timing delays and carrier phase.

[2] This Chapter will appear in IEEE Transactions on Communications [34].

The need for adaptation

The MMSE detector is of interest as an adaptive version can be implemented which does not require knowledge of the interfering signals' characteristics. The adaptive multiuser receiver which minimizes the mean-square-error (MMSE) between the outputs and the data eliminates the need to know the signature waveforms of the interferers, the timing and the interference powers [12]. However, these adaptive detectors need to have training data sequences for every active user during adaptation. Each transmitter sends a training sequence at start-up which the receiver uses for initial adaptation. After the training sequence is completed, the receiver switch to decision-directed mode.

The need for blind adaptation

The decision directed adaptation becomes unreliable whenever there is a drastic change in the interference environment, and consequently, data transmission of the desired user must be suspended and the training sequence must be retransmitted. Not only does this situation arise frequently in a shared frequency band, but it is also unrealistic to expect interferers from outside the spread-spectrum system to submit to the transmission of training sequences. We therefore consider the blind multiuser detection algorithm [14] that requires only knowledge of the spreading code of the desired user (in our case, the true SS user). We exploit the structure of the virtual CDMA system introduced in chapter two to analyze this detector. Indeed, this system model gives a special structure to the covariance matrix of the received signal, and we exploit this structure herein to characterize the signal space.

The brunt of our analysis is placed in examination of the signal space and how various receivers project energy in this space. We begin in the following section with defining several bases for the space spanned by all possible signature sequences, as well as important subspaces. We examine the eigenspaces of the received signal's covariance matrix to partition the signal space in three subspaces. We demonstrate the significance of these subspaces in terms of how energy from the desired user, the AWGN and the narrowband interference is distributed among them.

In section 3.3, we first consider the three most known fixed sub-optimal receivers introduced previously: 1) The matched filter or conventional detector, 2) the decorrelating detector, and 3) the MMSE receiver. We show that for this virtual CDMA system, the three fixed receivers of interest all project the received signal onto a two-dimensional subspace. Typical CDMA systems with wideband interference will not have this reduced dimension subspace. By identifying this space we are able to parameterize the receivers of interest by a single variable. Contrast this with m+2 wideband users leading a m+2 dimensional space and m+2 variables to characterize a receiver. In section 3.4 we go on to apply these results to the dynamics of the blind adaptive receiver. We examine the trajectory of the adaptive receiver's tap weights in section 3.5 and we identify certain convergence anomalies and propose a new receiver to avoid them. In section 3.6 we outline two new less restrictive stability constraints on the adaptation step size leading to faster convergence of the adaptive receiver to the MMSE receiver.

3.2. Subspace signal energy distribution

3.2.1. Received signal & covariance matrix

Received signal

We consider the virtual CDMA system as presented in chapter 2. This scenario has one SS signal and one digital narrowband signal in an otherwise AWGN channel with variance σ^2 (Figure 2.10). The narrowband signal and the SS signal are asynchronous, therefore we will have only partial narrowband bits at the beginning and end of the SS spreading code. These form a set of orthogonal interference users, uncorrelated with one another. However, in general, the i^{th} virtual user's signature sequence $s_i(t)$ ($\mathbf{s}_i$ in the discrete model), taken to have unit energy, will have some cross correlation, ρ_i, with the spread spectrum user: $\rho_i = \int_0^T s_0(t)s_i(t)dt$ (=$<\mathbf{s}_i,\mathbf{s}_0>$), for i from 1 to $m+1$, where $<\mathbf{u},\mathbf{v}>$ denotes the inner product between the two vectors **u** and **v**, forming the vector ρ. Without loss of

generality, we assume, as described in the previous chapter, that there is an integer relationship between the SS bits rate and the NB bits rate.

The received signal is sampled N times in a SS bit interval (N typically being the length of the direct sequence spreading code) using the chip matched filter presented in Figure 1.4. Similarly, each signature sequences can be sampled and represented as a finite dimensional vector. The received signal during one SS bit is the vector sum of each users' signature sequence weighted by the user's energy and bit value, plus the AWGN. The k^{th} virtual user's contribution can be written as $\mp\sqrt{w_I}\mathbf{s}_k$. The AWGN can be written as a Nx1 vector of independent, zero mean, unit variance random variable, **n**, weighted by the square root of the noise power spectral density σ^2. The discrete received signal during one bit interval of the SS user is thus

$$\mathbf{y} = \sqrt{w_0}b_0\mathbf{s}_0 + \sqrt{w_I}\sum_{i=1}^{m+1} b_i\mathbf{s}_i + \sigma\mathbf{n} \tag{1}$$

Here, it is assumed that the received signal strength for both signals remains constant for the SS bit interval. This assumption is reasonable for a slowly varying channel.

Covariance matrix

The covariance matrix of the received signal is

$$\mathbf{R}_{\mathbf{yy}} = E\{\mathbf{y}\mathbf{y}^T\} = w_0\mathbf{s}_0\mathbf{s}_0^T + w_I\sum_{i=1}^{m+1}\mathbf{s}_i\mathbf{s}_i^T + \sigma^2\mathbf{I}_N \tag{2}$$

The matrix $\mathbf{R}_{yy}$ has N dimensions. Mathematically, it is a linear transformation in the N-dimensional signal space. The eigenvectors of this correlation matrix describe the distribution of the signal energy in the signal space. The eigenvalues measure the mean energy concentrated in each eigenvector's direction.

3.2.2. Various Bases & Subspaces

In this section we define four sets of basis vectors for Γ, the space (dimension N) spanned by all possible signature sequence vectors. The set of standard basis vectors we call B_e=[e_0,...e_{N-1}] , with the definition: $e_j[i] = \begin{cases} 1 & i = j \\ 0 & i \neq j \end{cases}$ for j=0,...N-1. B_e is a canonical orthonormal basis of the space.

The space spanned by all active signature sequences we call Γ_{act}. Note that for our virtual CDMA system there are $m+2$ active users, therefore Γ_{act} has dimension $m+2$. The orthogonal complement of Γ_{act} we call Γ_{NO}, as it contains energy from noise only, with no energy from an active user. Γ_{act} and Γ_{NO} are presented in figure 3.1, and the space Γ is the direct sum of these two subspaces, *ie*.,

$$\Gamma_{act} \oplus \Gamma_{NO} = \Gamma \tag{3}$$

A new set of basis vectors for Γ_{act} is formed by the signature sequences themselves; we refer to this basis as B_{act}. These vectors span the space Γ_{act}, have unit length (from the signature sequence having unit energy), are linearly independent, but are not orthogonal. Only the independence between the signatures is required to characterize Γ_{act}. Let B_{NO} be a set of basis vectors to span Γ_{NO}, and complete this basis of Γ. The basis B_{NO} is composed of orthonormal vectors which are orthogonal to Γ_{act}. We refer to B_s as the complete basis of Γ

$$B_s = B_{act} \oplus B_{NO} \tag{4}$$

We define a third set of basis vectors B_{yy} that are formed by the eigenvectors of the covariance matrix $\mathbf{R}_{yy}$ of the received signal. In the following section, we calculate the eigenvectors and the eigenvalues of $\mathbf{R}_{yy}$. These eigenvectors will determine a special partition of the signal space into subspaces. The definition of B_{yy} is motivated by the geometric significance of the eigenvectors and associated eigenvalues. The eigenvectors represent the privileged directions of concentration of power in the space Γ. The eigenvalues quantify the amount of power concentrated in each direction.

Finally, we define a fourth set of basis vectors, B_{vy}, that is formed by the eigenvectors of $\mathbf{R}_{vy}$ as defined in section 3.4. The matrix $\mathbf{R}_{vy}$ governs the dynamics of the gradient descent algorithm. We will describe the evolution of the algorithm using the projections of the tap weight vector onto the eigenvectors of $\mathbf{R}_{vy}$. The eigenvectors of $\mathbf{R}_{vy}$ represent proper or privileged directions of the mean evolution of the blind adaptive detector, and the associated eigenvalues represent a measure of this mean dynamic evolution in each eigenvector direction.

3.2.3. Subspaces identification

In this section we demonstrate that the subspace Γ_{act} is invariant[3] under $\mathbf{R}_{yy}$ (or $\mathbf{R}_{yy}$-invariant). This allows us to define and calculate the restriction of $\mathbf{R}_{yy}$ in Γ_{act} which we denote by $\tilde{\mathbf{R}}_{yy}$. By definition, Γ_{act} is invariant by $\mathbf{R}_{yy}$ (or $\mathbf{R}_{yy}$-invariant) if for every vector $\mathbf{v}\in\Gamma_{act}$ we find that the transformed vector $\mathbf{R}_{yy}\mathbf{v}\in\Gamma_{act}$. Recall that Γ_{act} is spanned by the signatures sequences, therefore we calculate $\mathbf{R}_{yy}\mathbf{s}_i$ for i=0,...,m+1

$$\begin{aligned}
\mathbf{R}_{yy}\mathbf{s}_0 &= \left(w_0+\sigma^2\right)\mathbf{s}_0 + w_I\sum_{i=1}^{m+1}\rho_i\mathbf{s}_i \\
&\vdots \\
\mathbf{R}_{yy}\mathbf{s}_i &= w_0\rho_i\mathbf{s}_0 + \left(w_I+\sigma^2\right)\mathbf{s}_i \qquad 1\le i\le m+1
\end{aligned} \tag{5}$$

Note that each signature vector is transformed by $\mathbf{R}_{yy}$ to a linear combination of the signature vectors. Let $\tilde{\mathbf{R}}_{yy}$ be the restriction[4] of $\mathbf{R}_{yy}$ in Γ_{act} so that

$$\mathbf{R}_{yy}\left[\mathbf{s}_0 \quad \cdots \quad \mathbf{s}_{m+1}\right] = \left[\mathbf{s}_0 \quad \cdots \quad \mathbf{s}_{m+1}\right]\tilde{\mathbf{R}}_{yy} \tag{6}$$

---

[3] Let Γ_{sub} be an m dismensional subspace of Γ. Γ_{sub} is called **A**-invariant for matrix **A** if for every vector $\mathbf{u}\in\Gamma_{sub}$, the product $\mathbf{Au}\in\Gamma_{sub}$.

[4] Let $[\mathbf{u}_1\ \mathbf{u}_2\ \ldots\ \mathbf{u}_{m+1}]$ be an (N×m+1) matrix, where the column vectors $\mathbf{u}_1$, $\mathbf{u}_2$, . . ., and $\mathbf{u}_{m+1}$ span the subspace Γ_{sub}. If $\mathbf{A}[\mathbf{u}_1\ \mathbf{u}_2\ \ldots\ \mathbf{u}_{m+1}] = [\mathbf{u}_1\ \mathbf{u}_2\ \ldots\ \mathbf{u}_{m+1}]\mathbf{B}$, with Γ_{sub} **A**-invariant, the matrix **B** is called the restriction of **A** in Γ_{sub}.

Using the basis of signature sequences we can write $\tilde{\mathbf{R}}_{\mathbf{yy}}$ in an arrow structure as

$$\tilde{\mathbf{R}}_{\mathbf{yy}} = \begin{bmatrix} w_0 + \sigma^2 & w_0 \boldsymbol{\rho}^T \\ w_I \boldsymbol{\rho} & \left(w_I + \sigma^2\right)\mathbf{I}_{\mathbf{m+1}} \end{bmatrix} \tag{7}$$

The matrix is symmetric and nonnegative definite, therefore all eigenvalues are nonnegative and all eigenvectors are orthogonal.

For every $\mathbf{V} \in \Gamma_{NO}$, we have $\mathbf{R}_{\mathbf{yy}}\mathbf{V}=\sigma^2\mathbf{V}$, which means that Γ_{NO} is trivially $\mathbf{R}_{\mathbf{yy}}$-invariant and the matrix $\sigma^2\mathbf{I}_{N-(m+2)}$ is the restriction of $\mathbf{R}_{\mathbf{yy}}$ in Γ_{NO}. Since the eigenvalues and the eigenvectors of a matrix are the same as those of its restrictions, we focus on the matrices $\tilde{\mathbf{R}}_{\mathbf{yy}}$ and $\sigma^2\mathbf{I}_{N-(m+2)}$ to find the eigenvalues and eigenvectors of $\mathbf{R}_{\mathbf{yy}}$. The eigenvalues of $\tilde{\mathbf{R}}_{\mathbf{yy}}$ are equal to the first (m+2) eigenvalues of $\mathbf{R}_{\mathbf{yy}}$.

The matrix $\mathbf{R}_{\mathbf{yy}}$ can be viewed mathematically as a linear operator on the space Γ, and it can be decomposed into a combination of two independent linear operators 1) $\tilde{\mathbf{R}}_{\mathbf{yy}}(m+2 \times m+2)$ can be expressed in basis vectors B_{act}, and 2) $\sigma^2\mathbf{I}_{N-(m+2)}$ expressed in the basis vectors B_{NO}. Recall that B_s is the second N-vector basis of Γ, and it's the direct sum of B_{act} and B_{NO}. In order to eventually generate the third basis B_{yy} for Γ, we calculate in the appendix the eigenvalues and eigenvectors of the covariance matrix $\mathbf{R}_{\mathbf{yy}}$. We arrive to

$$\begin{aligned} \lambda_{0y} &= \frac{1}{2}\left(w_0 + w_I + 2\sigma^2 + \sqrt{\phi}\right) \quad , \quad \phi = \left(w_0 - w_I\right)^2 + 4w_0 w_I \boldsymbol{\rho}^T\boldsymbol{\rho} \\ \lambda_{1y} &= \frac{1}{2}\left(w_0 + w_I + 2\sigma^2 - \sqrt{\phi}\right) \\ \lambda_{iy} &= w_I + \sigma^2 \qquad 2 \le i \le m+1 \\ \lambda_{iy} &= \sigma^2 \qquad m+2 \le i \le N-1 \end{aligned} \tag{8}$$

For constants Δ^+, Δ^-, and γ_i defined in the appendix, the orthonormal set of eigenvectors is given by

$$
\begin{aligned}
\mathbf{V_{0y}} &= \gamma_0 \left[\Delta^- \quad -\boldsymbol{\rho}^T \right]_{B_{act}} \\
\mathbf{V_{1y}} &= \gamma_1 \left[\Delta^+ \quad -\boldsymbol{\rho}^T \right]_{B_{act}} \\
\mathbf{V_{iy}} &= \gamma_i \left[0 \quad \rho_i \rho_1 \quad \cdots \quad \rho_i \rho_{i-1} \; \delta_i \quad \cdots \quad 0 \right]_{B_{act}} \qquad \forall\, 2 \le i \le m+1 \\
\mathbf{V_{iy}} &= \gamma_i \left(e_i - \sum_{j=0}^{i-1} \left\langle e_i, \mathbf{V_{jy}} \right\rangle \mathbf{V_{jy}} \right) \qquad \forall\, m+2 \le i < N
\end{aligned}
\tag{9}
$$

where $\delta_i = -\sum_{j=1}^{i-1} \rho_j^2$

The eigenvalues describe the average energy of the received signal in the associated eigenvector's direction. The eigenvectors represent a privileged directions of concentration of energy. Only the constants Δ^+ and Δ^- are functions of the desired user's power $_0$. It is important to note that the nature of $\mathbf{V_{0y}}$ and $\mathbf{V_{1y}}$ allows us to form the linear combination

$$
\begin{aligned}
\gamma_1^{-1}\mathbf{V_{1y}} - \gamma_0^{-1}\mathbf{V_{0y}} &= \left(\Delta^+ - \Delta^-\right)\left[1 \quad 0 \quad \cdots \quad 0\right]_{B_s} \\
&= \left(\Delta^+ - \Delta^-\right)\mathbf{s_0}
\end{aligned}
\tag{10}
$$

which implies that $_0$ can be expressed as a linear combination of $\mathbf{V_{0y}}$ and $\mathbf{V_{1y}}$

$$
\begin{aligned}
\mathbf{s}_0 &= \frac{1}{\Delta^+ - \Delta^-}\left(\gamma_1^{-1}\mathbf{V_{1y}} - \gamma_0^{-1}\mathbf{V_{0y}}\right) \\
&= \frac{\alpha^2}{\sqrt{\left(\alpha^2 - 1\right)^2 + 4\alpha^2 \boldsymbol{\rho}^T \boldsymbol{\rho}}}\left(\gamma_1^{-1}\mathbf{V_{1y}} - \gamma_0^{-1}\mathbf{V_{0y}}\right)
\end{aligned}
\tag{11}
$$

Eigenvectors $\mathbf{V_{0y}}$ and $\mathbf{V_{1y}}$ span a subspace of dimension two that we call Γ_E, as it contains all the energy from the desired user and the *e e i e* energy from the interference and noise. We say effective energy, because we will show that three important fixed detectors (the matched filter receiver, decorrelating receiver, and MMSE receiver) project the received signal onto this subspace, as discussed in section 3.3, therefore it is only this subset of interference and noise energy which affects receiver performance. We should note that the decorrelating and the MMSE receivers may not project onto this space for all CDMA systems, however we will show that for this virtual CDMA system they do, as does the

adaptive version of the MMSE detector discussed in section 3.4.2. This subspace should not be confused with the subdivisions of Γ_{act} discussed in [12].

The set of eigenvectors for $\leq i \leq m$ are orthogonal to $_0$, and span a space we call $\Gamma_{I\&N}$; the orthogonal complement of Γ_E relative to the space Γ_{act}

$$\Gamma_{I\&N} \oplus \Gamma_E = \Gamma_{act} \tag{12}$$

That is, $\Gamma_{I\&N}$ and Γ_E form a partition of Γ_{act}. The remainder of eigenvectors for $m \leq i \leq N$ span the space Γ_{NO}. Note the eigenvalues associated with $\Gamma_{I\&N}$ are functions of the interference power and the noise power, while the eigenvalues associated with Γ_{NO} are functions of the noise power only. To recap the subspaces discussed, we have the relationship $\Gamma = \Gamma_{NO} \oplus \Gamma_{act} = \Gamma_{NO} \oplus \Gamma_{I\&N} \oplus \Gamma_E$. These subspaces are illustrated in Figure 3.1.

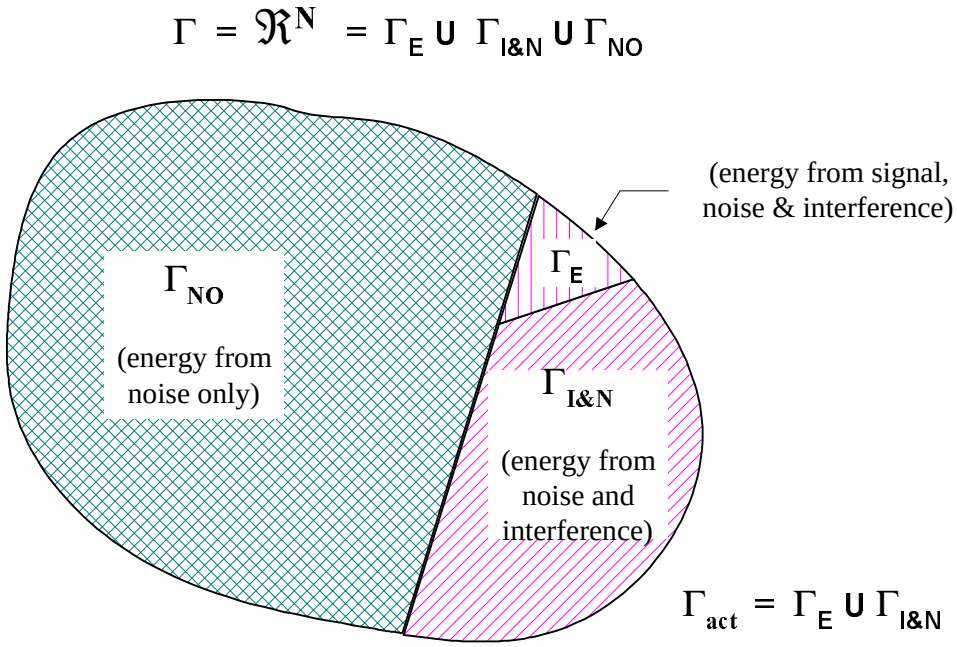

Fig re 3.1 S b pace Partitio

3.3. The fixed receivers

We demonstrated in the previous section that only the two dimensional subspace Γ_E contains energy from the desired user. This leads us to conclude that any detector of interest should not have a component outside Γ_E. In fact, any component outside Γ_E contributes to excess noise enhancement at the output of the receiver.

The canonical form of a receiver is defined in [14] as the sum of the desired user's spreading code, $_0$, plus a vector $\mathbf{x}_0$ orthogonal to $_0$, *i.e.*, $\mathbf{c} = _0 + \mathbf{x}_0$. The vector $_0$ can be written as a linear combination of $_{0y}$ and $_{1y}$ (see equation 31), and therefore falls in Γ_E. We construct a second vector $^{\perp}$ in Γ_E that is orthogonal to $_0$, and together they span Γ_E.

$$\begin{aligned}\mathbf{V}^{\perp} &= \frac{1}{\sqrt{\rho^T\rho\left(1-\rho^T\rho\right)}}\cdot\left[\rho^T\rho \quad -\rho_1 \quad \cdots \quad -\rho_{m+1}\right]_{B_{act}} \\ &= \frac{1}{\sqrt{\rho^T\rho\left(1-\rho^T\rho\right)}}\cdot\left[\rho^T\rho \quad -\rho^T\right]_{B_{act}}\end{aligned} \tag{13}$$

We can verify the inner product $< _0, \ ^{\perp} >=0$. To verify that $^{\perp}$ can be written as a linear combination of $_{0y}$ and $_{1y}$; we begin by writing the following two equations

$$\begin{aligned}\gamma_0^{-1}\mathbf{V}_{0y} &= \left[\Delta^- \quad -\rho^T\right]_{B_{act}} \\ \gamma_1^{-1}\mathbf{V}_{1y} &= \left[\Delta^+ \quad -\rho^T\right]_{B_{act}}\end{aligned} \tag{14}$$

and by forming the linear combination

$$\frac{1}{\Delta^- - \Delta^+}\left(\Delta^-\gamma_0^{-1}\mathbf{V}_{0y} - \Delta^+\gamma_1^{-1}\mathbf{V}_{1y}\right) = \left[0 \quad -\rho^T\right]_{B_{act}} \tag{15}$$

We can express

$$\sqrt{\rho^T\rho\left(1-\rho^T\rho\right)}\mathbf{V}^{\perp} = \left[\rho^T\rho \quad -\rho^T\right]_{B_{act}} = \rho^T\rho\mathbf{s}_0 + \left[0 \quad -\rho^T\right]_{B_{act}}$$

After some manipulations we get

e e i i e i e e e e i i

$$\mathbf{V}^{\perp} = \frac{1}{2\sqrt{\rho^T\rho(1-\rho^T\rho)}}\left[(1-\Theta^-)\gamma_0^{-1}\mathbf{V_{0y}} + (1+\Theta^+)\gamma_1^{-1}\mathbf{V_{1y}}\right] \tag{16}$$

where $\Theta^{\pm} = \dfrac{1-\alpha^{-2} \pm 2\rho^T\rho}{\sqrt{(1-\alpha^{-2})^2 + 4\alpha^{-2}\rho^T\rho}}$

As the three fixed receivers we will examine all project the received signal onto Γ_E, the vector $\mathbf{x_0}$ orthogonal to $\mathbf{s_0}$ must be a constant times the vector $\mathbf{V}^{\perp}$. This will allow us to parameterize these receivers by the constant multiplying $\mathbf{V}^{\perp}$, a constant we will call β, *i.e.*,

$$\mathbf{c} = \mathbf{s}_0 + \beta\ \mathbf{V}^{\perp} \tag{17}$$

Conventional detector

The conventional receiver (or matched filter) is given by $\mathbf{c_{MF}} = \mathbf{s_0}$, so that clearly β = 0 in our parameterization.

Decorrelating detector

From section 2.5

$$\mathbf{c_{DEC}} = \left[1, \quad -\rho^T\right]_{B_s}^T \tag{18}$$

The form of $\mathbf{V}^{\perp}$ and $\mathbf{c_{DEC}}$ allows us to write the following linear combination

$$\mathbf{c_{DEC}} = \sqrt{\rho^T\rho(1-\rho^T\rho)}\cdot\mathbf{V}^{\perp} + (1-\rho^T\rho)\mathbf{s_0} \tag{19}$$

To arrive at the canonical form of the decorrelating detector we normalize with respect to $\langle \mathbf{s_0}, \mathbf{c_{DEC}} \rangle$ and we arrive at

$$\begin{aligned}\mathbf{c_{DEC}} &= \frac{1}{\sqrt{1-\rho^T\rho}}\cdot\left[1 \quad -\rho^T\right]_{B_s} \\ &= \mathbf{s_0} + \sqrt{\frac{\rho^T\rho}{1-\rho^T\rho}}\cdot\mathbf{V}^{\perp} \\ &= \mathbf{s_0} + \beta_{DEC}\cdot\mathbf{V}^{\perp}\end{aligned} \tag{20}$$

which demonstrates that this detector does indeed fall in Γ_E.

The MMSE detector

We now derive an expression for the detector which minimizes the mean square error (MMSE) reported simultaneously in [31] and [33]. Per [12], the detector which minimizes the MSE is determined by the inverse of the matrix $\mathbf{R}+\sigma^2\mathbf{W}^{-1}$ where $\mathbf{R}$ is the cross correlation matrix and $\mathbf{W}$ is the diagonal matrix of user powers. As previously explained in section 2.5, for our system this inverse can be found explicitly as a function of the interference power, the noise power and the cross correlation vector ρ, yielding

$$\mathbf{c}_{\mathrm{MMSE}} = \frac{1}{1-\rho^T\rho+\sigma^2/w_I}\cdot\left[\left(1+\sigma^2/w_I\right) \quad -\rho^T\right]_{B_{\mathrm{act}}} \tag{21}$$

We normalize this expression to arrive at

$$\begin{aligned}\mathbf{c}_{\mathrm{MMSE}} &= \mathbf{s}_0 + \frac{\sqrt{\rho^T\rho\left(1-\rho^T\rho\right)}}{1-\rho^T\rho+\sigma^2/w_I}\,\mathbf{V}^{\perp} \\ &= \mathbf{s}_0 + \beta_{MMSE}\,\mathbf{V}^{\perp}\end{aligned} \tag{22}$$

The decision statistic, the near far ratio, and the probability of error of the MMSE detector are derived in section 2.5.

The parametrization introduced is possible as any interesting linear receiver will lie in Γ_E. In chapter 4 we derive the decision statistic, the near far resistance, the mean output energy, the signal to interference ratio, and the probability of error of a generalized linear detector as function of only a single variable, β.

3.4. Subspace Approach for Blind Adaptation

In this section we examine the stochastic gradient algorithm which converges to the minimum of the MOE, and hence the MMSE receiver [14], reproduced in section 1.5. As mentioned previously, the approach is based on the decomposition of the linear multiuser

detector into the sum of two orthogonal components. One of these components is equal to the signature waveform of the desired user which is assumed known. The canonical representation of the detector can be expressed by the following equation [14]

$$\mathbf{c}_0=\mathbf{s}_0+\mathbf{x}_0, \text{ where } <\mathbf{s}_0, \mathbf{x}_0> = 0$$

3.4.1. Adaptation algorithm

Minimization criteria

We consider the linear detector in canonical form that minimizes (over all $\mathbf{x}_0$ orthogonal to $\mathbf{s}_0$) the mean output energy of a detector. We calculate first the mean output voltage of this detector given the true SS bit value

$$\mathrm{E}\left\{\left\langle \mathbf{s}_0+\mathbf{x}_0,\mathbf{y}\right\rangle \middle| \mathrm{b}_0\right\} = \mathrm{E}\left\{\left\langle \mathbf{s}_0+\mathbf{x}_0,\sqrt{w_0}\mathrm{b}_0\mathbf{s}_0+\sqrt{w_0}\sum_{i=1}^{m}\mathrm{b}_i\mathbf{s}_i+\mathbf{n}\right\rangle \middle| \mathrm{b}_0\right\}$$

Given that the noise is zero mean and that the bits are equiprobable ±1, we arrive to

$$\begin{aligned}\mathrm{E}\left\{< \mathbf{s}_0+\mathbf{x}_0,\mathbf{y} > /\mathrm{b}_0\right\} &= \sqrt{w_0}\mathrm{b}_0 < \mathbf{s}_0+\mathbf{x}_0,\mathbf{s}_0 > \\ &= \sqrt{w_0}\mathrm{b}_0\end{aligned}$$

Recall that the output voltage of the detector is its decision statistic (D.S.). The mean output energy is statistically the second order moment of the output voltage given the true SS bit value

$$\mathrm{MOE}(\mathbf{x}_0) = E\left\{< \mathbf{s}_0+\mathbf{x}_0,\mathbf{y} >^2 \middle| \mathrm{b}_0\right\} \tag{23}$$

The mean square error (MSE) at the output can be viewed as the variance of this linear detector. It's clear that MSE($\mathbf{x}_0$) can be written using the first order and the second order moments of the detector output voltage. We calculate the function MSE($\mathbf{x}_0$)

$$\begin{aligned}\mathrm{MSE}(\mathbf{x}_0) &= \mathrm{E}\left\{\left(\sqrt{w_0}b_0 - < \mathbf{s}_0+\mathbf{x}_0,\mathbf{y} >\right)^2\right\} \\ &= w_0 + \mathrm{MOE}(\mathbf{x}_0) - 2w_0 < \mathbf{s}_0+\mathbf{x}_0,\mathbf{s}_0 > \\ &= \mathrm{MOE} - w_0\end{aligned} \tag{24}$$

b b wb

verifying

$$\mathrm{Var}\{\mathrm{D.S.}|\mathrm{b}_0\} = \mathrm{E}\{\mathrm{D.S.}^2|\mathrm{b}_0\} - \mathrm{E}\{\mathrm{D.S.}|\mathrm{b}_0\}^2 \tag{25}$$

From this equation, it can be seen that the MMSE and MOE differ by a constant. This means that the MMSE detector necessarily minimizes the MOE as well. It is shown in [14] that the function MOE is strictly convex, so that the MSE is also a convex function. The stochastic gradient algorithm will use the MSE as the minimization function for adaptation.

Adaptation rule

The output energy function MOE lends itself to a simple stochastic gradient-descent adaptation rule. Let $\mathbf{y}(i)$ be the observed waveform in the i^{th} bit interval [iT, iT+T]. Let $z_{MF}(i)$ be the output of the conventional detector during this bit interval

$$z_{MF}(i) = <\mathbf{s}_0, \mathbf{y}(i)> \tag{26}$$

and z(i) the output of the adaptive detector during the i^{th} bit interval

$$z(i) = <\mathbf{s}_0 + \mathbf{x}_0(i-1), \mathbf{y}(i)> = <\mathbf{c}(i), \mathbf{y}(i)> \tag{27}$$

To derive the adaptation rule for $\mathbf{x}_0(i)$ we take the unconditioned gradient of MOE($\mathbf{x}_0$), that is equal to a scaled version of the observations

$$2 < \mathbf{s}_0 + \mathbf{x}_0, \mathbf{y} > \mathbf{y} \tag{28}$$

The component of $\mathbf{y}$ orthogonal to $\mathbf{s}_0$ is given by $\mathbf{y} - <\mathbf{s}_0, \mathbf{y}> \mathbf{s}_0$. Therefore, the stochastic gradient adaptation rule is

$$\mathbf{x}_0(i) = \mathbf{x}_0(i-1) - \mu\, z(i)\left[\mathbf{y}(i) - z_{MF}(i)\mathbf{s}_0\right] \tag{29}$$

As mentioned previously, interest in the MMSE receiver is motivated by the existence of this adaptive version. The stochastic gradient algorithm does not require information about the interfering users' power, timing or signature sequences, nor does it requires a training sequence.

We adopt the same signal space approach introduced previously to examine the dynamics of the adaptive algorithm. We exploit the orthogonality of the interference signals to demonstrate that the adaptive receiver is, on average, confined to the two dimensional subspace Γ_E. This contrasts with previous analysis of arbitrary interferers (non-orthogonal), which isolated the receiver only within the $m+2$ dimensional space $\Gamma_{act.}$ Because of the lower dimensionality of the subspace Γ_E, we are able to identify a less restrictive stability constraint on the step-size in the adaptation, allowing for significantly faster convergence. Note that the stochastic gradient is a noisy algorithm. Noise outliers will lead the algorithm out of Γ_E, with no zero components in the noise only subspace Γ_{NO}. To avoid this behavior the receiver should switch to a fixed receiver or decision-directed least mean squares (LMS) algorithm after nominal convergence to the MMSE receiver.

3.4.2. System Dynamics - Eigenspaces of $\mathbf{R}_{vy}$

As mentioned earlier, the receiver that minimizes the MOE also minimizes the MSE. A gradient descent algorithm was proposed to adaptively minimize the convex function MOE. This linear detector is written in the canonical form, that is, as the sum of the desired user's signature sequence plus a vector orthogonal to this signature sequence, $\mathbf{c} = \mathbf{s}_0 + \mathbf{x}_0$. The adaptation algorithm is

$$\mathbf{c}(n) = \mathbf{c}(n-1) - \mu \cdot \langle \mathbf{c}(n), \mathbf{y}(n) \rangle \cdot \left(\mathbf{y}(n) - \langle \mathbf{s}_0, \mathbf{y}(n) \rangle \cdot \mathbf{s}_0 \right) \tag{30}$$

where the index n refers to the iteration or bit interval. Note that at each iteration we are scaling the projection of the received signal onto the space orthogonal to $\mathbf{s}_0$ to update the vector $\mathbf{c}$. We define the vector $\mathbf{v}(n) = \left(\mathbf{I}_N - \mathbf{s}_0 \mathbf{s}_0^T \right) \mathbf{y}(n)$, that is, v(n) is the product of the projection matrix $\left(\mathbf{I}_N - \mathbf{s}_0 \mathbf{s}_0^T \right)$ and the received signal. With this definition the algorithm can be written as

$$\mathbf{c}(n) = \left[\mathbf{I}_N - \mu \mathbf{v}(n) \mathbf{y}^T(n) \right] \mathbf{c}(n-1) \tag{31}$$

Taking expectations of both sides we have

$$\begin{aligned} E\{\mathbf{c}(n)\} &= \left[\mathbf{I}_{\mathrm{N}} - \mu E\{\mathbf{v}(n)\mathbf{y}^{T}(n)\}\right] E\{\mathbf{c}(n-1)\} \\ &= \left[\mathbf{I}_{\mathrm{N}} - \mu \mathbf{R}_{\mathbf{vy}}\right] E\{\mathbf{c}(n-1)\} \end{aligned} \tag{32}$$

To study the dynamics of the adaptive system, we therefore examine the covariance matrix $\mathbf{R}_{\mathbf{vy}}$.

Eigenvalue calculation

As in the previous section for $\mathbf{R}_{\mathbf{yy}}$, we demonstrate that Γ_{act} is $\mathbf{R}_{\mathbf{vy}}$ invariant and we determine the restriction $\tilde{\mathbf{R}}_{\mathbf{vy}}$ of $\mathbf{R}_{\mathbf{vy}}$ in Γ_{act}. We calculate the eigenvalues and eigenvectors of $\tilde{\mathbf{R}}_{\mathbf{vy}}$ using the same method as that used for the $\tilde{\mathbf{R}}_{\mathbf{yy}}$ eigenvalue calculation, and note that the eigenvalues were simultaneously reported in [33] and [34]. In the basis B_{act} we obtain the special arrow structure

$$\tilde{\mathbf{R}}_{\mathbf{vy}} = \begin{bmatrix} -w_I \rho^{\mathrm{T}} \rho & -\left(w_I + \sigma^2\right)\rho^{\mathrm{T}} \\ w_I \rho & \left(w_I + \sigma^2\right)\mathbf{I}_{\mathrm{m+1}} \end{bmatrix}_{\mathrm{B_{act}}} \tag{33}$$

After column elimination, we arrive at the upper triangular matrix

$$\left(w_I + \sigma^2 - \lambda\right)\left[\tilde{\mathbf{R}}_{\mathbf{vy}} - \lambda \mathbf{I}_{\mathbf{m+2}}\right]_{\Gamma_{act}} = \begin{bmatrix} -\left(w_I \rho^T \rho + \lambda\right)\left(w_I + \sigma^2 - \lambda\right) + w_I\left(w_I + \sigma^2\right)\rho^T \rho & -\left(w_I + \sigma^2\right)\rho^T \\ 0 & \left(w_I + \sigma^2 - \lambda\right)\mathbf{I}_{\mathbf{m+1}} \end{bmatrix}_{B_{\mathrm{act}}}$$

which yields the characteristic polynomial

$$P_c(\lambda) = -\lambda\left(w_I\left(1 - \rho^T \rho\right) + \sigma^2 - \lambda\right)\left(w_I + \sigma^2 - \lambda\right)^m \tag{34}$$

The eigenvalues which solve this characteristic polynomial are

$$\begin{aligned} &\lambda_{0v} = 0 \\ &\lambda_{1v} = w_I\left(1 - \rho^T \rho\right) + \sigma^2 \\ &\lambda_{iv} = w_I + \sigma^2 \qquad\qquad 2 < \mathrm{i} < \mathrm{m} + 1 \end{aligned} \tag{35}$$

Similarly as for $\mathbf{R}_{\mathbf{yy}}$, we demonstrate that Γ_{NO} is $\mathbf{R}_{\mathbf{vy}}$-invariant and we determine the restriction

$$\begin{aligned}
&\lambda_{0v} = 0 \\
&\lambda_{1v} = w_I\left(1-\rho^T\rho\right)+\sigma^2 \\
&\lambda_{iv} = w_I + \sigma^2 \qquad\qquad 2 < \mathrm{i} < \mathrm{m}+1 \\
&\lambda_{iv} = \sigma^2 \qquad\qquad m+2 < \mathrm{i} < \mathrm{N}-1
\end{aligned} \tag{36}$$

Eigenvector determination

As noted earlier, $\tilde{\mathbf{R}}_{\mathbf{vy}}$ can be expressed as

$$\tilde{\mathbf{R}}_{\mathbf{vy}} = \left(\mathbf{I_N} - \mathbf{s_0}\mathbf{s_0}^T\right)\tilde{\mathbf{R}}_{\mathbf{yy}} \tag{37}$$

The matrix $\mathbf{I}_N - \mathbf{s}_0\mathbf{s}_0^T$ is well described in Householder's book[38]. In fact, it defines a projection of the N dimensional space along the direction of $\mathbf{s}_0$. The matrix $\mathbf{I}_N - \mathbf{s}_0\mathbf{s}_0^T$ has these important properties:

$I.\ I\quad \mathbf{V}\perp\mathbf{s}_0,\qquad \left(\mathbf{I}_N - \mathbf{s}_0\mathbf{s}_0^T\right)\mathbf{V} = \mathbf{V}\qquad y\ V \in\quad \Gamma\ .$

$.\ I\quad \mathbf{V}\ /\ /\ \mathbf{s}_0,\qquad \left(\mathbf{I}_N - \mathbf{s}_0\mathbf{s}_0^T\right)\mathbf{V} = 0.$

These properties allow us to conclude

$$\mathbf{s_0} \perp \Gamma_{I\&N} \quad\Rightarrow\quad \left\langle\left(\mathbf{I_N} - \mathbf{s_0}\mathbf{s_0}^T\right), \Gamma_{I\&N}\right\rangle = \Gamma_{I\&N} \quad\Rightarrow\quad \mathbf{V_{iv}} = \mathbf{V_{iy}} \quad \text{for} \quad 2 \le i \le m+1$$

$$\mathbf{s_0} \perp \Gamma_{NO} \quad\Rightarrow\quad \left\langle\left(\mathbf{I_N} - \mathbf{s_0}\mathbf{s_0}^T\right), \Gamma_{NO}\right\rangle = \Gamma_{NO} \quad\Rightarrow\quad \mathbf{V_{iv}} = \mathbf{V_{iy}} \quad \text{for} \quad m+2 \le i \le \mathrm{N}-1$$

The projection matrix changes only the two first eigenvectors of $_{yy}$ that span Γ_E, because they are the only eigenvectors in Γ which are not orthogonal to the SS signature vector $\mathbf{s_0}$. Since all the other eigenvectors spanning the subspaces $\Gamma_{I\&N}$ and Γ_{NO} are orthogonal to $\mathbf{s_0}$, they do not change with the projection operator $\mathbf{I}_N - \mathbf{s}_0\mathbf{s}_0^T$. The two eigenvectors $\mathbf{V_{0v}}$ and $\mathbf{V_{1v}}$ relate respectively to the two eigenvalues λ_{0v} and λ_{1v}, and they span the planar subspace Γ_E. We arrive at

$$\mathbf{V}_{0v} = \frac{1}{\gamma_0'}\left[1 + \frac{\sigma^2}{w_I} \quad -\rho^T\right] \quad , \quad \gamma_0' = \sqrt{\left(1+\frac{\sigma^2}{w_I}\right)^2\left(1-\rho^T\rho\right)+\left(\frac{\sigma^2}{w_I}\right)^2\rho^T\rho}$$

$$\mathbf{V}_{1v} = \frac{1}{\gamma_1'}\left[\rho^T\rho \quad -\rho^T\right] \quad , \qquad \gamma_1' = \sqrt{\rho^T\rho\left(1-\rho^T\rho\right)}$$

The eigenvector $\mathbf{V}_{0v}$ is a normalized version of the MMSE detector. $\mathbf{V}_{1v}$ is equal to $\mathbf{V}^{\perp}$, the normalized vector in Γ_E orthogonal to the desired user signature $_0$. $_0$ can be expressed as linear combination of the eigenvectors $\mathbf{V}_{0v}$ and $\mathbf{V}_{1v}$

$$\mathbf{s}_0 = \frac{1}{1-\rho^T\rho+\sigma^2/w_I}\left(\gamma_0'\mathbf{V}_{0v} - \gamma_1'\mathbf{V}_{1v}\right) \tag{39}$$

Extension of results in [33]

In [33], Poor and Wang define the matrix $\tilde{\mathbf{R}}_{vv} = \left(\mathbf{I}_N - \mathbf{s}_0\mathbf{s}_0^T\right)\tilde{\mathbf{R}}_{yy}\left(\mathbf{I}_N - \mathbf{s}_0\mathbf{s}_0^T\right)$. In order to simplify calculation of the tap weight error correlation matrix, they made the approximation $\Lambda_{yy} \approx \Lambda_{vy} \approx \Lambda_{vv}$, where Λ_{yy}, Λ_{vy}, and Λ_{vv}, are respectively the diagonal forms of, $\tilde{\mathbf{R}}_{yy}$, $\tilde{\mathbf{R}}_{vy}$ and $\tilde{\mathbf{R}}_{vv}$. We write $\tilde{\mathbf{R}}_{vv} = \tilde{\mathbf{R}}_{vy}\left(\mathbf{I}_N - \mathbf{s}_0\mathbf{s}_0^T\right)$ and use the properties of the projection matrix to determine the eigenvalues and eigenvectors of $\tilde{\mathbf{R}}_{vv}$.

$\tilde{\mathbf{R}}_{vv}\mathbf{s}_0 = 0$, so $_0$ is the first eigenvector of $\tilde{\mathbf{R}}_{vv}$, relative to a zero eigenvalue. All the other eigenvectors of $\tilde{\mathbf{R}}_{vv}$ are orthogonal to $_0$, and therefore are invariant under the Householder transformation. $\tilde{\mathbf{R}}_{vv}$ has the same eigenvalues as $\tilde{\mathbf{R}}_{vy}$. We conclude that the approximation made in [33] is partially exact, *i.e.,*

$$\Lambda_{yy} \neq \Lambda_{vy} = \Lambda_{vv} \tag{40}$$

Because of the special form of the projection matrix, we expect the eigenvectors of $\tilde{\mathbf{R}}_{vy}$ to follow those of $\tilde{\mathbf{R}}_{vv}$, except those eigenvectors falling in Γ_E, *i.e.*, in directions containing energy from $_0$. Indeed our calculations show that the two matrices have the same eigenvectors for $2 \leq i \leq N-1$. The first two eigenvectors on the other hand are different.

We make two important observations: the first eigenvector is a multiple of the MMSE receiver, and the second eigenvector is the vector $^{\perp}$ defined in section 3.3 together they span the space Γ_E. Note that these eigenvectors are not orthogonal (because $\tilde{\mathbf{R}}_{\mathbf{vy}}$ is not symmetric), however $_{1v} \perp _{0}$. It should be noted that the set of basis vectors B_{yy} formed by the eigenvectors of R_{yy} and the set of basis vectors B_{vy} formed by the eigenvectors of $\tilde{\mathbf{R}}_{\mathbf{vy}}$ differ only in the first two vectors that describe the subspace Γ_E by $_{0y}$ and $_{1y}$, instead of B_{vy} describe it by $_{0v}$ and $_{1v}$.

3.5. Tap Weight Trajectory

Having analyzed the matrix $\tilde{\mathbf{R}}_{\mathbf{vy}}$, we are now prepared to follow the trajectory of the mean tap weight defined by

$$\bar{\mathbf{c}}(n) = E\{\mathbf{c}(n)\} = \left[\mathbf{I}_{\mathbf{N}} - \mu\tilde{\mathbf{R}}_{\mathbf{vy}}\right]\bar{\mathbf{c}}(n-1) \tag{41}$$

We will express the matrix $\tilde{\mathbf{R}}_{\mathbf{vy}}$ in a basis of its eigenvectors B_{vy} to yield a diagonal form. The initial value of the tap weight is taken to be the desired user's spreading code (*i.e.*, we initiate the algorithm with the matched filter receiver). Therefore, writing $_{0}$ in the basis B_{vy}, we arrive at

$$\begin{aligned}
\bar{\mathbf{c}}(n) &= \left[\mathbf{I}_{\mathbf{N}} - \mu\tilde{\mathbf{R}}_{\mathbf{vy}}\right]_{B_{vy}}^{n}\mathbf{s}_{\mathbf{0}} = \left[\mathbf{I}_{\mathbf{N}} - \mu\tilde{\mathbf{R}}_{\mathbf{vy}}\right]_{B_{vy}}^{n}\frac{1}{1-\rho^{T}\rho+\sigma^{2}/w_{I}}\cdot\left[\gamma_0' \quad -\gamma_1' \quad 0 \quad \cdots \quad 0\right]_{B_{vy}}^{T} \\
&= \frac{1}{1-\rho^{T}\rho+\sigma^{2}/w_{I}}\left[\mathrm{diag}\left[1 \; 1-\mu\lambda_{1v} \; 1-\mu\lambda_{2v} \; \cdots \; 1-\mu\lambda_{Nv}\right]_{B_{vy}}\right]^{n}\cdot\left[\gamma_0' \quad -\gamma_1' \quad 0 \quad \cdots \quad 0\right]^{T} \\
&= \frac{1}{1-\rho^{T}\rho+\sigma^{2}/w_{I}}\left[\gamma_0' \quad -\gamma_1'(1-\mu\lambda_{1v})^{n} \quad 0 \quad \cdots \quad 0\right]_{B_s}^{T} \\
&= \frac{\gamma_0'}{1-\rho^{T}\rho+\sigma^{2}/w_{I}}\mathbf{V}_{\mathbf{0v}} - \frac{\gamma_1'(1-\mu\lambda_{1v})^{n}}{1-\rho^{T}\rho+\sigma^{2}/w_{I}}\mathbf{V}_{\mathbf{1v}}
\end{aligned}$$

The mean tap weight vector falls entirely in the subspace Γ_E, therefore we can write it in canonical parametrized form as

n n w n n n n n

$$\bar{\mathbf{c}}(n) = \mathbf{s}_0 + \frac{\sqrt{\rho^T\rho(1-\rho^T\rho)}}{1-\rho^T\rho+\sigma^2/w_I}\left(1-\left[1-\mu\left(w_I(1-\rho^T\rho)+\sigma^2\right)\right]^n\right)\cdot\mathbf{V}^\perp$$

It is clear that the second term on the right hand side of the above equation represents the vector $\mathbf{x}_0(n)$ which is orthogonal to the SS user sequence $\mathbf{s}_0$. We demonstrate here that the direction of $\mathbf{x}_0(n)$ does not change with n. $\mathbf{x}_0(n)$ has the fixed direction of $\mathbf{V}^\perp$ all the time. Thus, only the norm of $\mathbf{x}_0(n)$ changes with the time, the instantaneous value of β.

Parametrized mean trajectory

We demonstrate that only the length of $\mathbf{x}_0$ changes with the mean evolution of the blind adaptive detector. Let $\beta(n)$ be the length of $\mathbf{x}_0(n)$, we write

$$\beta(n) = \frac{\sqrt{\rho^T\rho(1-\rho^T\rho)}}{1-\rho^T\rho+\sigma^2/w_I}\left(1-\left[1-\mu\lambda_{1v}\right]^n\right) \tag{44}$$

which is an alternate mono-variable representation of the adaptive algorithm.

Asymptotic behavior of the adaptive algorithm

If the convergence conditions are met, as n tends to infinity $\mathbf{c}(n)$ approaches the MMSE detector.

$$\lim_{n\to\infty}\bar{\mathbf{c}}(n) = \mathbf{s}_0 + \frac{\sqrt{\rho^T\rho(1-\rho^T\rho)}}{1-\rho^T\rho+\sigma^2/w_I}\cdot\mathbf{V}^\perp = \mathbf{s}_0 + \beta_{MMSE}\mathbf{V}^\perp \tag{45}$$

we verify also that

$$\lim_{\substack{n\to\infty \\ \sigma^2/w_I\to 0}} = \mathbf{s}_0 + \beta_{DEC}\cdot\mathbf{V}^\perp = \mathbf{c}_{\mathrm{DEC}} \tag{46}$$

3.6. Two new step sizes

Using the results of [14], it can be shown that the algorithm, derived in section 3.4.1, converges regardless of the initial condition to the MMSE detector, provided that the step size shrinks as one over the iteration number

$$\mu[i] < \frac{1}{i} \tag{47}$$

In [12], Honig shows that for stability, we must have

$$0 \le \mu < \min_k \frac{2}{\left|\lambda_k^{vy}\right|} = \frac{2}{\max_k \left|\lambda_k^{vy}\right|} \tag{48}$$

Alternatively, Honig show in [14] that stability is also generated if the step size meets the following criterion

$$0 \le \mu < \frac{2}{tr\,\mathbf{R}_{\mathbf{vy}}} = \frac{2}{\sum_{i=0}^{m+1} \lambda_k^{vy}} \tag{49}$$

however, convergence is very slow. In the following we derive a new step size that provides much faster convergence [33].

New fixed step size

Given that $\lambda_{0v} = 0$, the only eigenvalue that effects the stability of the algorithm is λ_{1v}, so that

$$\mu < \frac{2}{w_I\left(1-\rho^T\rho\right)+\sigma^2} \tag{50}$$

ensures convergence of the mean tap vector. Using the iterative expression $\beta(n)$, we calculate the limit of $\beta(n)$ as n tends to infinity.

$$\lim_{n\to\infty}\beta(n) = \frac{\sqrt{\rho^T\rho\left(1-\rho^T\rho\right)}}{1-\rho^T\rho+\sigma^2/w_I}\lim_{n\to\infty}\left(1-\left[1-\mu\lambda_{1v}\right]^n\right)$$
$$= \frac{\sqrt{\rho^T\rho\left(1-\rho^T\rho\right)}}{1-\rho^T\rho+\sigma^2/w_I}\left(1-\lim_{n\to\infty}\left[1-\mu\lambda_{1v}\right]^n\right) \qquad (51)$$
$$= \frac{\sqrt{\rho^T\rho\left(1-\rho^T\rho\right)}}{1-\rho^T\rho+\sigma^2/w_I} = \beta_{\text{MMSE}}$$

This is a less restrictive stability constraint than the maximum eigenvalue of $\mathbf{R}_{vy}$ proposed in [14], and reproduced below for the system under consideration.

$$\mu < \frac{2}{\max\left(\left|\lambda_{\mathbf{R}_{vy}}\right|\right)} = \frac{2}{w_I+\sigma^2} \qquad (52)$$

It is of interest to mention that for a different scenario where there are many CDMA users operating in the presence of several narrowband interferers, the adaptive receiver would not be confined to a 2-D space. In fact, any additional CDMA user introduces a new dimension in the effective energy eigenspace. In interpreting the narrowband interference as m+1 CDMA users we would expect Γ_E to grow similarly in dimension. However, we show that being a single signal it, in fact, only contributes one dimension to Γ_E and we exploit this fact for faster convergence. In terms of generalization, while analytic expressions would become more complicated, the existence of faster convergence criteria is nevertheless established.

New variable step size[5]

Using the expression of the instantaneous parameter $\beta(i)$, we define the instantaneous mean evolution of the algorithm (IME) as a function of the step size

[5] This variable constraint was presented in the *Interference Rejection and Signal Separation in Wireless Communications Symposium*, George Washington University, March 18, 1997 [37]

$$\begin{aligned}\mathrm{IME}(\mu) &= \beta(i)-\beta(i-1)\\ &= \frac{\sqrt{\rho^T\rho\left(1-\rho^T\rho\right)}}{1-\rho^T\rho+\sigma^2/w_I}\left(\left[1-\mu\lambda_{1v}\right]^{i-1}-\left[1-\mu\lambda_{1v}\right]^{i}\right)\\ &= \mu\lambda_{1v}\frac{\sqrt{\rho^T\rho\left(1-\rho^T\rho\right)}}{1-\rho^T\rho+\sigma^2/w_I}\left[1-\mu\lambda_{1v}\right]^{i-1}\\ &= \mu w_I\sqrt{\rho^T\rho\left(1-\rho^T\rho\right)}\left[1-\mu\lambda_{1v}\right]^{i-1}\end{aligned} \tag{53}$$

We define also the relative mean evolution of the algorithm (RIME), as the ratio of the IME to β_{MMSE}.

$$\frac{\beta(i)-\beta(i-1)}{\beta_{\mathrm{MMSE}}} = \mu\lambda_{1v}\left[1-\mu\lambda_{1v}\right]^{i-1} \tag{54}$$

We propose to find the step size that maximizes the ratio RIME. As the logarithm is a monotone function we maximize

$$\ln\left[\frac{\beta(i)-\beta(i-1)}{\beta_{\mathrm{MMSE}}}\right] = \ln[\mu]+\ln\left[\lambda_{1v}\right]+(i-1)\ln\left[1-\mu\lambda_{1v}\right] \tag{55}$$

We take the derivative and set it equal to zero

$$\frac{\partial}{\partial\mu}(\cdot) = \frac{1}{\mu}-\frac{(i-1)\lambda_{1v}}{1-\mu\lambda_{1v}} = 0 \tag{56}$$

This equation has solution

$$1-\mu\lambda_{1v} = (i-1)\mu\lambda_{1v} \Rightarrow \quad \mu = \frac{1}{i\lambda_{1v}}$$

To verify that the derived μ effectively maximizes the RIME, we calculate the second derivative and we compare it to zero

$$\frac{\partial^2}{\partial \mu^2}(\cdot) = -\frac{1}{\mu^2} - \frac{(i-1)\lambda_{1v}^2}{(1-\mu\lambda_{1v})^2} = -\left[\frac{1}{\mu^2} + \frac{(i-1)\lambda_{1v}^2}{(1-\mu\lambda_{1v})^2}\right] \le 0 \tag{57}$$

Since the second derivative is always negative, the derived expression m maximizes the RIME. Thus, we arrive at a new time variant constraint to the step size

$$\mu(i) < \frac{1}{i\lambda_{1v}} \tag{58}$$

It is of interest to show that the new variable constraint to the step size is a product of our previous fixed step size, and that of [14]. The new step size limit is able to increase the convergence rate of the algorithm by employing a large step sizes in the beginning of adaptation. The step size decreases with time, which provides an important enhancement of the quality of convergence.

Performance analysis and a new detector[6]

4.1. Introduction

In chapter 3, the brunt of our analysis is placed in examination of the signal space and how various receivers project energy in this space. We examined the eigenspaces of the received signal's covariance matrix to partition the signal space in three subspaces, Γ_{NO}, $\Gamma_{I\&N}$ and Γ_E. We discovered that Γ_E is a two dimensional subspace which contains all the energy of the desired signal and a subset of the interference and noise energies. We showed that for our virtual CDMA system, the three fixed receivers of interest all project the received signal onto this two-dimensional subspace. By identifying this space we were able to parameterize the receivers of interest by a single variable. The low dimension of the effective energy space allowed us to define a general form of a linear receiver as function of one parameter. Each receiver of interest was characterized by a particular value of this parameter.

---

[6] This Chapter was presented in IEEE Globecom 1996 [35].

In section 4.2, we use the simple parametrized form of the linear detector to formulate a parametrized version of the probability of error, the asymptotic efficiency, the near far resistance, the mean output energy MOE, and the signal to interference ratio SIR. This parameterization allows an alternate derivation of the MMSE receiver and also allows us to see the effect of weak interference on the mean output energy (MOE). Using our single parameter model of the MOE we identify an anomaly in the convergence of the algorithm for weak interferers. In section 4.3, we show that while the MOE is always convex, it is extremely shallow for weak interference signals. The shallow convexity ensures that the algorithm will not be trapped by local minima, however it is easily lead astray by spurious noise samples. We examine how system parameters affect the efficiency of the convergence of the adaptive algorithm. We find the algorithm cannot effectively converge to the MMSE receiver when the narrowband interference power is weaker than the spread spectrum signal's power. We present simulation results for the fixed and adaptive receivers. Monte Carlo simulations confirm theoretical calculations of the probability of error for all receivers. We show faster convergence of the stochastic gradient algorithm when the constant new, looser constraint is applied to the step size, focusing on convergence along the eigenvectors of interest. We also match Monte Carlo results to theoretical results for the parameterized mean output energy illustrating sensitivity to interference power.

Finally, in section 4.4, we propose a new detector which avoids the convergence anomalies and use the new constraint on the step size to achieve faster convergence.

4.2. Parametrized performance measures

4.2.1. Probability of error

As mentioned previously, every linear filter which is intended to recover the true SS user bits in our virtual CDMA system model described by Figure 2.10, can be expressed in the simple canonical parametrized form

$$\mathbf{c}_0 = \mathbf{s}_0 + \beta\, \mathbf{V}^{\perp} \tag{1}$$

as function of a single parameter β. As explained in the previous chapter, the parameter β entirely characterize any linear receiver for our system model. Recall that the NB interferer is cast as m+1 mutually orthogonal virtual CDMA signal. We generate the detector estimate of the SS bit using

$$\hat{b}_0 = \mathrm{sgn}\left[\int_0^T \mathbf{c}_0(t)\mathbf{y}(t)dt\right] \tag{2}$$

equivalently, in the discrete model version

$$\begin{aligned}\hat{b}_0 &= \mathrm{sgn}\left[<\mathbf{c}_0, \mathbf{y}>\right] \\ &= \mathrm{sgn}\left[<\mathbf{s}_0, \mathbf{y}> + \beta <\mathbf{s}_0, \mathbf{V}^{\perp}>\right] \\ &= \mathrm{sgn}\left[\mathrm{D.S.}\right]\end{aligned}$$

where D.S. is the decision statistic, or the output voltage, of the receiver.

Decision statistic calculation

In order to determine the probability of error we examine the decision statistic D.S. for the SS bit. Using (1) and (3) we calculate

$$\mathrm{D.S.} = <\mathbf{s}_0, \mathbf{y}> + \beta <\mathbf{V}^{\perp}, \mathbf{y}> \tag{3}$$

Then first term is

$$\begin{aligned}<\mathbf{s}_0, \mathbf{y}> &= <\mathbf{s}_0, b_0\mathbf{s}_0 + \sqrt{w_I}\sum_{i=1}^{m+1} b_i\mathbf{s}_i + \sigma\,\mathbf{n}> \\ &= b_0 + \sqrt{w_I}\sum_{i=1}^{m+1} b_i <\mathbf{s}_0, \mathbf{s}_i> + \sigma <\mathbf{s}_0, \mathbf{n}> \\ &= b_0 + \sqrt{w_I}\rho^{\mathrm{T}}\mathbf{b} + \sigma <\mathbf{s}_0, \mathbf{n}>\end{aligned} \tag{4}$$

The second term is

$$\begin{aligned}<\mathbf{V}^{\perp}, \mathbf{y}> &= <x\left(\rho^{\mathrm{T}}\rho\mathbf{s}_0 - \sum_{i=1}^{m+1}\rho_i\mathbf{s}_i\right), b_0\mathbf{s}_0 + \sqrt{w_I}\sum_{i=1}^{m+1} b_i\mathbf{s}_i + \sigma\,\mathbf{n}> \\ &= x\left(-\sqrt{w_I}\left(1-\rho^{\mathrm{T}}\rho\right)\rho^{\mathrm{T}}\mathbf{b} + \sigma\left(\rho^{\mathrm{T}}\rho <\mathbf{s}_0, \mathbf{n}> - \sqrt{w_I}\sum_{i=1}^{m+1}\rho_i <\mathbf{s}_0, \mathbf{n}>_i\right)\right)\end{aligned}$$

where $x = \left[\rho^{\mathrm{T}}\rho\left(1-\rho^{\mathrm{T}}\rho\right)\right]^{-1/2}$.

We consider now the entire expression for the decision statistics

$$\begin{aligned}
&\text{D.S.} = <\mathbf{s}_0, \mathbf{y}> + \beta <\mathbf{V}^{\perp}, \mathbf{y}> \\
&= \mathrm{b}_0 + \sqrt{w_I}\sum_{i=1}^{m+1} \mathrm{b}_{\mathrm{i}}\rho_{\mathrm{i}} + \sigma <\mathbf{s}_0, \mathbf{n}> + \beta x\left(-\sqrt{w_I}\left(1-\rho^{\mathrm{T}}\rho\mathbf{s}\right)\rho^{\mathrm{T}}\mathbf{b}\right) \\
&\quad + \beta x\sigma\left(\rho^{\mathrm{T}}\rho <\mathbf{s}_0, \mathbf{n}> - \sqrt{w_I}\sum_{i=1}^{m+1}\rho_{\mathrm{i}} <\mathbf{s}_0, \mathbf{n}>\right) \\
&= \mathrm{b}_0 + \sqrt{w_I}\left[\left(1-\beta x\left(1-\rho^{\mathrm{T}}\rho\right)\right)\rho^{\mathrm{T}}\mathbf{b}\right] + \sigma\left[\left(1-\beta x\rho^{\mathrm{T}}\rho\right) <\mathbf{s}_0, \mathbf{n}> - \beta x\sum_{i=1}^{m+1}\rho_{\mathrm{i}} <\mathbf{s}_0, \mathbf{n}>\right]
\end{aligned}$$

which can be expressed as the sum of the contributions of the SS signal $\tilde{\mathrm{S}}$, the interference $\tilde{\mathrm{I}}$, and the noise $\tilde{\mathrm{N}}$

$$\text{D.S.} = \tilde{\mathrm{S}} + \tilde{\mathrm{I}} + \tilde{\mathrm{N}} \tag{5}$$

where

$$\tilde{\mathrm{S}} = \mathrm{b}_0,\ \tilde{\mathrm{I}} = \sqrt{w_{\mathrm{I}}}\left[\left(1-\beta x\left(1-\rho^{T}\rho\right)\right)\rho^{T}\mathbf{b}\right] \tag{6}$$

and

$$\tilde{\mathrm{N}} = \sigma\left[\left(1-\beta x\rho^{\mathrm{T}}\rho\right) <\mathbf{s}_0, \mathbf{n}> - \beta x\sum_{i=1}^{m+1}\rho_{\mathrm{i}} <\mathbf{s}_{\mathrm{i}}, \mathbf{n}>\right] \tag{7}$$

The effective additive white Gaussian noise, $\tilde{\mathrm{N}}$, has zero mean and variance

w

$$
\begin{aligned}
\tilde{\sigma}^2 &= \mathrm{E}\left\{\tilde{\mathrm{N}}^2\right\} \\
&= \sigma^2 \mathrm{E}\left\{\left[\left(1-\beta x \boldsymbol{\rho}^{\mathrm{T}}\boldsymbol{\rho}\right) < \mathbf{s}_0, \mathbf{n} > -\beta x \sum_{i=1}^{m+1} \rho_{\mathrm{i}} < \mathbf{s}_{\mathrm{i}}, \mathbf{n} >\right]^2\right\} \\
&= \sigma^2 \left[\begin{array}{l} \left(1-\beta x \boldsymbol{\rho}^{\mathrm{T}}\boldsymbol{\rho}\right)^2 \mathrm{E}\left\{< \mathbf{s}_0, \mathbf{n} >^2\right\} + \beta^2 x^2 \sum_{i=1}^{m+1} \rho_i^2 \mathrm{E}\left\{< \mathbf{s}_{\mathrm{i}}, \mathbf{n} >^2\right\} \\ -2\beta x\left(1+\beta x \boldsymbol{\rho}^{\mathrm{T}}\boldsymbol{\rho}\right) \sum_{i=1}^{m+1} \rho_{\mathrm{i}} \mathrm{E}\left\{< \mathbf{s}_{\mathrm{i}}, \mathbf{n} >< \mathbf{s}_0, \mathbf{n} >\right\} \end{array}\right] \\
&= \sigma^2 \left[\left(1+\beta x \boldsymbol{\rho}^{\mathrm{T}}\boldsymbol{\rho}\right)^2 + \boldsymbol{\rho}^{\mathrm{T}}\boldsymbol{\rho}\left(\beta^2 x^2 - 2\beta x\left(1+\beta x \boldsymbol{\rho}^{\mathrm{T}}\boldsymbol{\rho}\right)\right)\right] \\
&= \sigma^2 \left[1+\beta^2 x^2 \boldsymbol{\rho}^{\mathrm{T}}\boldsymbol{\rho}\left(1-\boldsymbol{\rho}^{\mathrm{T}}\boldsymbol{\rho}\right)\right] \\
&= \sigma^2 \left[1+\beta^2\right]
\end{aligned}
$$

Probability of error

The probability of error using this decision statistic against a zero threshold is

$$
\begin{aligned}
P_e &= \frac{1}{2}\Pr\left(\hat{b}_0 = 1 / b_0 = -1\right) + \frac{1}{2}\Pr\left(\hat{b}_0 = -1 / b_0 = 1\right) \\
&= \frac{1}{2}\Pr\left(\mathrm{D.S.} > 0 / b_0 = -1\right) + \frac{1}{2}\Pr\left(\mathrm{D.S.} < 0 / b_0 = 1\right) \\
&= \frac{1}{2}\Pr\left(\tilde{\mathrm{N}} > 1 - \sqrt{w_I}\left[\left(1-\beta x\left(1-\boldsymbol{\rho}^{\mathrm{T}}\boldsymbol{\rho}\right)\right)\boldsymbol{\rho}^{\mathrm{T}}\mathbf{b}\right]\right) + \frac{1}{2}\Pr\left(\tilde{\mathrm{N}} < 1 + \sqrt{w_I}\left[\left(1-\beta x\left(1-\boldsymbol{\rho}^{\mathrm{T}}\boldsymbol{\rho}\right)\right)\boldsymbol{\rho}^{\mathrm{T}}\mathbf{b}\right]\right) \\
&= \frac{1}{2^{\mathrm{m+1}}} \sum_{i=0}^{2^{\mathrm{m+1}}-1} Q\left(\frac{1-\sqrt{w_I}\left[\left(1-\beta x\left(1-\boldsymbol{\rho}^{\mathrm{T}}\boldsymbol{\rho}\right)\right)\boldsymbol{\rho}^{\mathrm{T}}\mathbf{b}^{\mathrm{i}}\right]}{\sigma\sqrt{1+\beta^2}}\right)
\end{aligned}
$$

we arrive

$$
P_e = \frac{1}{2^{\mathrm{m+1}}} \sum_{i=0}^{2^{\mathrm{m+1}}-1} Q\left(\frac{1-\sqrt{w_I}\left[\left(1-\beta\sqrt{\left(\boldsymbol{\rho}^{\mathrm{T}}\boldsymbol{\rho}\right)^{-1}-1}\right)\boldsymbol{\rho}^{\mathrm{T}}\mathbf{b}^{\mathrm{i}}\right]}{\sigma\sqrt{1+\beta^2}}\right) \tag{8}
$$

where $\mathbf{b}^{\mathrm{i}}$ is an ordering of the m+1 narrowband bits.

P w

Using the parametrized form of the probability of error we can derive the probability of error of each receiver of interest: the matched filter, the decorrelating detector, and the MMSE detector.

An alternate derivation of the decorrelating detector

This parametrization allows an alternate derivation of the decorrelating detector. We know that the decorrelating detector is independent of the near far ratio, therefore we must have

$$1-\beta x\left(1-\rho^{\mathrm{T}}\rho\right)=0 \;\; \beta=\frac{1}{x\left(1-\rho^{\mathrm{T}}\rho\right)}=\sqrt{\frac{\rho^{\mathrm{T}}\rho}{1-\rho^{\mathrm{T}}\rho}}=\beta_{DEC} \tag{9}$$

The probability of error of the decorrelating detector is

$$P_e\big|_{\beta=\beta_{DEC}}=Q\left(\frac{\sqrt{1-\rho^{\mathrm{T}}\rho}}{\sigma}\right) \tag{10}$$

Asymptotic behavior of the probability of error

From equation (8) we derive some asymptotic results and other observations. As the near far ratio goes to zero, the probability of error for the linear detector approaches the limit

$$\lim_{w_1\to 0} P_e=Q\left(\frac{1}{\sigma\sqrt{1+\beta^2}}\right) \tag{11}$$

The near far ratio approaching zero corresponds to the single user channel. Using this expression the probability of error is minimized for $\beta=0$, that is, for the matched filter

$$\lim_{w_1\to 0} P_e\big|_{\beta=\beta_{\mathrm{MF}}=0}=Q\left(\frac{1}{\sigma}\right) \tag{12}$$

The correlation between the signatures sequences goes to zero as orthogonal codes. In this case the probability of error approaches the same limit in (12), *i.e.* A single user channel; and the matched filter is optimal. In most practical multiple access systems, the

signature sequences can not be kept orthogonal. If we nonetheless apply the matched filter to such system, the probability of error will be

$$P_e\big|_{\beta=\beta_{\mathrm{MF}}=0} = \frac{1}{2^{\mathrm{m+2}}} \sum_{i=0}^{2^{\mathrm{m+2}}-1} Q\left(\frac{1-\sqrt{w_I}\boldsymbol{\rho}^{\mathrm{T}}\mathbf{b}^{\mathrm{i}}}{\sigma}\right) \tag{13}$$

In the high SNR region ($\sigma \to 0$), the bit error rate is dominated by the largest term in the sum (13).

4.2.2. Asymptotic multiuser efficiency

The effective energy of the true SS user

Because of the presence of interference in the channel the probability of error can only increase. It is usually of interest to quantify the multiuser error probability relative to that of single CDMA AWGN channel (12). To that end, we define the *effective energy* of the true SS user, $e_0(\sigma)$, that the energy that this user would require to achieve the probability of error equal to that of single CDMA user Gaussian channel with the same background noise level, *i.e.*,

$$P_e = Q\left(\frac{\sqrt{e_0(\sigma)}}{\sigma}\right) \tag{14}$$

Since the probability of error of any multiuser detector is lower bounded by the single user probability of error (12). The effective energy of user zero is always upper bounded by the it's actual energy

$$e_0(\sigma) \le 1$$

moreover, the probability of error expression (8) is dominated by the Q(.) function with the lowest argument. This argument is

e *Pe* *e* *e* *e*

$$\frac{1-\sqrt{w_I}\left[\left(1-\beta\sqrt{\left(\rho^{\mathrm{T}}\rho\right)^{-1}-1}\right)\sum_{i=1}^{m+1}|\rho_i|\right]}{\sigma\sqrt{1+\beta^2}} \tag{15}$$

which corresponds to replace $\rho^{\mathrm{T}}\mathbf{b}^{\mathrm{i}}$ by $\sum_{i=1}^{m+1}|\rho_i|$. Using this argument we can derive a lower bound to the effective energy of the desired user as function of the single variable β

$$e_0(\beta) \le \left(\frac{1-\sqrt{w_I}\left[\left(1-\beta\sqrt{\left(\rho^{\mathrm{T}}\rho\right)^{-1}-1}\right)\sum_{i=1}^{m+1}|\rho_i|\right]}{\sqrt{1+\beta^2}}\right)^2 \tag{16}$$

We normalized the true SS user energy to one, The *u* *u* *e* *e* *e* which is defined as the ratio between the effective and actual energies has the same expression as the effective energy. By definition, the multiuser efficiency lies in the interval [0,1] and quantifies the performance loss (in dB) due to the existence of the narrowband user in the channel.

The asymptotic multiuser efficiency

Recall that the asymptotic multiuser efficiency of the true SS user is defined as the limit of its multiuser efficiency, (or the effective energy in our case), as the background noise tends to zero. The asymptotic multiuser efficiency measures the slope with which the logarithm of the probability of error decreases to zero as the signal to noise ratio increases. The expression (16) does not depend on σ, that is, the asymptotic multiuser efficiency denoted by η_0 is

$$\eta_0(\beta) = \frac{\max^2\left[0,1-\sqrt{w_I}\left[\left(1-\beta\sqrt{\left(\rho^{\mathrm{T}}\rho\right)^{-1}-1}\right)\sum_{i=1}^{m+1}|\rho_i|\right]\right]}{\left(1+\beta^2\right)} \tag{17}$$

If we suppose the following inequality is true

e e e ew e e

$$\sqrt{w_I}\left[\left(1-\beta\sqrt{\left(\rho^{\mathrm{T}}\rho\right)^{-1}-1}\right)\sum_{i=1}^{m+1}|\rho_i|\right]\geq 1 \tag{18}$$

in this case the linear detector characterized by β is not efficient, and its probability of error does not vanish as the background noise goes to zero, thus, $\eta_0(\beta)=0$. However, if

$$\sqrt{w_I}\left[\left(1-\beta\sqrt{\left(\rho^{\mathrm{T}}\rho\right)^{-1}-1}\right)\sum_{i=1}^{m+1}|\rho_i|\right]\leq 1 \tag{19}$$

the asymptotic efficiency of a linear detector characterized by β is

$$\eta_0(\beta)=\frac{\left(1-\sqrt{w_I}\left[\left(1-\beta\sqrt{\left(\rho^{\mathrm{T}}\rho\right)^{-1}-1}\right)\sum_{i=1}^{m+1}|\rho_i|\right]\right)^2}{1+\beta^2} \tag{20}$$

the expression (17) combines the asymptotic multiuser efficiency in both regions (18) and (19).

Using this expression we can derive the asymptotic multiuser efficiency of the conventional detector, by setting β=0

$$\eta_0(0)=\left(1-\sqrt{w_I}\sum_{i=1}^{m+1}|\rho_i|\right)^2 \tag{21}$$

matching the expression derived by Verdù [2], for the special case where the interferers are of equal powers and the mutual cross-correlation between them is equal to zero.

The asymptotic multiuser efficiency of the decorrelating detector can be easily derived from the equation (17) and using the variable β_{DEC}

$$\eta_0(\beta_{DEC})=\frac{1}{1+\beta_{DEC}^2}=1-\rho^{\mathrm{T}}\rho \tag{22}$$

which does not depend on the near far ratio; it is then equal to it's near far resistance.

For the MMSE we use it's the proper variable β_{MMSE} expression, and we tend the noise variance to zero

$$\lim_{\sigma\to 0}\beta_{MMSE}=\lim_{\sigma\to 0}\frac{\sqrt{\rho^T\rho\left(1-\rho^T\rho\right)}}{1-\rho^T\rho+\sigma^2/w_I}=\sqrt{\frac{\rho^T\rho}{1-\rho^T\rho}}=\beta_{DEC} \tag{23}$$

which leads to the same expression as that derived for the decorrelating detector. The asymptotic multiuser efficiency of the decorrelating detector and the MMSE detector are identical.

4.2.3. The near far resistance

The ( ) of the desired SS user is defined as the minimum asymptotic efficiency over the relative energies of the interferers. In our case, all the virtual interferers have the same power but not necessarily the same correlation with the desired user.

$$\eta(\beta)=\min_{w_I}\left(\eta_0(\beta)\right) \tag{24}$$

To find the minimum of the asymptotic multiuser efficiency, we minimize the numerator of (20)

$$\left(1-\sqrt{w_I}\left[\left(1-\beta\sqrt{\left(\rho^{\mathrm{T}}\rho\right)^{-1}-1}\right)\sum_{i=1}^{m+1}|\rho_i|\right]\right) \tag{25}$$

Clearly for large w_I the interference dominates and have zero near far resistance. However, if the term multiplying $\sqrt{w_I}$ is zero the dependence on the interference power is eliminated, and we can have a non-zero . This occurs for

$$\left(1-\beta\sqrt{\left(\rho^{\mathrm{T}}\rho\right)^{-1}-1}\right)=0$$

which is just β_{DEC}. Thus the decorrelating detector leads to an expression independent of the near far ratio w_I. This confirms that among all the detectors independent of the interference

power, only the decorrelating detector [11] has non zero near far resistance. In our case the

is equal to

$$\eta(\beta_{DEC}) = \frac{1}{1+\beta_{DEC}^2} = 1-\rho^{T}\rho \tag{26}$$

matching the previous results of Rusch [28].

4.2.4. Parametrized MOE

In [14], Honig, ., demonstrated that the receiver which minimizes the MSE also minimizes the mean output energy (MOE), defined as $MOE(\mathbf{c}) = E\left\{\langle \mathbf{c}, \mathbf{y}\rangle^2\right\}$. We now find an alternate derivation of the vector **c** which minimizes this expression, using our subspace partition. Any two vectors **c** and **y** can be decomposed into their components falling into each of the spaces Γ_E, $\Gamma_{I\&N}$, and Γ_{NO} as follows

$$\mathbf{c} = \mathbf{c}_E + \mathbf{c}_{I\&N} + \mathbf{c}_{NO}, \text{ and } \mathbf{y} = \mathbf{y}_E + \mathbf{y}_{I\&N} + \mathbf{y}_{NO} \tag{27}$$

The component $\mathbf{c}_{NO}$ contributes only to noise enhancement at the receiver output, and $\mathbf{c}_{I\&N}$ contributes only interference and noise energies to the mean output energy. It is preferable to avoid theses noise and interference contributions. Indeed, for the received signal **y**, only the component in Γ_E will contain energy from the desired user. The component of **y** in Γ_{NO} contains only energy from the AWGN, and the component of **y** in $\Gamma_{I\&N}$ has energy only from the AWGN and the narrowband interference. We will minimize the noise and interference energy in the output by choosing the components of $\mathbf{c}_{opt}$ in $\Gamma_{I\&N}$ and Γ_{NO} to be zero.

$$\mathbf{c}_{I\&N} = \mathbf{c}_{NO} = 0$$

This choice minimizes the mean output energy directly

$$\begin{aligned} MOE(\mathbf{c}) &= E\left\{\langle \mathbf{c}_E, \mathbf{y}_E\rangle^2\right\} + E\left\{\langle \mathbf{c}_{I\&N}, \mathbf{y}_{I\&N}\rangle^2\right\} + E\left\{\langle \mathbf{c}_{NO}, \mathbf{y}_{NO}\rangle^2\right\} \\ &= E\left\{\langle \mathbf{c}_E, \mathbf{y}_E\rangle^2\right\} \end{aligned}$$

Therefore $\mathbf{c}_{\text{opt}}$ falls in the two-dimensional space Γ_E and can be written as $\mathbf{c}_{\mathbf{opt}} = \mathbf{s}_0 + \beta_{\min}\mathbf{V}^{\perp}$. To find the value of β minimizing the MOE, we write the MOE as a function of β and differentiate.

$$\begin{aligned} MOE(\beta) &= w_0 < \mathbf{c}, \mathbf{s}_0 >^2 + w_I \sum_{i=1}^{m+1} < \mathbf{c}, \mathbf{s}_i >^2 + \sigma^2 < \mathbf{c}, \mathbf{c} >^2 \\ &= w_0 < \mathbf{s}_0 + \beta\mathbf{V}^{\perp}, \mathbf{s}_0 >^2 + w_I \sum_{i=1}^{m+1} < \mathbf{s}_0 + \beta\mathbf{V}^{\perp}, \mathbf{s}_i >^2 + \sigma^2 < \mathbf{s}_0 + \beta\mathbf{V}^{\perp}, \mathbf{s}_0 + \beta\mathbf{V}^{\perp} >^2 \\ &= w_0 + \sigma^2 + w_I \rho^T \rho + \beta^2 \left(w_I \left(1 - \rho^T \rho \right) + \sigma^2 \right) - 2\beta w_I \sqrt{\rho^T \rho \left(1 - \rho^T \rho \right)} \end{aligned}$$

The value of β which minimizes this expression is

$$\beta_{\min} = \frac{\sqrt{\rho^T \rho \left(1 - \rho^T \rho \right)}}{1 - \rho^T \rho + \sigma^2 / w_I} = \beta_{\text{MMSE}} \tag{28}$$

matching the previous result for the MMSE detector that we derived in section 2.5.

In Figure 4.1 we plot the MOE as a function of β and the interference power (relative to the desired user's power). The minimum of the function MOE(β_{MMSE}) is traced in the plot. Note that β_{DEC} does not vary with interference power and the MOE(β_{DEC}) is a straight line. The adaptive version of the MMSE receiver minimizes the MOE. As the MOE is convex in β, the algorithm will not be trapped in local minima. However, the function is much less convex as the interference power approaches the desired user's power, as is evident in Figure 4.1, and is nearly flat for very weak interference. This leads us to anticipate that the adaptive algorithm will be much less effective in the presence of a weak interferer, as is demonstrated in the simulations of section 4.3.3.

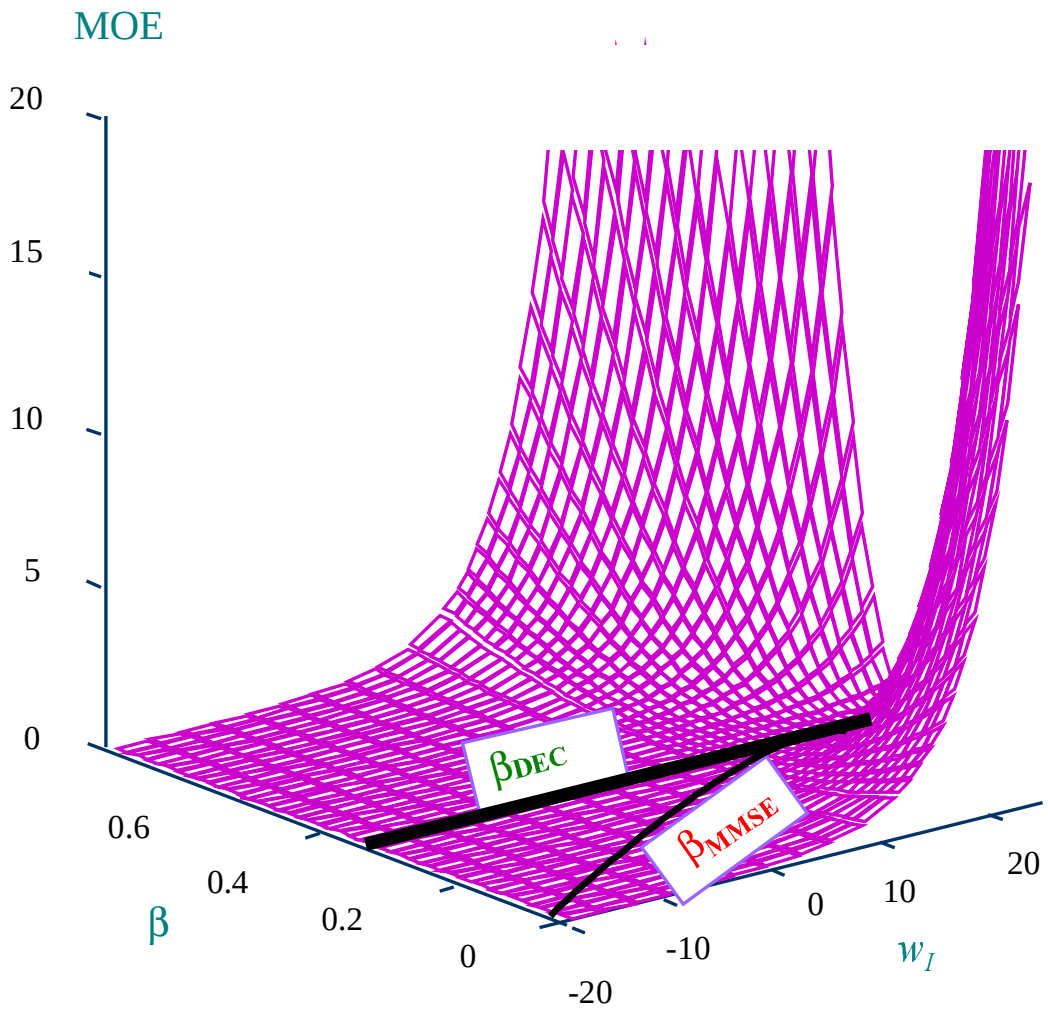

Figure 4.1 MOE as a function of interference power and parameter β

4.2.5. Parametrized SIR

This parameterization β can also be used to facilitate calculation of the SIR defined as

$$\mathrm{SIR}(\mathbf{c}) = \frac{\text{signal power}}{\mathrm{MOE}(\mathbf{c}) - \text{signal power}}$$

For the three fixed receivers, we can write this as a function of β

$$SIR(\beta) = \frac{w_0}{\sigma^2 + w_I \rho^T \rho + \beta^2 \left(w_I \left(1 - \rho^T \rho\right) + \sigma^2 \right) - 2\beta w_I \sqrt{\rho^T \rho \left(1 - \rho^T \rho\right)}} \qquad (29)$$

In Figure 4.2 we plot the SIR as a function of β and the interference power. It is clear that β_{min} gives a peak in the SIR for high values of interference power, whereas this peak is lost for weak interferers.

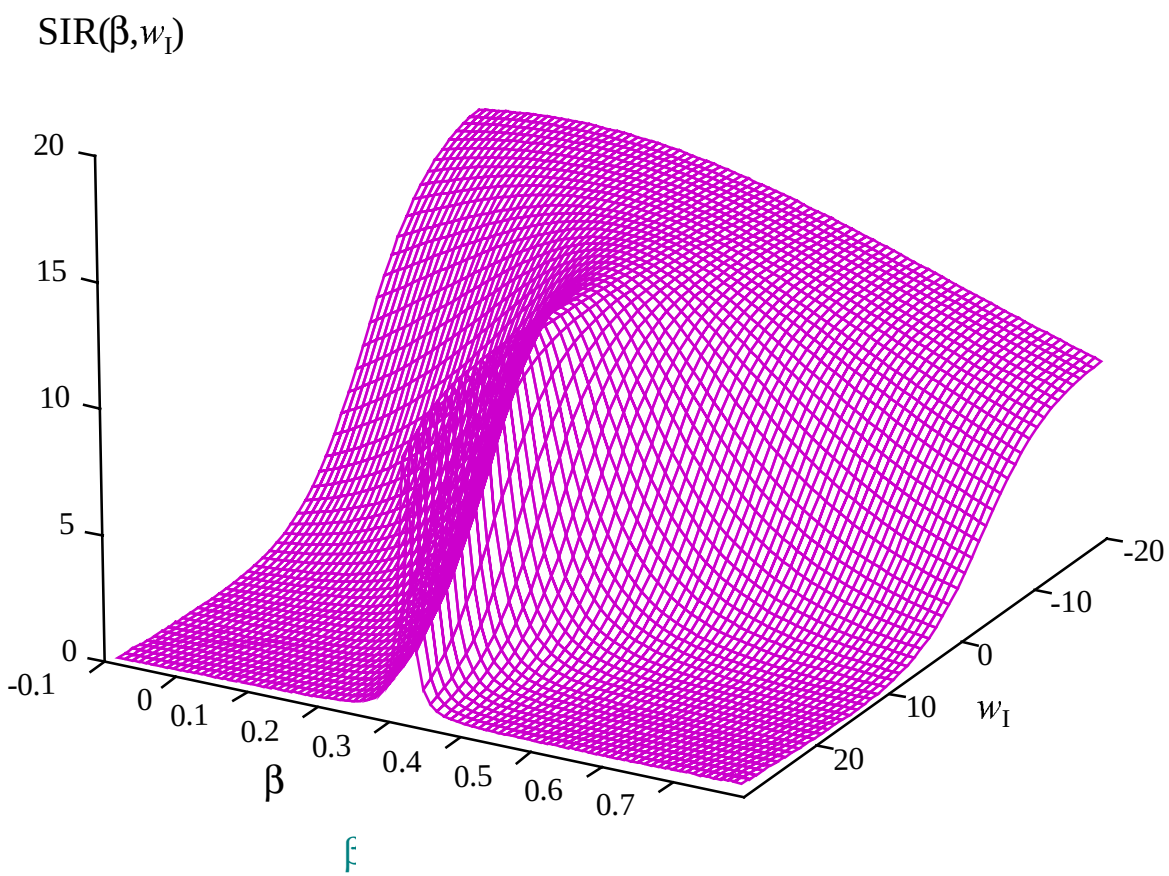

Figure 4.2 SIR as a function of interference power and parameter β

4.3. Simulation results vs theory

4.3.1. Convergence Anomalies

Using our subspace approach to analyze the stochastic gradient algorithm, we can examine new performance tests for the convergence of the algorithm by projecting the mean tap weights onto the three subspaces Γ_E, $\Gamma_{I\&N}$ and Γ_{NO}. Ideally the algorithm should only have a non-zero projection onto the space Γ_E, and this should asymptotically approach the MMSE detector. The projection of the tap weight vector on the first eigenvector is

$$\left\langle \bar{\mathbf{c}}(n), \mathbf{V}_{0\mathbf{v}} \right\rangle = \frac{\gamma_0'}{1-\rho^T\rho+\sigma^2/w_I}\left(1-\left(\frac{\gamma_1'}{\gamma_0'}\right)^2\left[1-\mu\left(w_I\left(1-\rho^T\rho\right)+\sigma^2\right)\right]^n\right) \xrightarrow[n\to\infty]{} \frac{\gamma_0'}{1-\rho^T\rho+\sigma^2/w_I} \quad (30)$$

and its projection on the second eigenvector is

$$\left\langle \bar{\mathbf{c}}(n), \mathbf{V}_{1\mathbf{v}} \right\rangle = \frac{\gamma_1'}{1-\rho^T\rho+\sigma^2/w_I}\left(1-\left[1-\mu\left(w_I\left(1-\rho^T\rho\right)+\sigma^2\right)\right]^n\right) \xrightarrow[n\to\infty]{} \frac{\gamma_1'}{1-\rho^T\rho+\sigma^2/w_I} \quad (31)$$

and finally, its projection on the other eigenvectors are

$$\left\langle \bar{\mathbf{c}}(n), \mathbf{V}_{i\mathbf{v}} \right\rangle = 0 \qquad \text{for} \quad 2 \le i \le N-1$$

This shows that ideally, the mean tap weight vector lies entirely in the effective energy eigenspace. In Figure 4.3 we examine the sensitivity of the gradient algorithm to the interference power via simulation. We project the tap weights as proposed in equations (30-32) and plot the simulation projections versus the theoretical values. We project along $\mathbf{V_{0v}}$ and $\mathbf{V_{1v}}$ in Γ_E and $\mathbf{V_{2v}}$, $\mathbf{V_{3v}}$ and $\mathbf{V_{4v}}$ in $\Gamma_{I\&N}$. In Figure 4.3 (a) we have a very weak interferer, 10 dB down from the CDMA signal, and it is difficult for the tap weight vector to achieve the desired dynamics. We note that nonzero components and found outside Γ_E. Due to the weak interference signal, the adaptation is being driven by noise samples. In Figure 4.3 (b) we have a moderate interference power, 10 dB up from the CDMA signal, and the gradient follows the theoretical mean values more closely, but still varies significantly from the optimal values.

n n i n n

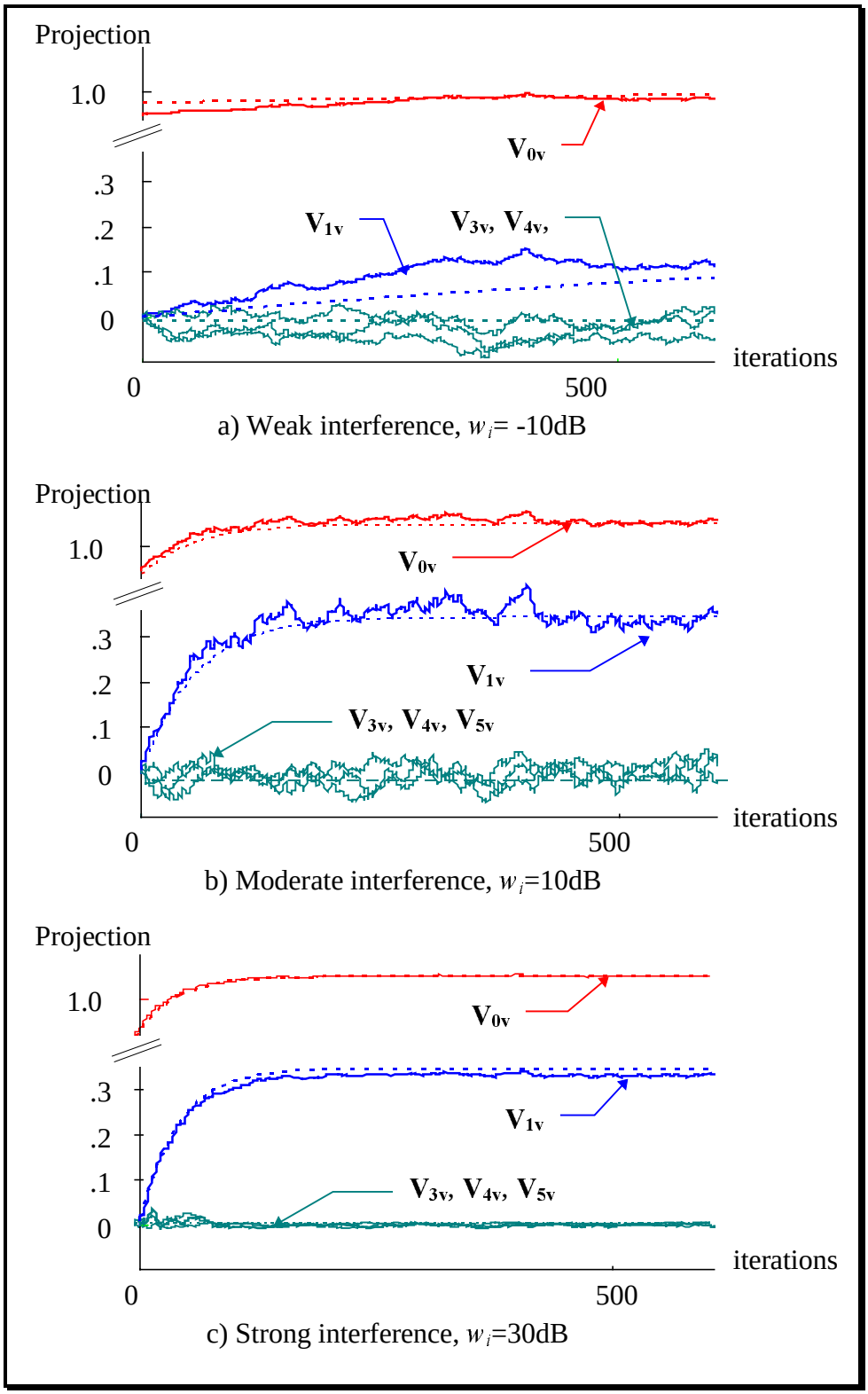

Figure 4.3 a,b,c) Convergence along various eigenvectors, (theory = dashed, simulation = solid)

In Figure 4.3 c) we have a strong interferer, 30 dB up from the CDMA signal, and the gradient attains the optimal tap weights.

This important convergence anomaly becomes evident using the subspace analysis. The extreme difficulty of the algorithm to converge, and possibly diverge, when only a small interference power is present, is a serious problem. This anomaly is explained by the very weak convexity of the mean output energy for weak interferers, as demonstrated in Figure 4.1. While the algorithm will not be trapped by local minima, it is easily lead astray by spurious noise samples.

In Figure 4.5 we simulate the stochastic gradient and project the detector energy onto the three subspaces Γ_E, $\Gamma_{I\&N}$ and Γ_{NO}. As the interference power diminishes we see a more and more significant portion of the detector energy appearing in Γ_{NO}. This corresponds to a large component of the detector output being attributable to noise only. While [14] and [33] alluded to the inefficiency of the gradient and the desirability of switching quickly to a decision-directed LMS detector, we now see that when the interference power is weak it is unlikely that the gradient will ever produce meaningful output.

A second anomaly which we highlight is the possible divergence of the algorithm when allowed to operate indefinitely. The gradient is always sensitive to a large noise sample. The longer the algorithm is allowed to run, the more likely that an outlier noise sample will occur and force the gradient to follow the noise into the space Γ_{NO}. Once displaced into Γ_{NO} the algorithm has great difficulty in returning to Γ_E. This problem is alluded to in [12], where a step size that shrinks as one over the iteration number is suggested to effectively stop adaptation after a certain point.

w

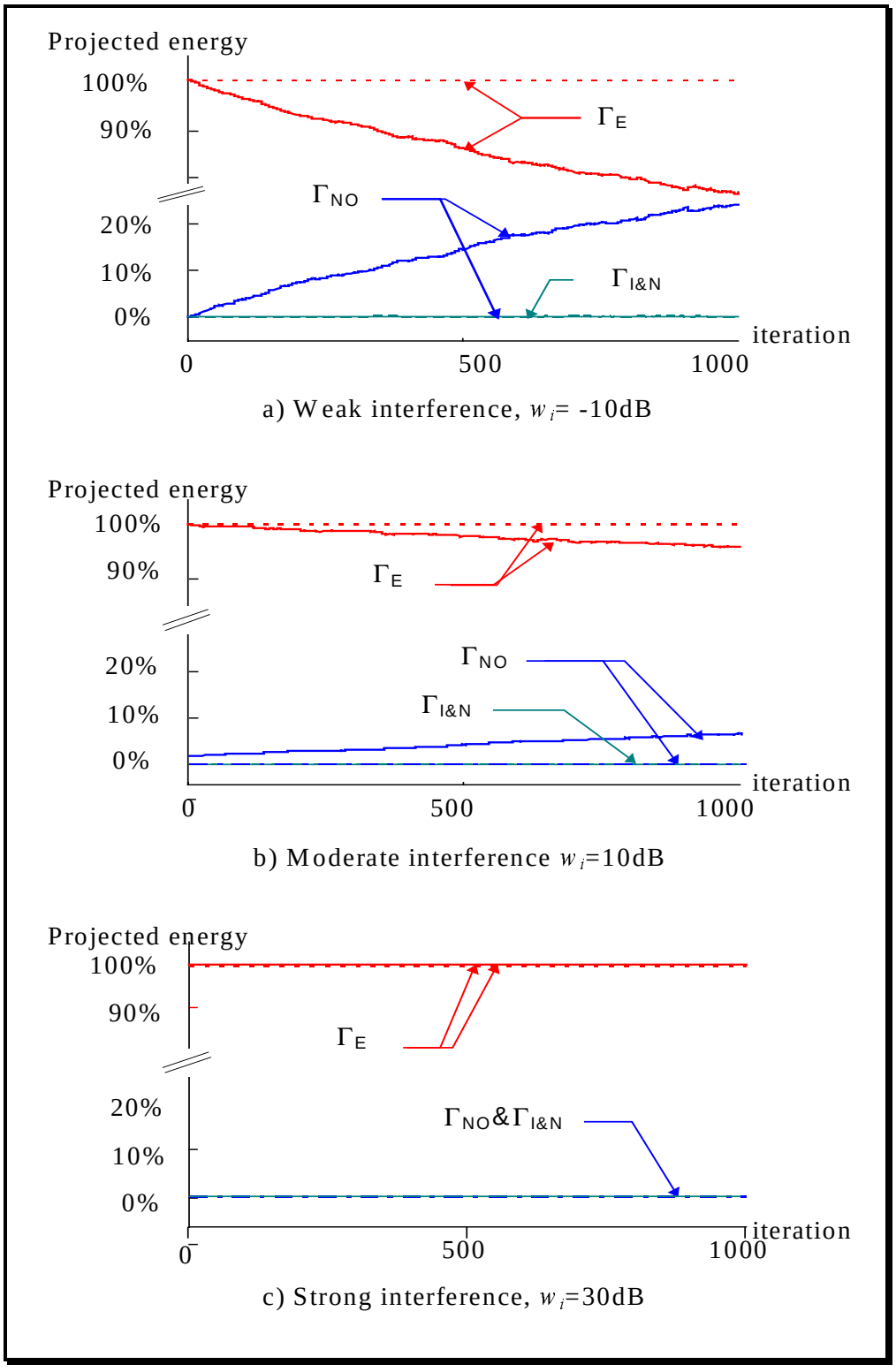

Figure 4.4 a,b,c) receiver output energy projected onto eigenspaces, (theory = dashed, simulation = solid)

4.3.2. Convergence Time with New Step Size

We now examine the improved convergence time of the new step-size constraint presented in equations (30-32) as opposed to the old criteria proposed in [14] and [33]. Figure 4.4 presents curves for the theoretical simulation results of the projections of the mean tap weight vector versus iterations for an interference power of 30 dB and m = 4. We project the tap weights as proposed in equation (30-32) onto the subspaces Γ_E and $\Gamma_{I\&N}$. It is clear that the new step size allows convergence in dozens of iterations, versus hundreds of iterations for the old step size. Given that we wish to switch out of the stochastic gradient adaptation as soon as possible, the new step size criteria is an important improvement to the algorithm. Note though that we also see in these plots the additional excess noise caused by the faster convergence.

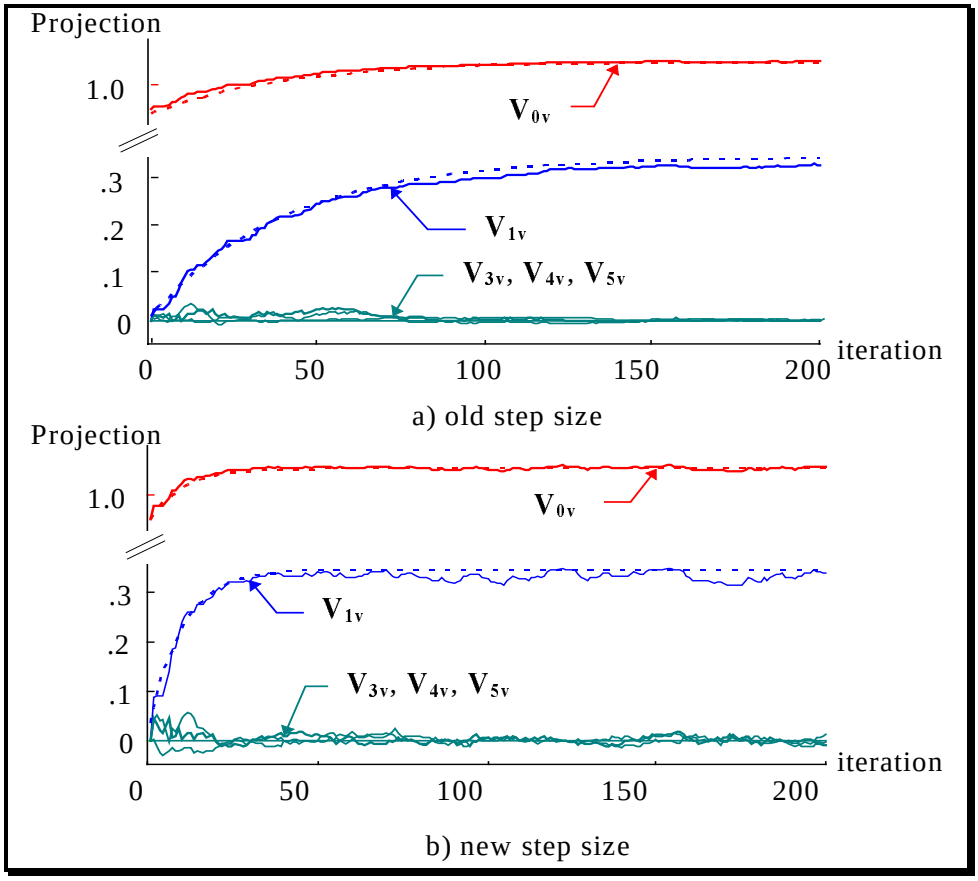

Figure 4.5 Projections onto eigenvectors: Comparison of convergence rates

w

4.3.3. Probability of error of various receivers

In Figure 4.6 we present Monte Carlo simulation results and theoretical calculations of the probability of error for three fixed receivers: the matched filter (MF), the decorrelating detector (DEC), and the MMSE detector. We also present simulation results for the stochastic gradient algorithm. All simulations use a maximal length sequence of length 63 for the true spread spectrum user, a noise power 6 dB down from the despread CDMA signal (as proposed in [17] during field trials), interference powers that vary from parity with the CDMA signal to 40 dB stronger, and one or two virtual CDMA users. We see that for MF, DEC, and MMSE simulation and theory match well. The decorrelating and MMSE detectors yield very similar performance. The blind stochastic gradient algorithm achieves better performance in strong interference environment. Its probability of error decreases as the near far ratio increases. We note similar performance with m=4, and 8. The gradient's performance improves as the interference power increases. To arrive at reliable estimates of the probability of error it was necessary to run the algorithm for millions of bits. This allowed adequate opportunity for the gradient algorithm to be lead astray by noise and significantly differ from the MMSE detector, even for very strong interference.

w

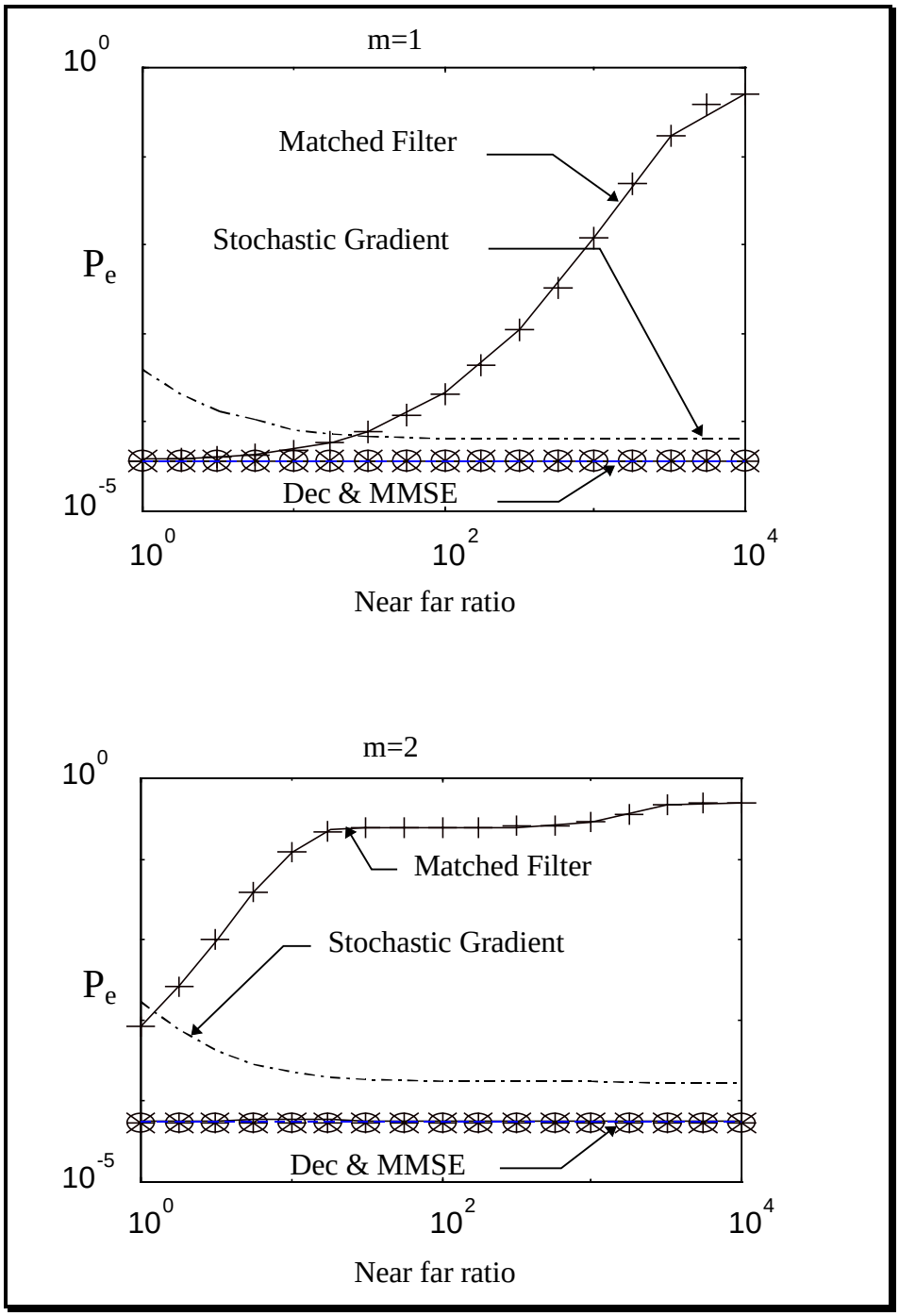

Figure 4.6 The probability of error, m=1, 2 (theoretical values as points, simulation values as curves)

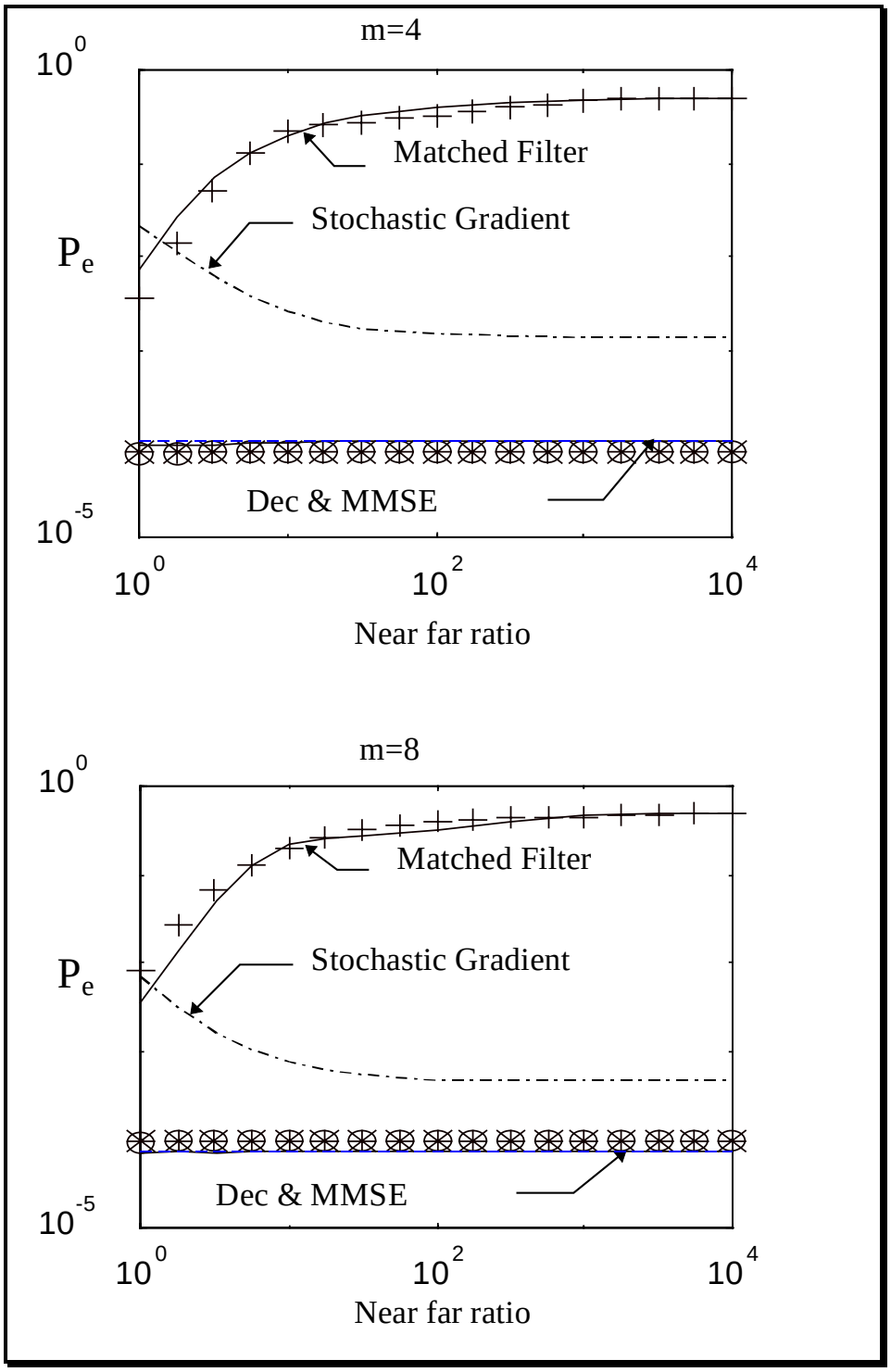

Figure 4.7 The probability of error, m=4, 8 (theoretical values as points, simulation values as curves)

w

4.4. The new detector

In view of the mentioned anomalies, we propose a new detector which takes advantage of the new step size for quicker convergence, while avoiding adaptation when the interference power is weak. A functional block diagram of the proposed receiver is given in Figure 4.8. There are two factors that determine the algorithm's continuing adaptation: iteration number and interference power. When the interference power is very weak, . ., no power is detected, the matched filter is nearly optimal, and the control forces the receiver to the matched filter.

If the interference power is strong, the algorithm has a good chance of converging to the MMSE receiver. In this region the MMSE detector is closely approximated by the decorrelating receiver, and we will effectively be converging to the decorrelating detector. Once enough iterations have passed for convergence, we average over several dozen bits to find the mean value for the tap weights and use this as a fixed receiver (alternately we could use this as the initial state for a decision-directed version of the LMS algorithm). If the interference power degrades significantly we also stop the adaptation, as the likelihood of drifting out of Γ_E and into Γ_{NO} is quite great.

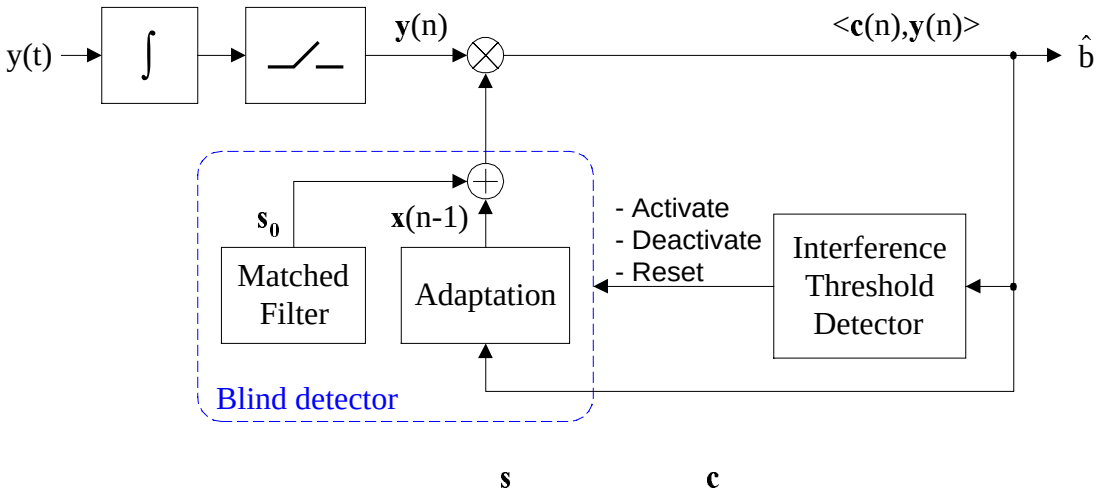

Figure 4.9 and Figure 4.10 show simulation results for the proposed blind detector vs. MF, DEC, MMSE, and the blind stochastic gradient algorithm for m=1, 2, 4,

and 8. The proposed detector achieves better performance, notably for weak interference scenario (unless otherwise indicated the old step-size is used). For most plots the proposed receiver achieves the performance of the decorrelating or MMSE detector. This detector ran adaptively at an interference power of 30 dB for 1000 bits. The tap weight values were then averaged over the last 100 iterations. This receiver (now fixed) was used to calculate the probability of error for the range of interference powers. At the time the gradient algorithm was stopped, it had formed a good estimate of the MMSE detector (noise outliers being unlikely is so few samples).

w

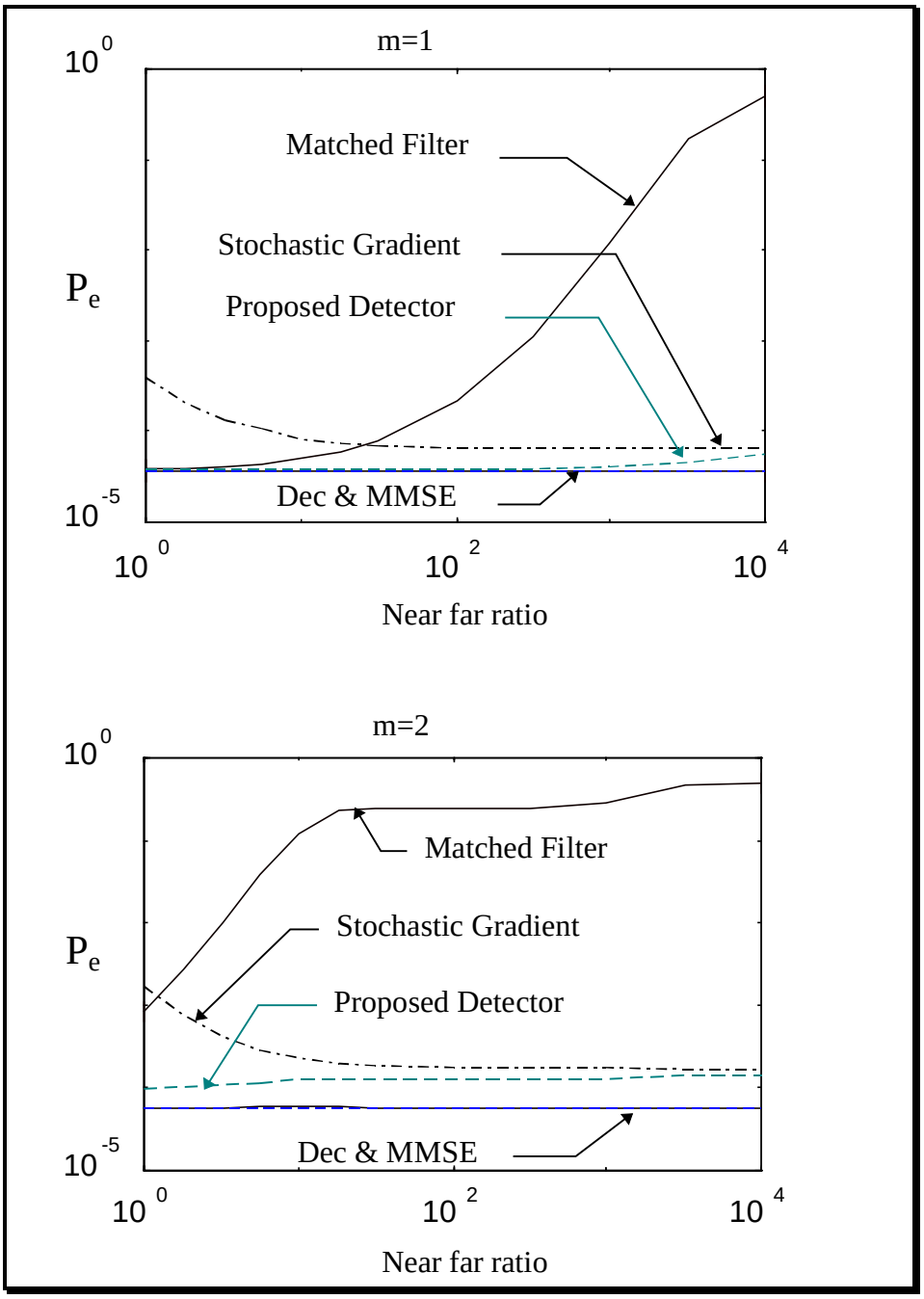

9 s c s M DE MMSE s c s c

w

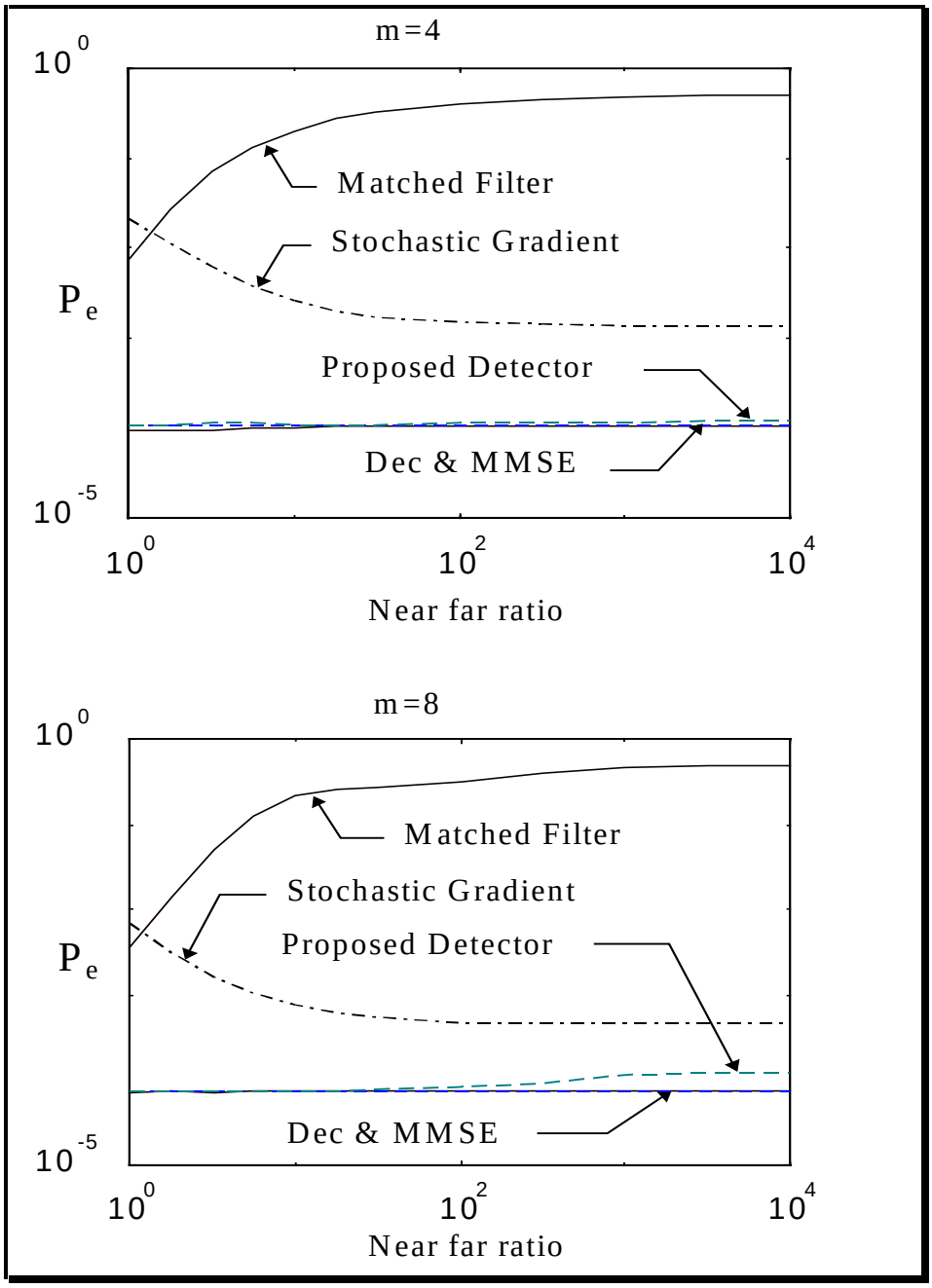

0 s c s M DE MMSE s c s c

Conclusion

In this work we addressed the problem of coexistence of spread spectrum communications with pre-existing digital narrowband (NB) system. We considered the digital narrowband signal as an interference in a code division multiple access (CDMA) system implemented with direct sequence spread spectrum (DSSS). We examined the feasibility of employing signal detection techniques from multiuser CDMA to combat the interference caused by the presence of strong narrowband digital interferer. We adopted the channel model of Rusch and Poor [29,30], where they treated the scenario of one NB and one SS signal, and they modeled it as a virtual multiuser CDMA system. They addressed the conventional (MF) and the decorrelating detectors (DEC), while we investigate in section 2.5, (and in [31]), the minimum mean square error (MMSE) receiver. We applied this detector to the narrowband suppression problem, arriving at a closed form solution for the MMSE detector, a closed form expression of its decision statistic as well as its probability of error. The derived closed form of the MMSE detector as well as that of the decorrelating detector have the advantage that they can be implemented in a simple form of modified matched filters.

Even though it was demonstrated that the DEC and the MMSE are efficient against digital NB interferer, these detectors require (or must acquire) the knowledge of all the users' signatures, timing, and powers. However in a practical context, this information is not readily available especially in our case of narrowband interference. This led us to investigate the feasibility of adaptive and blind detection techniques for the narrowband suppression problem.

In multiuser detection theory, Honig, Madhow, and Verdù [14] proposed a blind adaptive version of the MMSE detector by applying the gradient descent algorithm on the mean output energy (MOE). This stochastic algorithm leads adaptively to the MMSE

u

solution, and it requires only the desired user's signature. We focused on this blind suppression technique, applying it to our narrowband suppression problem.

We adopted a subspace strategy to describe the mean evolution trajectory of the blind detector (or the tap weight vector of the gradient descent algorithm). Our strategy clarified the dependence of the blind detector performance on some environment (or interference) parameters. We highlighted severe problems and inherent anomalies of the stochastic blind adaptive detector.

Firstly, we identified a special distribution of the received energy in the signal space, which led us to determine the eigenspaces of the system dynamics and to analyze the convergence of the blind adaptive algorithm for our channel. Using this eigenspace analysis, we partitioned the signal space into different significant subspaces. We demonstrated the significance of these subspaces in terms of how energy from the desired SS user, the AWGN and the narrowband interference is distributed among them. In particular the subspace Γ_E, which is a two dimensional subspace, contains all the energy of the desired signal and a subset of the interference and noise energies.

We discovered that the minimized function, the MOE, exists entirely in the only two dimensional subspace Γ_E. This observation allowed us to express the mean output energy of every linear canonical form detector as a single variable function. We denoted this single variable β, and we defined a general expression of every canonical linear detector as function of β. We expressed the most useful performance measure parameters such as the probability of error, the signal to interference ratio, the effective energy, the asymptotic multiuser efficiency, and the near-far ratio as function of the single variable β. We discovered also that the most useful fixed detectors such as the conventional detector and the decorrelating detector [30], as well as the MMSE receiver all lie in the two dimensional eigenspace Γ_E. We identified each investigated fixed detector by a special value of β, (β_{Mf} for the matched filter, β_{DEC} for the DEC detector, β_{MMSE} for the MMSE detector). We also derived the useful performance measures of each fixed detector from those of the general canonical linear detector.

u

Secondly, we identified two new constraints on the step size of the stochastic algorithm which can decrease the convergence time considerably. The first constraint is constant, and is derived from the fact that the minimized function, MOE, is a single parameter function, that is, only one eigenvalue must be taken into account. This eigenvalue is not necessarily the maximum. In our case, the minimum non-zero eigenvalue must be used to fix the constraint on the step size (denoted λ_{1v} in the text).

The second constraint is time-variable, and is derived via a new criteria we defined in the text. Using this criteria we maximize the convergence rate of the algorithm. We expressed the relative instantaneous mean evolution (RIME) of the algorithm as function of the iteration number and the step size. We derived the step size value which maximizes the RIME as function of the iteration number. This time-variable constraint is of great practical interest demonstrating that we can begin the convergence with relatively large step size, and decrease the step size as the iteration number increases (or we approach the convergence). It can be used to effectively reduce the excess noise energy viewed by the stochastic algorithm.

Thirdly, we demonstrated that the convexity of the mean output energy depends of the interference environment. The function MOE is much less convex as the interference power approaches the desired user's power, as is evident in Figure 4.1, and is nearly flat for very weak interference. We demonstrated with simulation results that the blind adaptive algorithm is much less effective in the presence of a weak interferer. The performance of the blind adaptive detector decreases dramatically in the weak near-far ratio situation.

A second convergence anomaly we detected in the possible diverge of the algorithm when allowed to operate indefinitely. Since the gradient is always sensitive to a large noise sample, the longer the algorithm is allowed to turn, the more likely that an outlier noise sample will occur and force the detector to leave the desired trajectory.

Fourthly, we proposed a new blind adaptive receiver that avoids the convergence anomalies, while capitalizing on the new step size for faster and better quality of convergence.

u

Finally, we recall that in our work we analyzed the scenario of only one CDMA user plus only one narrowband user. We believe that for a different scenario where there are many CDMA users operating in the presence of several narrowband interferers, the adaptive receiver would not be confined to a 2-D space. In fact, any additional CDMA user introduces a new dimension in the effective energy eigenspace. In interpreting the narrowband interference as m+1 CDMA users we would expect Γ_E to grow similarly in dimension. However, we showed that being a single signal it, in fact, only contributes one dimension to Γ_E .

Generalizing our results for multiple SS users, or multiple NB signals is not trivial; however, the convergence anomalies we identified exist naturally for such more general scenarios. Our analysis for the restricted case highlights the origins of these convergence anomalies of the blind detector, especially the dependence on the interference power level. While analytic expressions would become more complicated in the general, the existence of faster convergence criteria is nevertheless established.

Appendix : Eigenvalues and eigenvectors of $\mathbf{R_{yy}}$

Eigenvalues of $\tilde{\mathbf{R}}_{\mathbf{yy}}$

Using equation (8) we intend to calculate directly the characteristic polynomial of $\tilde{\mathbf{R}}_{\mathbf{yy}}$ defined by

$$P_c(\lambda) = \det\left(\tilde{\mathbf{R}}_{\mathbf{yy}} - \lambda \mathbf{I}_{\mathbf{m+2}}\right)$$

where λ is an eigenvalue, and $\mathbf{I_{m+2}}$ is the identity matrix with dimension $+2$. The matrix $\tilde{\mathbf{R}}_{\mathbf{yy}} - \lambda \mathbf{I}_{\mathbf{m+2}}$ also has an arrow structure

$$\tilde{\mathbf{R}}_{\mathbf{yy}} - \lambda \mathbf{I}_{\mathbf{m+2}} = \begin{bmatrix} w_0 + \sigma^2 - \lambda & w_I \rho^T \\ w_0 \rho & \left(w_I + \sigma^2 - \lambda\right)\mathbf{I}_{\mathbf{m+1}} \end{bmatrix}$$

We can triangularize this matrix in (m+1) steps. The first step is the row elimination of the last term of the first row. We multiply the first row by $\left(w_I + \sigma^2 - \lambda\right)$ and the last row by $\left(-w_I \rho_{m+1}\right)$; we put the sum of the two rows in place of the first row, after this operation we retain the last row in the previous state. We arrive at the equation

$$\left(w_I + \sigma^2 - \lambda\right)\left(\tilde{\mathbf{R}}_{yy} - \lambda I_{m+2}\right) = \begin{bmatrix} \left(w_0 + \sigma^2 - \lambda\right)\left(w_I + \sigma^2 - \lambda\right) - w_0 w_I \rho^T \rho & . & w_m \rho_m \left(w_I + \sigma^2 - \lambda\right) & 0 \\ w_0 \rho_1 & \left(w_I + \sigma^2 - \lambda\right) & 0 & 0 \\ . & 0 & . & 0 \\ w_0 \rho_m & 0 & 0 & \left(w_I + \sigma^2 - \lambda\right) \end{bmatrix}$$

In the ith step, we multiply the ith row by $\left(-w_I \rho_i\right)$. We put the sum of the first row and the resultant ith row in place of the first row. After all the (m+1) steps of row elimination, we arrive at the lower triangular matrix form

$$\begin{bmatrix} \left(w_0 + \sigma^2 - \lambda\right)\left(w_I + \sigma^2 - \lambda\right) - w_I w_0 \rho^T \rho & 0 \\ w_0 \rho & \left(w_I + \sigma^2 - \lambda\right)\mathbf{I}_{\mathbf{m+1}} \end{bmatrix}$$

The determinant of the above matrix is easily calculated to be

$$\left(\left(w_0+\sigma^2-\lambda\right)\left(w_I+\sigma^2-\lambda\right)-w_I w_0 \rho^T \rho\right)\left(w_I+\sigma^2-\lambda\right)^{m+1}$$

which yields the following characteristic polynomial

$$P_c(\lambda)=\left(\left(w_0+\sigma^2-\lambda\right)\left(w_I+\sigma^2-\lambda\right)-w_I w_0 \rho^T \rho\right)\left(w_I+\sigma^2-\lambda\right)^{m}$$

The eigenvalues which solve this polynomial are

$$\lambda_{0y}=\frac{1}{2}\left(w_0+w_I+2\sigma^2+\sqrt{\phi}\right) \quad , \quad \phi=\left(w_0-w_I\right)^2+4w_0 w_I \rho^T \rho$$
$$\lambda_{1y}=\frac{1}{2}\left(w_0+w_I+2\sigma^2-\sqrt{\phi}\right)$$
$$\lambda_{iy}=w_I+\sigma^2 \qquad 2\le i\le m+1$$
$$\lambda_{iy}=\sigma^2 \qquad m+2\le i\le N-1$$

Eigenvectors of $\tilde{\mathbf{R}}_{\mathbf{yy}}$

We define $\mathbf{V_{0y}} = [v_0 \ v_1,...,v_{m+1}]$ as the eigenvector relative to the eigenvalue λ_{0y} which solves

$$\left(\tilde{\mathbf{R}}_{\mathbf{yy}}-\lambda_{0y}\mathbf{I_{m+2}}\right)\mathbf{V_{0y}}=0$$

We arrive at the following system of $m+2$ equations for the eigenvector $\mathbf{V_{0y}}$

$$\left(w_0-w_I-\sqrt{\phi}\right)v_0+2w_I\sum_{i=1}^{m+1}\rho_i v_i=0$$
$$2w_0\rho_1 v_0+\left(w_I-w_0-\sqrt{\phi}\right)v_1=0$$
$$\vdots$$
$$2w_0\rho_{m+1}v_0+\left(w_I-w_0-\sqrt{\phi}\right)v_{m+1}=0$$

After simplifying we get the single variable equation $\left(\phi-\phi\right)v_0=0$. It is sufficient to take $v_0\neq 0$, and using the above system, determine the other components of the eigenvector $\mathbf{V}_{0y}$. The value $v_0=\frac{1}{2}\left(w_I-w_0-\sqrt{\phi}\right)$ offers a simple and compact expression for the other

i

eigenvector components.

We proceed similarly to find the second eigenvector $\mathbf{V}_{1y}=[v_0, v_1, ...v_{m+1}]$ relative to λ_{1y}

$$\left(\tilde{\mathbf{R}}_{\mathbf{yy}} - \lambda_{1y}\mathbf{I}_{\mathbf{m+2}}\right)\mathbf{V}_{\mathbf{1y}} = 0$$

and we arrive the following system of m+2 equations

$$\begin{aligned}
\left(w_0 - w_I + \sqrt{\phi}\right)v_0 + 2w_I \sum_{=1}^{+1} \rho\, v &= 0 \\
2w_0\rho_1 v_0 + \left(w_I - w_0 + \sqrt{\phi}\right)v_1 &= 0 \\
&\vdots \\
2w_0\rho_{+1} v_0 + \left(w_I - w_0 + \sqrt{\phi}\right)v_{+1} &= 0
\end{aligned}$$

After some manipulations, we get the following compact normalized form of the two eigenvectors

$$\mathbf{V}_{\mathbf{0y}} = \gamma_0\left[\Delta^-, -\rho^T\right] \text{ and } \mathbf{V}_{\mathbf{1y}} = \gamma_1\left[\Delta^+, -\rho^T\right]$$

where

$$\Delta^{\pm} = \frac{1}{2}\left(1-\alpha^{-2} \pm \sqrt{\left(1-\alpha^{-2}\right)^2 + 4\alpha^{-2}\rho^T\rho}\right), \quad \alpha = \sqrt{w_I / w_0}$$

and

$$\gamma_0 = \left(\left(\Delta^- - \rho^T\rho\right)^2 + \rho^T\rho\left(1-\rho^T\rho\right)\right)^{-\frac{1}{2}} \qquad \gamma_1 = \left(\left(\Delta^+ - \rho^T\rho\right)^2 + \rho^T\rho\left(1-\rho^T\rho\right)\right)^{-\frac{1}{2}}$$

The third eigenvalue is of multiplicity m. Thus, the associated eigenspace is of m+1 dimensions. Each eigenvector $\mathbf{V}_{iy}$ in this eigenspace solve the equation

$$\left(\mathbf{R}_{\mathbf{yy}} - \lambda_{iy}\mathbf{I}_{\mathbf{m+2}}\right)\mathbf{V}_{iy} = 0$$

Thus, the system of linear equations describing the eigenspace relative to the third

eigenvalue is

$$\sum_{i=1}^{m+1} \rho_i v_i = 0\,, \quad v_0 = 0$$

which defines an *m* dimensional convex hyperplane. We choose

$$\mathrm{V}_{2y} = \left[0, \rho_2\rho_1, -\rho_1^2, 0, \ldots, 0\right]\left(\rho_1^2\left(\rho_1^2 + \rho_2^2\right)\right)^{-\frac{1}{2}}$$

which solves the simple equation $\rho_1 v_1 + \rho_2 v_2 = 0$. The next eigenvector can be determined iteratively; it must meet the following condition

$$\rho_{1}\mathrm{v}_1 + \rho_{2}\mathrm{v}_2 + \rho_{3}\mathrm{v}_3 = 0$$

and preferably the second condition

$$<\mathbf{V_{3y}}, \mathbf{V_{2y}}> = 0$$

In this way all the orthonormal eigenvectors describing the eigenspace associated to the third eigenvalue λ_{iy} have the form

$$\mathrm{V}_{iy} = \left[0, \rho_i\rho_1, \ldots, \rho_i\rho_{i-1}, -\sum_{j=1}^{i-1}\rho_j^2, 0, \ldots, 0\right]\gamma_i$$

where

$$\gamma_i^{-1} = \sqrt{\left(\sum_{j=1}^{i-1}\rho_j^2\right)\left(\sum_{j=1}^{i}\rho_j^2\right)}\,, \text{ for } i = 2, \ldots m+1$$

We demonstrate in the following that all the above m vectors from the eigenspace associated with the third eigenvalue are orthogonal to the real SS signature $\mathbf{s_0}$. We calculate the inner product between the SS signature vector $\mathbf{s_0}$ and each every eigenvector $\mathbf{V}_{iy}$ relative to λ_{iy}, for $i = 2, \ldots m+1$

i

$$\left\langle \mathbf{s}_0, \mathrm{V}_{iy} \right\rangle = \left\langle \mathbf{s}_0, \left[0, \rho_i\rho_1, \ldots, \rho_i\rho_{i-1}, -\sum_{j=1}^{i-1}\rho_j^2, 0, \ldots, 0 \right]\gamma_i \right\rangle$$
$$= \rho_i\gamma_i\left(\sum_{j=1}^{i-1}\rho_j^2\right) - \rho_i\gamma_i\left(\sum_{j=1}^{i-1}\rho_j^2\right) = 0$$

This result is of great interest, as it allows us to define an m-dimensional subspace spanned by the m eigenvectors relatives to the third eigenvalue. This subspace is included in Γ_{act} and we call it $\Gamma_{I\&N}$.

The remaining *N-m-2* eigenvectors of the covariance matrix $\tilde{\mathbf{R}}_{\mathbf{yy}}$ relating to the remaining eigenvalues $\lambda_{iy} = \sigma^2, i = m+2, \ldots, N$ can be easily determined by combining the above m+1 eigenvectors and the standard basis vectors, using Gram-Schmidt orthogonalization.

For constants Δ^+, Δ^-, and γ_i defined in the appendix, the orthonormal set of eigenvectors is given by

$$\mathbf{V_{0y}} = \gamma_0\left[\Delta^- \quad -\rho^T\right]_{B_{act}}$$
$$\mathbf{V_{1y}} = \gamma_1\left[\Delta^+ \quad -\rho^T\right]_{B_{act}}$$
$$\mathbf{V_{iy}} = \gamma_i\left[0 \quad \rho_i\rho_1 \quad \cdots \quad \rho_i\rho_{i-1}\ \delta_i \quad \cdots \quad 0\right]_{B_{act}} \qquad \forall\ 2 \le i \le m+1$$
$$\mathbf{V_{iy}} = \gamma_i\left(e_i - \sum_{j=0}^{i-1}\left\langle e_i, \mathbf{V_{jy}}\right\rangle \mathbf{V_{jy}}\right) \qquad \forall\ m+2 \le i < N$$

where $\delta_i = -\sum_{j=1}^{i-1}\rho_j^2$

References

1. Pickholtz R. L., Schilling D. L., Milstein L. B., "Theory of Spread-Spectrum Communications-A Tutorial", *IEEE Transactions on Communications*, vol. COM-30, no.5, May 1982.
2. Verdù S. and Thomas, J. B., *Multiuser Detection.* Greenwich, CT: JAI Press, 1993.
3. Peterson R., Ziener R. E., Borth D. E., *Introduction to spread spectrum communications*, Prentice Hall. PTR, Englewood Cliffs, NJ 07632.
4. Rappaport T. S., *Wireless Communications Principles & Practice*, Prentice Hall, Upper Saddle River, NJ 07458.
5. Lee, William C. Y., *Mobile communications design fundamentals*, 2nd edition, W. series in telecommunications, T. Wiley, New York, 1993.
6. Poor H. V., and Verdù S., "Single-User Detectors for Multiuser Channel", *IEEE Transactions on Communications,* vol. 36, no. 1, pp. 50-88, January 1988.
7. Verdù S., "Minimum Probability of Error for Asynchronous Gaussian Multiple-Access Channels", *IEEE Transactions on Information Theory,* vol. IT-32, no. 1, pp. 85-96, January 1986.
8. Verdù S., "Optimum Multiuser Asymptotic Efficiency", *IEEE Transactions on Communications,* vol. COM-34, no. 9, pp. 890-897, September 1986.
9. Xie Z., Short R. T., and Rushforth C. K., "A family of Suboptimum Detectors for Coherent Multiuser Communications", *IEEE Journal on Selected Areas in Communications*, vol. 8, no. 4, pp. 683-690, May 1990.
10. Lupas R., and Verdù S., "Linear Multiuser Detectors for Synchronous Code-Division Multiple-Access Channels", *IEEE Transactions on Information Theory,* vol. 35, no. 1, pp. 123-136, January 1989.
11. Lupas R., and Verdù S., "Near-Far Resistance of Multiuser Detectors in Asynchronous Channels", *IEEE Transactions on Communications,* vol. 38, no. 4, pp. 496-508, April 1990.

12. Madhow U., and Honig M. L., "MMSE Interference Suppression for Direct-Sequence Spread-Spectrum CDMA", *IEEE Transactions on Communications*, vol. 42, no. 12, pp. 3178-3188, December 1994.
13. Hongya G., and Bar-Ness Y., "Comparative study of the linear minimum mean squarred (LMMSE) and the adaptive Bootstrap multiuser detectors for CDMA communications", in *Interference Rejection And Signal Separation In Wireless Communications Symposium*, New Jersey Institute of Technology, March 19, 1996.
14. Honig M., Madhow U., and Verdú S., "Blind Adaptive Multiuser Detection", *IEEE Transactions on Information Theory*, vol. 41, pp. 944-960, July, 1995.
15. Miller S. L., "An adaptive direct-sequence code-division multiple-access receiver for multiuser interference rejection", *IEEE Transactions on Communications*, Vol. 43, pp. 1746-1755, April, 1995.
16. Honig M. L., and Messerschmitt D. G., *Adaptive Filters Structures, Algorithms, and Applications*, Kluwer Academic Publishers, 1985.
17. Milstein L. B., Schilling D. L., Pickholtz R., Erceg V., Kullback M., and Kanterakis, "On the Feasibility of a CDMA Overlay for Personal Communications Networks", *IEEE Journal on Selected Areas in Communications*, vol. 10, pp. 655-668, May, 1992.
18. Schilling D. L., Milstein L.B., Pickholtz R., Kullback M., and Miller F., "Spread spectrum for commercial communications", *IEEE Communications Magazine*, pp. 66-79, Apr. 1991.
19. Schilling D. L., Pickholtz R., and Milstein L.B., "Spread spectrum goes commercial", *IEEE Spectrum*, pp. 41-45, Aug. 1990.
20. Utlaut W., "Spread spectrum: Principles and possible application to spectrum utilization and allocation", *IEEE Communications Magazine*, pp. 21-31, Sept. 1978.
21. Gilhousen K. S., Jacobs I. M., Padovani R., Viterbi A. J., Weaver L. A., Jr., and Wheatly C.E., "On the Capacity of a Cellular CDMA System", *IEEE Journal on Selected Area in Communications*, 1991.

22. Milstein, L. B., "Interference rejection techniques in spread spectrum communications," in *Proceedings of the IEEE,* vol. 76, pp. 657-671, 1988.
23. Poor H. V., "*An introduction to Signal Detection and Estimation*". Springer-Verlag, 1988.
24. Masreliez C. J., "Approximate non-Gaussian filtering with linear state and observation relations", *IEEE Transactions on Automatic Control,* pp. 107-110, February 1975.
25. Ketchum J. W., and Proakis J. G., "Adaptive algorithms for estimating and suppressing narrowband interference in PN spread spectrum systems", *IEEE Transactions on Communications*, vol. COM-30, pp. 913-924, May 1982.
26. Vijayan R. and Poor H. V., "Nonlinear techniques for interference suppression in spread spectrum systems", *IEEE Transactions on Communications*, vol. 38, pp. 1060-1065, July 1991.
27. Rusch L. A. and Poor H. V. "Narrowband Interference Suppression in CDMA Spread Spectrum Communications", *IEEE Transactions on Communications*, vol. 42, no. 2/3/4, 1994.
28. Rusch L. A. "*Interference Suppression in Spread Spectrum Code Division Multiple Access Communications*", PhD thesis, Princeton university, 1994.
29. Poor H. V., and Rusch L. A. "Narrowband Interference Suppression in Spread Spectrum CDMA", *IEEE Personal Communications,* 1994.
30. Rusch L. A. and Poor H. V., "Multiuser Detection Techniques for Narrowband Interference Suppression in Spread Spectrum", *IEEE Transactions on Communications*, vol. 43, pp. 1725-1745, April, 1995.
31. Rusch, L. A. and Fathallah, H., "MMSE Detector for Narrowband Interference Suppression in DS Spread Spectrum", in *Interference Rejection And Signal Separation In Wireless Communications Symposium*, New Jersey Institute of Technology, March 19, 1996.
32. Sandberg D., Delmarco S., Jagler K., and Tzannes M.A., "Some Alternatives in Transform-Domain Suppression of Narrowband Interference for Signal Detection

and Demodulation" *IEEE Transactions on Communications,* vol. 43, no. 12 December 1995.

33. Poor H. V. and Wang X., "Adaptive Suppression of Narrowband Digital Interferers from Spread Spectrum Signals", *Special Issue on Interference in Mobile Wireless Systems,* submitted 1995.
34. Fathallah H., and Rusch L. A., "A Subspace Approach to Adaptive Narrowband Interference Suppression in DSSS", *IEEE Transactions on Communications,* accepted, July, 1997.
35. Fathallah H., and Rusch L. A., "Enhanced Blind Adaptive Narrowband Interference Suppression in DSSS", *Globecom proceedings*, vol. 1 of 3, pp. 545-549, Nov., 1996.
36. Duel-Hallen A., "Decorrelating Decision-Feedback Multiuser Detector for Synchronous Code-Division Multiple-Access", *IEEE Transactions on Communications*, vol. 41, pp. 285-290, February 1993.
37. Fathallah, H and Rusch, L. A., "Blind Adaptive Narrowband Interference Suppression DSSS via Subspace Analysis", in *Interference Rejection And Signal Separation In Wireless Communications Symposium*, George Washington University, Washington DC, March 18, 1996.
38. Householder, Alston S., "*The Theory of Matrices in Numerical Analysis*", Blaisdell, 1964.